



GDAŃSKI UNIWERSYTET MEDYCZNY
WYDZIAŁ FARMACEUTYCZNY Z ODDZIAŁEM
MEDYCZYNY LABORATORYJNEJ

Renata Barbara Bujak

**NIECELOWANA ANALIZA METABOLICZNYCH „ODCISKÓW
PALCA” W PRÓBKACH OSOCZA W NADCIŚNIENIU PŁUCNYM
Z WYKORZYSTANIEM CHROMATOGRAFII CIECZOWEJ
I GAZOWEJ SPRZĘŻONYCH ZE SPEKTROMETRIĄ MAS**

Zakład Biofarmacji i Farmakokinezyki

Katedry Biofarmacji i Farmakodynamiki

Gdańskiego Uniwersytetu Medycznego

Promotor:

**dr hab. n. farm. Michał Jan Markuszewski,
prof. GUMed**

Promotor pomocniczy:

prof. Coral Barbas

Centre of Metabolomics and Bioanalysis

Uniwersytet San Pablo w Madrycie

Gdańsk 2015



MEDICAL UNIVERSITY OF GDAŃSK
FACULTY OF PHARMACY WITH SUBFACULTY
OF LABORATORY MEDICINE

Renata Barbara Bujak

**PLASMA METABOLIC FINGERPRINTING IN PULMONARY
ARTERIAL HYPERTENSION BY LIQUID AND GAS
CHROMATOGRAPHY COUPLED WITH MASS SPECTROMETRY**

Department of Biopharmaceutics and Pharmacokinetics

Chair of Biopharmaceutics and Pharmacodynamics

Medical University of Gdańsk

Supervisor:

assoc. prof. Michał J. Markuszewski, Ph.D.

Co-supervisor:

prof. Coral Barbas

Centre of Metabolomics and Bioanalysis

San Pablo University in Madrid

Gdańsk 2015

Praca doktorska finansowana była ze środków:

1. Umowy Offsetowej z Hiszpanią- EADS CASA (Eurocopter and Airbus Operations)
2. Krajowego Naukowego Ośrodka Wiodącego (KNOW) przyznanych na podstawie decyzji nr MNiSW-DS-6002-4693-23/WA/12 z dnia 12 lipca 2012 r. na lata 2012-2017
3. Narodowego Centrum Nauki, grant PRELUDIUM nr 2014/13/N/NZ7/04231

The doctoral thesis was supported by:

1. Offset Agreement with Spain- EADS CASA (Eurocopter and Airbus Operations)
2. The Ministry of Science and Higher Education of the Republic of Poland, from the quality - promoting subsidy, under the Leading National Research Centre (KNOW) programme for the years 2012 – 2017".
3. National Science Centre, grant no 2014/13/N/NZ7/04231

Abbreviations:

ALP- alkaline phosphatase

ALT- alanine aminotransferase

APAH- pulmonary arterial hypertension associated with other diseases

BMPR2- bone morphogenetic protein receptor 2

APCI- atmospheric pressure chemical ionization

AST- aspartate aminotransferase

bFGF- basic fibroblast growth factor

BMI- body mass index

BNP- B-type natriuretic peptide

BSTFA- N,O-Bis(trimethylsilyl)trifluoroacetamide

BUN- blood urea nitrogen

CA- cluster analysis

CCM- central carbon metabolism

CCR- correct classification rate

CE-MS- capillary electrophoresis coupled with mass spectrometry

CERK- ceramide kinase

CHD- congenital heart diseases

SCD- sickle cell disease

CI- chemical ionization

CID- collision-induced dissociation

CO- cardiac output

COW- correlation optimized warping

COX- cyclooxygenase

LOX- lipoxygenase

CYP-450- cytochrome P 450

cPLA2- cytosolic phospholipase A2

CSF- cerebrospinal fluid

CV- coefficient of variation

DIMS- direct infusion mass spectrometry

DTW- dynamic time warping

ECC- extracted compound chromatogram

ECM- extracellular matrix

EI- electron impact

EPCs- endothelial progenitor cells

ERA- endothelin receptor antagonists

ESI- electrospray ionization

FFA- free fatty acids

FT-IR- Fourier-transform infrared spectroscopy

GC-MS- gas chromatography coupled with mass spectrometry

GSH- glutathione

HCA- hierarchical cluster analysis

HGF- hepatocyte growth factor

HIF- hypoxia-inducible factor

HILIC- hydrophilic interaction liquid chromatography

HR- heart rate

ICR- ion cyclotron resonance

IMS- ion mobility spectrometer

IS- internal standard

IT-ion trap analyzer

IVDE- in-vial dual extraction

JK- jack knife confidence interval

k-NN- k-nearest neighbors algorithm

LC-ESI-MS- liquid chromatography coupled with electrospray ionization mass spectrometry

LOOCV- leave-one-out cross validation

LV- latent variable

MALDI- matrix-assisted laser desorption ionization

MFC- median fold change

MFE- molecular feature extraction

MMPs- metalloproteinases

mPAP- mean pulmonary arterial pressure

MS- mass spectrometry

MS/MS- tandem mass spectrometry

mSBP- mean systemic blood pressure

MSGUS- MS group useful signal

MSTFA- N-methyl-N (trimethylsilyl)-trifluoroacetamide

MSTS- MS total signal

MSTUS- MS total useful signal

mTOR- mammalian target of rapamycin

NMR- nuclear magnetic resonance

NO- nitric oxide

nSMase- neutral sphingomyelinase

OPLS- orthogonal partial least squares regression

PAH- pulmonary arterial hypertension

PASMCs- pulmonary artery smooth muscle cells

PCA-principal component analysis

PCs- principal components

PCWP- pulmonary capillary wedge pressure

PDE-5- phosphodiesterase type 5

PDGF- platelet-derived growth factor

PE- pulmonary embolism

PFAMs- primary fatty acids amides

PH- pulmonary hypertension

PLA2- phospholipase A2

PLS-DA- partial least squares discriminant analysis

PLS- partial least squares regression

PPARs- peroxisome proliferator-activated receptors

PPHN- persistent pulmonary hypertension of the newborn

PUFA- polyunsaturated fatty acids

PVR- pulmonary vascular resistance

PWP- pulmonary wedge pressure

QC- quality control samples

QqQ- triple quadrupole

Q- quadrupole analyzer

Q-TOF- quadrupole analyzer coupled with time of flight analyzer

RAS- renin-angiotensin system

RHC- right heart catheterization

RI- retention index

ROS- reactive oxygen species

RP- reversed-phase

RT- retention time

SD- standard deviation

sGC- soluble guanylate cyclase

SIM- single ion monitoring

SMC- smooth muscle cell

SOP- standard operating procedure

SVM- support vector machine

TCA cycle- tricarboxylic acid cycle

TGF- β - transforming growth factor- β

TIC- total ion chromatogram

TMCS- trimethylchlorosilane

TMS- trimethylsilyl

TOF- time of flight analyzer

UHPLC- ultra high-performance liquid chromatography

UV scaling- unit variance scaling

UVol- urine volume

VEGF- vascular endothelial growth factor

VIP- vasoactive intestinal polypeptide

WU- Wood units

α -HB- α -hydroxybutyrate

β -HB- β -hydroxybutyrate

5-HT- 5-hydroxytryptamine

TABLE OF CONTENTS

I. THEORETICAL PART	11
1. INTRODUCTION	11
2. METABOLOMICS IN THE CONTEXT OF SYSTEMS BIOLOGY	12
2.1 <i>Research strategies in metabolomics</i>	14
2.2 <i>Typical workflow in untargeted metabolic fingerprinting</i>	17
2.2.1. Study design and metabolite extraction	18
2.2.2 Analytical platforms in sample analysis	21
2.2.3 Raw data extraction and preprocessing	26
2.2.4 Multivariate data analysis	28
2.2.5 Metabolite identification and biochemical interpretation.....	30
3. MASS SPECTROMETRY BASED METABOLOMICS	31
3.1 <i>Ionization modes</i>	32
3.2 <i>Mass analyzers</i>	36
3.3 <i>Tandem mass spectrometry</i>	37
4. PULMONARY ARTERIAL HYPERTENSION	39
4.1 <i>Clinical definitions and epidemiology</i>	39
4.2 <i>Clinical classification</i>	41
4.3 <i>Pathomechanisms of pulmonary arterial hypertension</i>	46
4.4 <i>Current diagnosis and treatment in pulmonary arterial hypertension</i>	51
II. THE OBJECTIVE OF THE DOCTORAL THESIS.....	55
III. EXPERIMENTAL PART	56
5. MATERIALS AND METHODS	56
5.1 <i>Instrumentation</i>	56
5.2 <i>Disposable materials and reagents</i>	58
5.2.1 Disposable materials.....	58
5.2.2 Reagents	59
5.2.3 Solutions.....	60
5.3 <i>Biological samples</i>	62
5.3.1. Animal model	62
5.3.2. Human model	65
5.4 <i>Biological sample preparation</i>	67
5.4.1. Plasma sample pretreatment for LC-QTOF-MS metabolic fingerprinting	67
5.4.2. Plasma sample pretreatment for GC-Q-MS metabolic fingerprinting	69
5.5 <i>Analytical platforms used in plasma metabolic fingerprinting</i>	71
5.5.1. Plasma metabolic fingerprinting with LC-ESI-QTOF-MS.....	71
5.5.2. Plasma metabolic fingerprinting with GC-Q-MS	74
5.6 <i>The data extraction and processing methods</i>	75
5.6.1. Data acquired with LC-ESI-QTOF-MS plasma metabolic fingerprinting	75
5.6.2. Data acquired with GC-Q-MS plasma metabolic fingerprinting	76
5.7 <i>Univariate and multivariate statistical data analysis</i>	77
5.8 <i>Metabolite identification and biochemical interpretation</i>	79
IV. RESULTS AND DISCUSSION	81

6. PLASMA METABOLIC FINGERPRINTING WITH LC-ESI-QTOF-MS AND GC-Q-MS IN AN ANIMAL MODEL OF ACUTE PULMONARY HYPERTENSION	81
6.1 <i>Univariate and multivariate statistical analysis</i>	87
6.2 <i>Discriminant models validation</i>	90
6.3 <i>Metabolite identification</i>	93
6.4 <i>Biochemical interpretation and discussion</i>	97
7. PLASMA METABOLIC FINGERPRINTING WITH LC-ESI-QTOF-MS AND GC-Q-MS IN A HUMAN MODEL OF PULMONARY ARTERIAL HYPERTENSION	103
7.1 <i>Univariate and multivariate statistical analysis</i>	109
7.2 <i>Discriminant models validation</i>	112
7.3. <i>Metabolite identification</i>	114
7.4 <i>External validation of potential markers of pulmonary hypertension</i>	117
7.5 <i>Biochemical interpretation and discussion</i>	119
V. CONCLUSIONS	126
VI. SUMMARY	127
TABLE CONTENT	131
FIGURE CONTENT	133
VII. REFERENCES	136
VIII. ABSTRACT	152
IX. STRESZCZENIE	153

I. THEORETICAL PART

1. Introduction

So far, all known living systems as plants, microorganisms, animals and human beings, are characterized by dynamic homeostasis state which means that they are changing over time. Thus the key task of each organism is to keep internal balance in response to exogenous stimuli. During whole life various biological systems are exposed to different factors that can disturb their own homeostasis. For instance, the pathological processes related to disease initiation can cause changes on all biological organization levels. However, the prediction of the living systems' behavior may be difficult in view of a single biochemical component. Therefore to describe diversity of the networked interactions in a specific biological organism, the multidisciplinary platforms based on both measurement technologies and mathematical models are mandatory. In biomedical research, to understand pathomechanisms of complex disorders, usually, single factor as gene, protein or enzyme has been concerned. Recently, the extensive development in the field of systems biology, has provided a new multifactorial insight into pathological processes responsible for disease initiation, progress or recurrence.

Thanks to significant improvements in sensitive analytical techniques and advanced bioinformatics tools, there are constant possibilities to expand the knowledge on human metabolites composition. Similarly to well defined genome or proteome, metabolome determines complement of all small molecule metabolites in biological system under particular state. Since, the genome or proteome modifications predict what may occur, metabolite alterations reflect what had already happened on cellular level of the living system. In this sense, metabolome is a chemical representation of the molecular phenotype of an particular organism. Thus new approaches, such as: metabonomics or metabolomics have recently emerged in existing *-omics* revolution. However, comprehensive understanding of pathological hallmarks of complex diseases may be achieved by integrative insight into all molecular levels. Integration of the existing systems biology branches may completely define

biological phenotype of disorders, especially those with unexplained pathomechanisms. Only such approaches guarantee the holistic, against to reductionistic, view into the life systems [1].

2. Metabolomics in the context of systems biology

To understand the complex and dynamic living systems the holistic and integrative approach, namely systems biology (systeomics), is required. Systeomics looks into the structure and dynamics of various biological organization levels of the living systems such as: cells, tissues or organisms [2]. Therefore, the systems biology aims to predict the behavior of the whole system on the basis of the set of biological components and interactions between them. Among these systems biology tools, so-called *-omics* sciences, genomics, transcriptomics, proteomics or metabolomics, play a crucial role in understanding molecular processes at the different biological organization levels. The development of genomics provided the sequencing of any organisms genome and initiated the progress of other systeomics branches as transcriptomics and proteomics which are focused on measurement of mRNA transcription level (transcriptome) or proteins abundance (proteome), respectively. Subsequently, the changes at proteome level stimulated further determination of low-molecular-weight molecules, namely metabolites. Therefore, the general flow of biological information through *-omic* cascade (Figure 1) in living systems goes from genes via transcripts, and proteins to metabolites. However, it should be underlined that there are numerous feedback interactions from metabolites to proteins, transcripts or genes, as well as others. For that reason, the development of new *-omic* approaches in the field of systems biology have recently been reported. For instance, the fluxomics studies turnover of the molecules in the metabolic flux which determines all the biological processes such as: cellular signaling, transport or regulation [3]. Additionally, metabolites level reflect the dynamic changes in the genome, transcriptome and proteome so that it is thought to be the chemical representation of phenotype of an organism. Therefore, metabolome, defined as the total complement of all metabolites in a cell, tissue or organism at a given point of time, became the main point of interest in the

systems biology research. The intensive studies on the metabolome of the various living systems have resulted in metabolomics dominance in the postgenomic area.

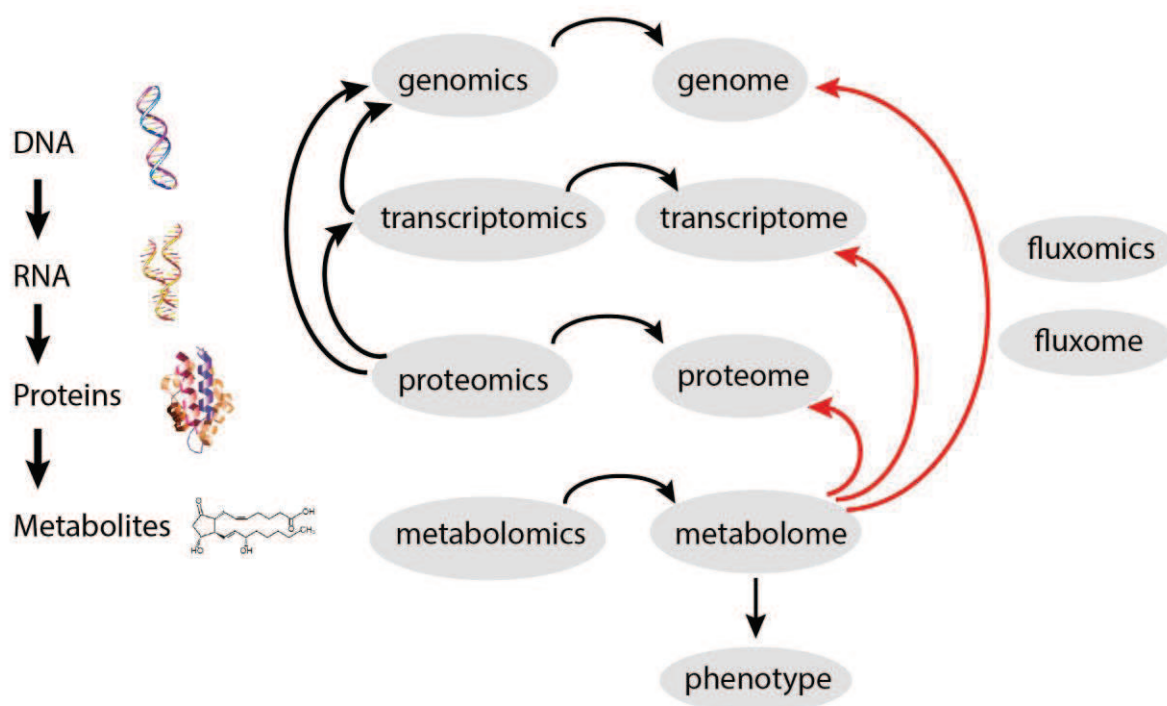


Figure 1. The general flow of biological information in the network –omic cascade.

Although, the beginning of metabolomics is dated back to the 1970s, at least as far as in ancient Greece, the urine colour, smell and taste, that are metabolic in origin, were used to diagnose the diabetes, for instance [4]. Nevertheless, the studies initiated in the 1970s by Horning et al. [5,6] and also by Robinson and Pauling [7] brought new insight into metabolomics research, which was focused not only on single metabolite analysis but also on total state-specific metabolic profile in biological matrices. During the last decades, modern definitions of metabonomics and metabolomics have been introduced. Metabonomics was defined by Nicholson [8], as the quantitative measurement of the dynamic multiparametric metabolic response of living systems to pathophysiological stimuli or genetic modification. Subsequently, Fiehn [9] set metabolomics as a

comprehensive and quantitative analysis of all metabolites in a system. It can be noticed, that the difference between these terms is subtle and rather philosophical than technical. So that, in practice, these definitions are often used interchangeably and employ the same analytical and modeling procedures [4].

Nowadays, metabolomics is becoming the dominant and integral technique in systems biology. As a terminal representation downstream from the genome, transcriptome and proteome, metabolome is considered to be the link of genotype-to-phenotype gap. Additionally, the continuous development in an analytical instrumentation and bioinformatics improves the metabolome measurement and identification. Therefore, the metabolomics is often implicated in clinical, pharmaceutical, toxicological and environmental research.

Summarizing, to understand complex and dynamic response of living systems to various stimuli, such as: pathological process, drug treatment, genetic modification or environmental factors, the integration of networked *-omics* technologies is required.

2.1 Research strategies in metabolomics

The metabolome size is related to species or organisms genus. In case of microorganisms it usually consists of a few hundreds of metabolites (for instance 500 metabolites in *Escherichia coli*) [10]. The metabolome of plants contains around a few thousands of small molecular-weight metabolites. However, metabolome composition of each organism as well as metabolome size have not been fully specified yet. There are few commercially available databases containing information about metabolites presented in human biological matrices. For example, *Human Metabolome Database* (www.hmdb.ca) comprises around 40000 human metabolites, however it has been constantly updated and expanded. Additionally, it should be taken into account that any metabolome size may be overestimated due to the presence of various exogenous metabolites derived from diet, drugs as well as compounds produced by endogenous gut microflora [11]. Therefore, the human metabolome is still of great interest and has been extensively studied.

In existing area of systems biology revolution, metabolomics which aims at identification and quantification of metabolites present in a biological system, has achieved a dominant position.

There are few research strategies that have emerged in the metabolomics experiments such as: metabolic profiling, metabolic fingerprinting and metabolic footprinting [12]:

- a) Metabolic profiling, as a targeted approach, relies on the identification and quantification of a selected group of metabolites characterized by similar physicochemical properties (i.e. carbohydrates, amino acids, organic acids, nucleosides) or belonging to the same biochemical pathway (i.e., glycolysis, gluconeogenesis, β -oxidation or citric acid cycle). In this approach the hypothesis on metabolite profile which is altered due to specific gene mutation, disease progression, drug treatment or diet intervention, is given beforehand. Therefore, analytical techniques applied in sample preparation and determination should provide selectivity for selected metabolites. Metabolic profiling may be termed as the extension of metabolite targeted analysis which refers to precise detection of one or small subset of chosen low-molecular-weight compounds in order to define the effects of the specific stimuli on the metabolism.
- b) Metabolic fingerprinting, as an approach that is not driven by any preliminary assumption, focuses on the whole metabolome determination. There is no previous knowledge on compounds that should be investigated. The fingerprint can be defined as a unique pattern describing the metabolite perturbations under a particular condition. Therefore the main goal of the metabolic fingerprinting is to identify and qualify as many metabolites as possible in biological matrices. Due to the complexity of the biological systems and physicochemical diversity of all compounds present in the metabolome, there is no single analytical platform for metabolic fingerprinting analysis. However, in case of sample treatment procedure, non-selective methods should be used to provide efficient extraction of metabolites, especially from complex matrices. Metabolic fingerprinting is often used in a comparative analysis of two groups (i.e. healthy vs. disease, untreated vs. treated) which makes it a promising tool in disease diagnosis and prognosis as well as in pharmaceutical research.

- c) Metabolic footprinting is a methodology often applied in microbiological or biotechnological studies. This approach, as compared to the previous ones, is not focused on the intracellular metabolites, but rather on compounds secreted or failed to be taken by cells from specific media. Therefore the metabolic footprint is defined as exometabolome. Due to close relationship between intracellular and extracellular metabolism, metabolic footprinting can provide the integrative interpretation of metabolic network of specific living system.

The graphical representation of common research strategies in metabolomics was displayed in Figure 2. To sum up, the choice of a proper approach for successful metabolomics study is strictly related to the nature of the biological questions designed to answer. As a general rule, it can be considered that metabolic profiling is dedicated rather for targeted metabolomic experiment, while metabolic fingerprinting is preferred in untargeted studies. However, the terms: profiling and fingerprinting are often used interchangeably in the literature. Therefore, as the real terms, targeted and untargeted metabolomics, should be considered. Due to the fact that plasma metabolic fingerprinting has been applied in this thesis the further sections of this chapter are limited to this particular metabolomics strategy.

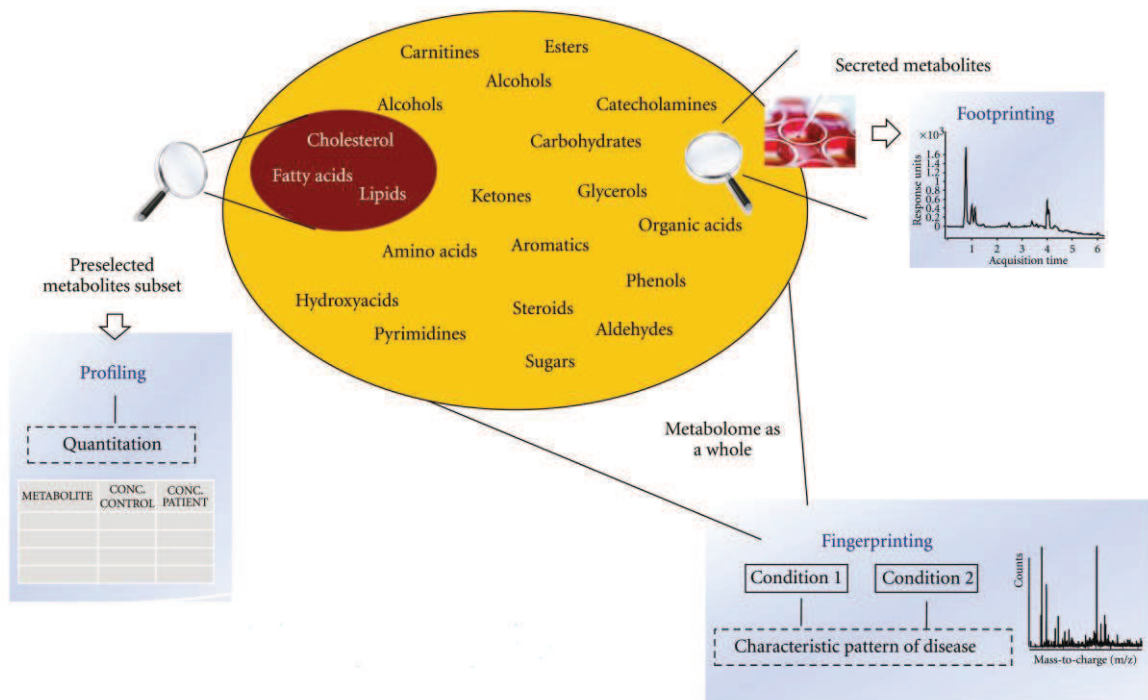


Figure 2. Common research strategies in metabolomics [12].

2.2. Typical workflow in untargeted metabolic fingerprinting

Untargeted metabolic fingerprinting is rather hypothesis generating than hypothesis-driven investigation. Thus the careful arrangement of the whole experiment is mandatory in order to maximize the number of metabolites detected, as well as to provide reliable final results. Crucial steps comprise study design followed by sample collection; metabolite extraction; sample analysis; data acquisition, processing and analysis; finally the identification of metabolites which leads to biochemical interpretation [13]. Recent development in analytical instrumentation mainly sensitivity, acquisition speed, resolution and accuracy, as well as complexity of the biological systems investigated during untargeted metabolic fingerprinting lead to generation of multidimensional data matrices obtained after automated processing step. Therefore, the use of advanced bioinformatic and computational tools is required to extract biologically relevant information from complex data sets. To select metabolite changes that may be correlated to the specific biological question, multivariate

statistical methods must be applied to provide holistic view of the system under study [13]. Finally, selected metabolites identification and biochemical pathways analysis provide the understanding of biological processes that determine metabolic signature of specific phenotype. The typical workflow in the untargeted metabolomics was shown in Figure 3.

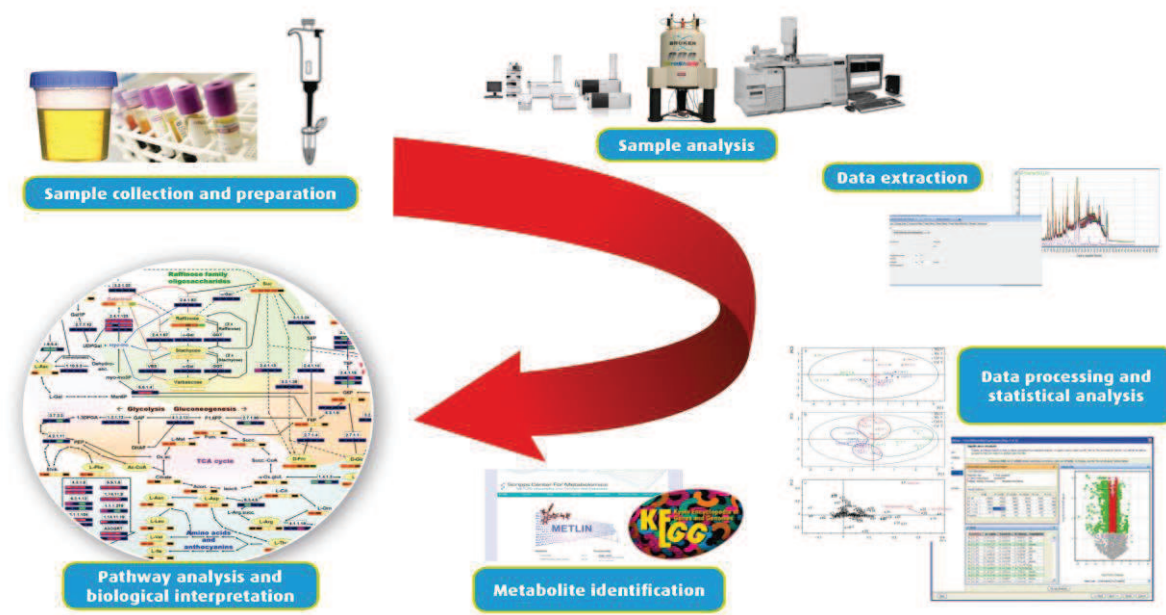


Figure 3. Scheme of the typical workflow in untargeted metabolic fingerprinting approach.

2.2.1. Study design and metabolite extraction

The biological, pre-analytical and analytical variation can affect each metabolomic experiment. In comparison to animal studies in which experimental conditions or sample handling are usually easy to standardize, clinical experiments based on human population are more exposed to variation introduced by biological or process factors. Thus, the careful planning of the study constitutes a critical step in metabolic fingerprinting experiment to ensure robust and reliable biological conclusions. First of all, when two study groups (case vs.

case or case *vs.* control) are to be investigated, it is crucial to match them by age, gender or body mass index (BMI), to avoid significant differences that are not related to the biological aim of the study. These factors have been reported to have a huge influence on global metabolic fingerprints [14]. Additionally, in large-scale metabolomics studies concerning human population, samples are often collected at multiple research institutions either from one or different countries. Therefore, the standard operating procedure (SOP) is mandatory during the sample collection and processing steps. Especially, collection tubes, time of sampling, time on ice before freezing, temperature and time of storage, the number of thaw-freeze cycles and condition of sample transport, should be standardized due to possible introduction of undesirable bias [15]. These factors mainly affect blood plasma or serum which are composed of enzymes that can be active after sample collection, and subsequently are able to change the metabolic composition of the biological matrix [16]. Another factor is collection time, as the diurnal variation has a huge impact also on urine metabolic fingerprints [17]. To sum up, the careful study design and standardized sample collection are critical points during human-based untargeted metabolomics studies and provide robust and biologically significant results, mainly of clinical investigations.

The next step in metabolic fingerprinting experiment is metabolite extraction from obtained matrices before sample analysis. Since, the untargeted metabolomics approach aims to determine as many metabolites as possible in biological samples, the sample preparation should provide their efficient extraction and minimize metabolites losses. Therefore, in metabolic fingerprinting study the choice of proper sample treatment procedure will strictly depend on the type of biological matrix and analytical platform that is going to be used in the sample analysis. The blood (both plasma or serum), urine, saliva, cerebrospinal fluid (CSF) or various tissue extracts are examples of biological samples, which are the most commonly used in untargeted metabolomics to define the metabolic signature in particular state, such as: disease progression, pharmacotherapy, genetic modification or environmental stress. However, due to almost noninvasive sampling and reflection of global metabolic response to different stimuli, the blood and urine samples dominate in metabolic fingerprinting approach.

Due to small amount of high molecular mass compounds (i.e., lipoproteins) in urine, the sample treatment is much simpler as compared to blood or tissues. Firstly, the

centrifugation is performed to remove solid particles and subsequently the dilution with water (from 1:1 to 1:3 v/v, depending on urine origin) is adopted. As an alternative technique to remove urinary proteins and solid particles, the use of molecular weight cut-off filters was proposed [18], however the higher sample contamination risk should be considered during this approach. In case of urine fingerprinting by liquid chromatography coupled with mass spectrometry with the use of electrospray ionization mode (LC-ESI-MS) the direct injection technique was reported [19]. Although this approach provides rapid metabolic fingerprinting and minimizes the metabolites' losses, it can result in ion suppression, ion source contamination or column back-pressure [19].

Blood plasma or serum, due to high proteins concentration and enzymatic activity, require more complex sample preparation for LC-MS based metabolic fingerprinting, as compared to urine samples. Thus, the first step involves sample deproteinization with the use of organic solvents (1:3 v/v ratio and low temperature are recommended). Then, the centrifugation is performed followed by supernatant filtration before sample analysis. Such approach, mainly provides the hydrophobic compounds extraction. Therefore, the new methodology, called in-vial dual extraction (IVDE) was introduced in the area of plasma metabolic fingerprinting research [20]. IVDE approach is a one-step extraction method, that allows to obtain two separated layers: lipophilic and hydrophilic ones, in one vial which provides the wide metabolite coverage from a single plasma aliquot.

Using nuclear magnetic resonance (NMR) spectroscopy to urine or blood metabolic fingerprinting, the sample preparation step is often omitted or reduced to sample dilution as well as phosphate buffer, deuterated water, saline or deionized water addition [21]. Moreover, NMR possesses benefits by means of its non-destructiveness and therefore samples may be subjected for the analysis together with the use of other analytical platform. While gas chromatography coupled with mass spectrometry (GC-MS) is chosen to global metabolic fingerprinting of both urine or blood samples, metabolite extraction requires complicated and time-consuming procedures. Due to the fact, that many interesting groups of compounds present in metabolome, as sugars, amino acids, nucleosides are characterized by high polarity and lack of volatility, the chemical derivatization is essential before GC-MS analysis. Due to the wide diversity of metabolites, two-stage derivatization is the most commonly employed

procedure [22]. After sample deproteinization, the extract is dried up and then dissolved in pyridine and subsequently reacts with methoxyamine hydrochloride and *N*-methyl-*N*-(trimethylsilyl)-trifluoroacetamide (MSTFA). The first methoximation step provides the carbonyl groups conversion to oximes. During the second stage, the trimethylsilyl (TMS) esters are formed to replace exchangeable protons in the molecules. In case of urine sample, an additional step, providing urea depletion via treatment with urease, is required to avoid urea interference with other important metabolites [23]. Unfortunately, the chemical derivatization, even though is mandatory before GC-MS analysis, has a huge potential to introduce pre-analytical variation as well as metabolites losses during the sample preparation step.

2.2.2 Analytical platforms in sample analysis

Due to physicochemical diversity of the metabolome as well as complexity of the living systems, there is no single analytical platform to cover all metabolites in biological matrices and for that reason the numerous analytical techniques are applied in metabolic fingerprinting approach [24]. However, NMR and mass spectrometry (MS) coupled with various separation techniques have become emerging and comprehensive platforms in untargeted metabolomics. The main advantages and drawbacks of MS in comparison with NMR technique in the context of untargeted metabolomics were summarized in Table 1.

Table 1. The main advantages and drawbacks of MS and NMR application in metabolomics studies [25].

	MS	NMR
Quantitation	Low	High
Reproducibility	Low	High
Sensitivity	High	Low
Detection range	Wider Coupled with chromatographic separation (i.e., LC,GC or CE)	Narrower Biased toward higher abundant metabolites Overlapping signals are not easily resolved
Sample volume requirement	200-400 μ l	Few μ l
Sample recovery	Destructive	Non-destructive
Tissue analysis	Yes, after extraction	Yes Application of magic angle spinning (MAS) NMR
Metabolite identification facility	Complicated Uncompleted databases provide only putative identification Confirmation by tandem MS required	Easier Databases availability 1D and 2D spectrum analysis

NMR determines the magnetic resonance of nuclei in molecules and it is dedicated practically to all compounds containing hydrogen atoms. MS aims to measure ionized molecules based on their mass-to-charge (m/z) ratio. NMR technology has been considered to be a pioneering platform in metabolomics and was successfully applied in toxicological and pharmaceutical studies [26,27] as well as MAS NMR approach was dedicated to the determination of solid-state matrices such as tissues or intact cells [28]. While NMR is an unbiased, robust, reproducible, non-destructive and non-selective technique with almost no sample treatment requirement it suffers from low sensitivity and lack of separation component. Therefore, MS hyphenated with an initial separation method has been the most frequently used platform in untargeted metabolic fingerprinting. Among these approaches, LC-MS, GC-MS or capillary electrophoresis coupled with mass spectrometry (CE-MS) have emerged in the area of metabolome analysis.

The widespread availability and continuous development of instrumentation have resulted in extensive LC-MS applications in metabolic fingerprinting. LC-MS is a suitable technique in non-volatile, thermally unstable, high- or low-molecular-weight compounds that are characterized by wide range of polarity. Thus, it is a preferable platform for biofluids (either urine or blood) determination and does not require derivatization step, which makes the sample pretreatment more simple in comparison to GC-MS technique. The selectivity of LC system strictly depends on the chemical characterization of the chromatographic column. Generally, in metabolic fingerprinting with the use of LC-MS, metabolites' separation might be provided with the use of reversed-phase (RP) columns and electrospray ionization (ESI) both in positive and negative mode to obtain metabolome coverage in biological matrices. Since, the gradient RP separations are intended for medium or low polar compounds, they do not provide proper retention of water-soluble metabolites belonging to the class of amino acids or sugars. To overcome this limitation, the newly designed columns such as: hydrophilic interaction liquid chromatography (HILIC) [29] or weak-ion exchange column (i.e., Waters Atlantis metabonomics column) have been developed. Additionally, the LC column dimensions (i.e., 4.6 mm x 150 mm) or particle sizes (i.e., 5 μm) will affect the sensitivity and separation power. To avoid this problem and improve chromatographic resolution, ultra high-performance liquid chromatography (UHPLC) with the use of 2.1 mm i.d. column packed with 2 μm particles, was successfully applied in metabolomics study of urine samples from different rodents (rat and mouse) [30]. There is one initial development of LC-NMR-MS which combines high-throughput of NMR with the high sensitivity and resolution of LC-MS [31].

GC employing high-resolution capillary column and combined with MS detection, is a powerful platform for the global metabolic fingerprinting analysis. However, it is strictly dedicated for volatile and thermally stable compounds, therefore the complicated sample derivatization step is necessary, which can result in undesirable metabolites' losses. When GC-MS is applied in untargeted metabolomic experiment, the electron impact (EI) or chemical ionization (CI) are commonly used, which provide putative identification of metabolites and the high availability of numerous structural and mass spectral libraries. Recent development of multidimensional GC, defined as GCxGC, improved the resolution, robustness and sensitivity as compared to GC in one dimension mode. In this technology, the first longer column

(typically 30 m) separates analytes based on their volatility, whereas the second and shorter column (typically 1.5 m) separates the investigated compounds based on their polarity. Thus, after elution from the first column, analytes are trapped, cryogenically focused and subsequently separated [21]. Multidimensional GC-MS approach was used in global metabolic profiling to analyze the spleen extracts from obese and lean mice [32].

CE-MS technique, in comparison to LC-MS or GC-MS methodologies, has been relatively rarely used approach in untargeted metabolomics. In relation to metabolic fingerprinting, it is a technique suitable for polar and charged compounds as those present in urine samples or culture media, which requires minimal sample preparation before proper analysis. However, extensive research is being conducted concerning CE-MS application in global metabolite profiling of serum samples [33]. CE-MS has been a technique of choice for water-soluble and charged molecules, which provides highly complementary alternative to other separation methods as LC or GC. The main strengths of this analytical platform, including high resolution power, small amounts of sample or reagents requirements which ensures inexpensive analyses, confirm the potential interest of its application in untargeted metabolomics research. The main drawback of CE-MS platform is an unstable electroosmotic flow resulting in notable migration time shift during single run analysis [34]. For comparative purposes, the main strengths and limitations of LC-MS, GC-MS and CE-MS were collected in Table 2.

Other analytical methodologies, used in metabolomics studies include direct mass spectrometry infusion (DIMS) or Fourier-transform infrared (FT-IR) spectroscopy. DIMS technique is a high-throughput tool since typically one minute analysis time is applied, which allows to determine hundreds of samples during one day. This approach was successfully used in metabolomics studies of plant or microbial experiments [35]. However, DIMS technique is not fully suitable for complex biological samples such as urine or blood, due to matrix effects, which has a negative influence on ionization efficiency and subsequently on the analysis result. FT-IR spectroscopy enables rapid, nondestructive, reagentless and high-throughput determination of various types of samples, although with many limitations such as sensitivity, resolution and identification capability [36].

As a final conclusion, it should be underlined that multiplatform-based metabolome analysis is needed to reveal all biochemical perturbations which define the metabolic picture of biological phenotype. Thus, the continuous improvements both in resolution of separation methods and sensitivity of the MS detection, can be observed.

Table 2. The summary of advantages and limitations of the most commonly used analytical platforms in untargeted metabolomics [35].

Analytical technique	Advantages	Limitations
LC-MS	<ul style="list-style-type: none"> - high sensitivity and resolution - wide detection range due to chemical diversity of the available columns - coupled with time of flight analyzer provides high accuracy of mass determination - no derivatization required - shorter analysis time, lower reagents consumption and higher separation power in case of UHPLC 	<ul style="list-style-type: none"> - due to possible ion suppression the analytes separation is required for reliable determination and identification - matrix effect - lack of databases containing universal spectral libraries for automated compound identification - analysis depending on the mass analyzer - some restrictions on LC eluents
GC-MS	<ul style="list-style-type: none"> - high sensitivity and resolution - high reproducibility - easier compound identification due to numerous spectral libraries availability - coupled with time of flight analyzer provides high accuracy of compounds determination 	<ul style="list-style-type: none"> - the application limited to volatile and low-molecular-weight compounds - the extensive sample derivatization requirement - possible compounds losses in sample pretreatment step - cost of analysis depending on the mass analyzer
CE-MS	<ul style="list-style-type: none"> - higher resolution power comparing to LC-MS or GC-MS - low sample amount - low reagents consumption - low analysis cost 	<ul style="list-style-type: none"> - lower sensitivity as compared to LC-MS or GC-MS - lower reproducibility than in GC-MS or LC-MS - lack of databases containing universal spectral libraries for automated compound identification

2.2.3 Raw data extraction and preprocessing

Due to the high sensitivity of the analytical platforms currently used to measure metabolome and the diversity of the living systems under investigation, thousands of potential metabolites can be detected in a single biological sample. The accurate number of low-molecular-weight molecules closely depends on the selectivity and resolution of the separation technique as well as sensitivity of MS detectors. Moreover, the application of high throughput methodologies results in the increased quantity of data but mainly influences its properties. The consequences of these facts include [37]:

- a) notably high number of measured features relative to small number of observation used in the metabolomics study,
- b) large noise contribution,
- c) analytical bias variation,
- d) many possible missing values,
- e) analytical response drift.

The common feature of MS-based metabolomic raw data is its three-dimensional structure in which each detected point is characterized by m/z ratio, retention time (RT) and abundance. Additionally, ions with different m/z can have the same RT value, so the coelution is a common issue in MS-based technologies. To overcome this difficulties, some softwares for untargeted metabolomic data preprocessing, for instance MetAlign (www.metalign.wur.nl), MZmine (mzmine.sourceforge.net) and XCMS (metlin.scripps.edu/download) [38] have been designed recently to provide automated extraction of relevant information from thousands data points detected in a single biological sample. These free available tools, in case of LC-ESI-MS raw data, provide the background cutting off and single component extraction based on its accurate mass, RT, charge state, isotopic distribution, possible adducts during ionization process (H^+ , H^- , Na^+ , K^+ , $HCOO^-$ or neutral water loss). Some MS instrumentation manufacturers, such as Agilent Technologies deliver tools, mainly MassHunter Qualitative Analysis Software including algorithm called Molecular Feature Extraction (MFE), which is useful in untargeted metabolomic data preprocessing. However, the Automated Mass Spectral Deconvolution and Identification

System (AMDIS), is a dominant software for raw data extraction obtained in GC-MS-based metabolic fingerprinting experiment [39].

After data deconvolution, the alignment, normalization and scaling steps are recommended in untargeted metabolomics to provide proper data treatment before statistical analysis. Due to analytical variation during the samples analysis, the RT shift often occurs in MS-based analytical platforms, therefore the alignment is needed to ensure that the same molecular feature (ideally, metabolite) is marked as the same entity across all analyzed samples. Some multialignment tools such as Time Correlation Optimized Warping (COW), Parametric Time Warping or Dynamic Time Warping (DTW) have been developed [40,41]. While MS-based untargeted metabolomics study is being performed, an undesirable systematic bias derived from variation in sample concentration (i.e. urine, blood, saliva) often occurs. Additionally, measurement errors related matrix effects, especially ion suppression, can be another source of variability in signal intensities. To minimize problems derived from either biological or analytical variation the normalization is highly recommended. Depending on the matrix type under metabolic fingerprinting study there are various normalization strategies including internal standards (IS) addition, MS total signal (MSTS), MS total useful signal (MSTUS), MS group useful signal (MSGUS), median fold change normalization (MFC) and urine volume (UVol) or creatinine concentration dedicated for urine samples [42,43]. Data scaling aims to adjust weight of each potential metabolite with the scaling factor derived either from data dispersion (i.e. standard deviation) or size measurement (i.e. mean). The unit variance scaling (UV-scaling), also termed as autoscaling, and Pareto scaling belong to the most common scaling types applied in metabolomics studies [44]. The comparison of various scaling techniques was summarized in Table 3.

Table 3. The comparison of various scaling techniques [44].

Method	Scaling factor	Goal	Advantages	Disadvantages
Autoscaling	standard deviation	compare metabolites based on correlations	all metabolites become equally important	inflation of the measurement errors
Range scaling	biological range	compare metabolites relative to the biological response range	all metabolites become equally important.	inflation of the measurement errors and sensitive to outliers
Pareto scaling	square root of standard deviation	reduce the relative importance of large values	stays closer to the original measurement than autoscaling	sensitive to large fold changes
Vast scaling	coefficient of variation	focus on the metabolites that show small fluctuations	aims for robustness, can use prior group knowledge	not suited for large induced variation without group structure
Level scaling	mean	focus on relative response	suited for identification of e.g. biomarkers	inflation of the measurement errors

2.2.4 Multivariate data analysis

In untargeted metabolic fingerprinting experiment numerous both known or unknown metabolites are detected and need to be considered simultaneously, to provide holistic view of the biological system under study. Therefore, the univariate statistical methods are insufficient for this purpose and the multivariate chemometric approaches should be applied to reveal the correlation structure between selected metabolites. The leading multivariate techniques used in untargeted metabolomics are principal component analysis (PCA) and partial least squares regression (PLS) including derivative approaches such as partial least squares discriminant analysis (PLS-DA) or orthogonal PLS (OPLS).

PCA belongs to unsupervised methods (no class knowledge considered), which aims to explain variance existing in the data set by smaller number of newly constructed principal components (PCs) [45]. In metabolomics, the PCs represent the metabolites contribution into

variance of the obtained data set. Therefore, each PC is a linear combination of original variables and explains as much variance in the original data as possible without loss of significant information. In general, PCA method transforms original data into low dimensional model plane. PCA model can be displayed as either score plot or loading plot. The position of each sample in the score plot determines its similarity or dissimilarity in comparison to the rest of the objects. In turn, a loading plot, represents the relation among all used metabolites and determines their influence on the specific PC. PCA provides dimensionality reduction, data visualization, clustering and sample classification. Therefore is often used as a first exploratory technique in data analysis, especially in a hypothesis-free untargeted metabolomics.

PLS regression method, as a supervised technique, aims to reveal inherent patterns as distinct metabolite profiles that are strictly related to the predefined biological response. For instance, PLS-DA relates the data matrix (i.e. multivariate metabolite data) to the response vector (sample class label, like case-control) based on latent variables (LV) construction [46]. PLS-DA is usually used for discrimination purposes or even to predict class membership of undefined samples based on a training set of known class distributions. OPLS technique, as an extension of PLS, has also been developed [47]. A main drawback of supervised methods is the susceptibility to overfitting, which can be defined as excessive learning on a training dataset, which may confirm the noise included during the statistical model construction [48]. So far, some validation techniques like cross validation [49] or bootstrapping [50] have been proposed to overcome model overfitting of multivariate statistical model. It has to be noticed, that there are many other multivariate statistical techniques, both unsupervised and supervised, such as cluster analysis (CA), hierarchical cluster analysis (HCA), support vector machine (SVM) or k-nearest neighbors algorithm (k-NN), that can be successfully applied in metabolomics research [51].

2.2.5 Metabolite identification and biochemical interpretation

In untargeted metabolic fingerprinting, the metabolite identification is the most time-consuming step, especially in case of LC-MS based study. Significant compounds selected in multivariate analysis, are described only by monoisotopic mass value. To define the identity of potential metabolites of interest, their accurate masses are firstly searched in free available databases such as: METLIN (www.metlin.scripps.edu), KEGG (www.genome.jp/kegg), LIPIDMAPS (www.lipidmaps.org/), HMDB (www.hmdb.ca) and all simultaneously accessed by recently developed search engine, CEU MassMediator (<http://ceumass.eps.uspceu.es/mediator>). However, the match found in databases ensures only the putative identification and needs to be confirmed by tandem MS/MS analysis. The most reliable metabolite identification is provided by standard determination by tandem MS/MS platform. Then comparison of fragmentation pattern of both standard and metabolite candidate can confirm compound identity. Unfortunately, there are no available standards for many metabolites included in human metabolome. Moreover, although metabolite databases are still extensively developed and expanded, numerous metabolite features originated from biological samples do not have any matches. In comparison to LC-MS, metabolite identification detected in GC-MS based metabolic fingerprinting experiment is much easier. The application of high reproducible EI ionization mode results in universal mass spectral libraries availability, for instance NIST/EPA/NIH (www.nist.gov/srd/nist1.htm).

The final step in untargeted metabolomics approach focuses on biochemical interpretation. The identified metabolites are located in biochemical pathways which are characteristic for certain organism under the investigation. Moreover, the crucial task is to find connections between biochemical pathways involved in biological response induced by various stimuli such as disease process, treatment intervention or gene modification. There are few free available databases useful for biochemical pathways analysis, for instance KEGG or ExPASy (www.expasy.org).

3. Mass spectrometry based metabolomics

MS is an emerging analytical platform in metabolomics research. Among numerous advantages, the high sensitivity should be underlined. Additionally, its combination with various separation techniques (mainly chromatographic or electromigration) minimizes the complexity of mass spectra due to the fact, that potential metabolites are separated firstly in time dimension which also delivers complementary information about physico-chemical features of compounds.

Therefore, the MS technology is the most promising tool for untargeted metabolic fingerprinting approach. Although, numerous technical improvements have continuously been designed to enhance the MS sensitivity. There are few principal parts in mass spectrometer construction, including sample inlet, ion source, mass analyzer, detector and computer (Figure 4).

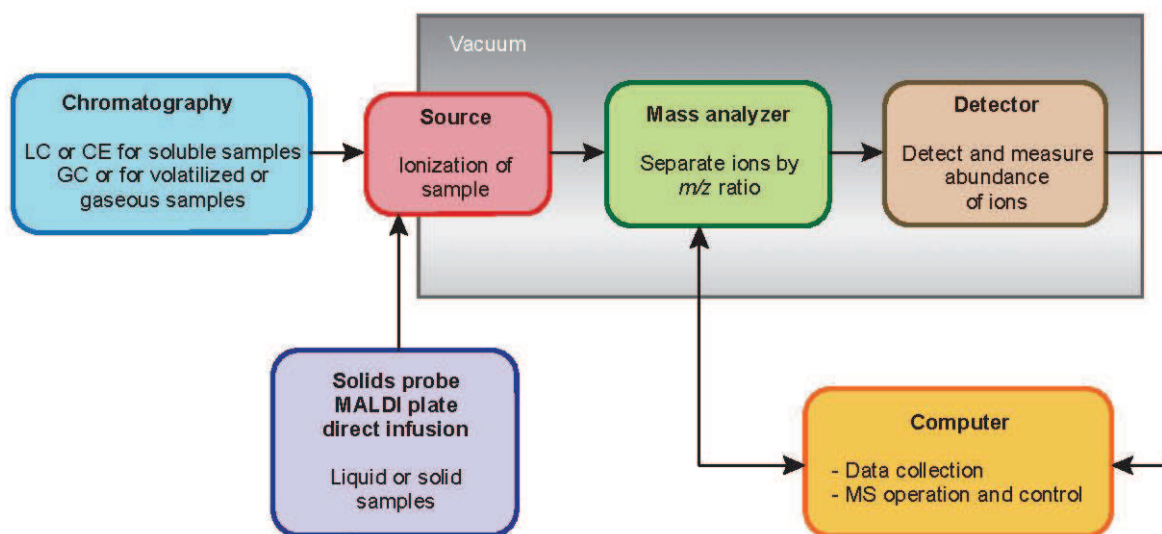


Figure 4. Typical mass spectrometer construction.

3.1 Ionization modes

Prior to MS analysis, samples must be ionized. There are numerous and various ionization techniques applied in MS-based experiments.

a) Electron ionization

Electron ionization (also termed as electron impact- EI) is mainly dedicated for relatively volatile, thermally stable and low-molecular-weight molecules. Thus, EI is a suitable ionization mode for GC-MS platform. In this case, a sample usually an effluent from GC part, is introduced into high vacuum source. Then, analytes present in gas-phase are exposed to high-energy electrons stream (usually 70 eV). As a result, single and positively charged ions occur. However, the energy excess remaining after ionization process results in fragmentation phenomenon. Thus, EI belongs to the “hard” ionization techniques. The high reproducibility of both ionization and fragmentation processes allows to create commercially available mass spectral libraries, containing hundred thousand spectra, which can be useful for both known and unknown metabolites identification.

b) Chemical ionization (CI)

Similarly to EI, chemical ionization (CI) is mostly applied in combination with GC-MS technique. In contrast to EI, CI is classified to “soft” ionization modes and was developed to reduce fragmentation process during ionization. In CI mode, sample is entered to a chamber with reagent gas, mainly methane, isobutene or ammonia (at pressure 0.3-1.0 torr). Firstly, the reagent gas is ionized by electrons beam to produce reagent ions. Then the analytes present in sample react with ionized gas reagent and both positive and negative analytes’ ions can be produced. For negative ionization mode, usually the mixture of CH₄ and NO₂ is used.

c) Electrospray ionization (ESI)

Electrospray ionization (ESI) is the most commonly applied mode in metabolomics research, especially in untargeted metabolic fingerprinting. Electrospray is performed under atmospheric pressure and so that the ionization is possible without previous sample evaporation. Thus, possible ionization of a sample in liquid state simplifies the MS combination with chromatographic or electromigration techniques. Electrospray process relies on formation and subsequent evaporation of ionized liquid droplets [52]. First, samples are introduced into the ion source directly by the syringe, but most often with mobile phase from LC part. The liquid sample is transferred via the metal nebulization capillary (held at high voltage 1-3 kV) and sprayed at atmospheric pressure by nebulizing gas (often nitrogen) in ionization chamber to form charged droplets. These droplets are constantly evaporated by drying gas and are subjected to decrease in size, which causes the increasing charge concentration in droplets. This process is continued till the charge repulsion overcomes surface tension, termed as “Rayleigh” limit and as a consequence the coulombic explosion occurs. This phenomenon is repeated several times until the produced ions are desorbed into the gas phase. Finally, the ions are transported into the heated capillary, which is an inlet of mass spectrometer. The ESI mechanism is shown in Figure 5 [53].

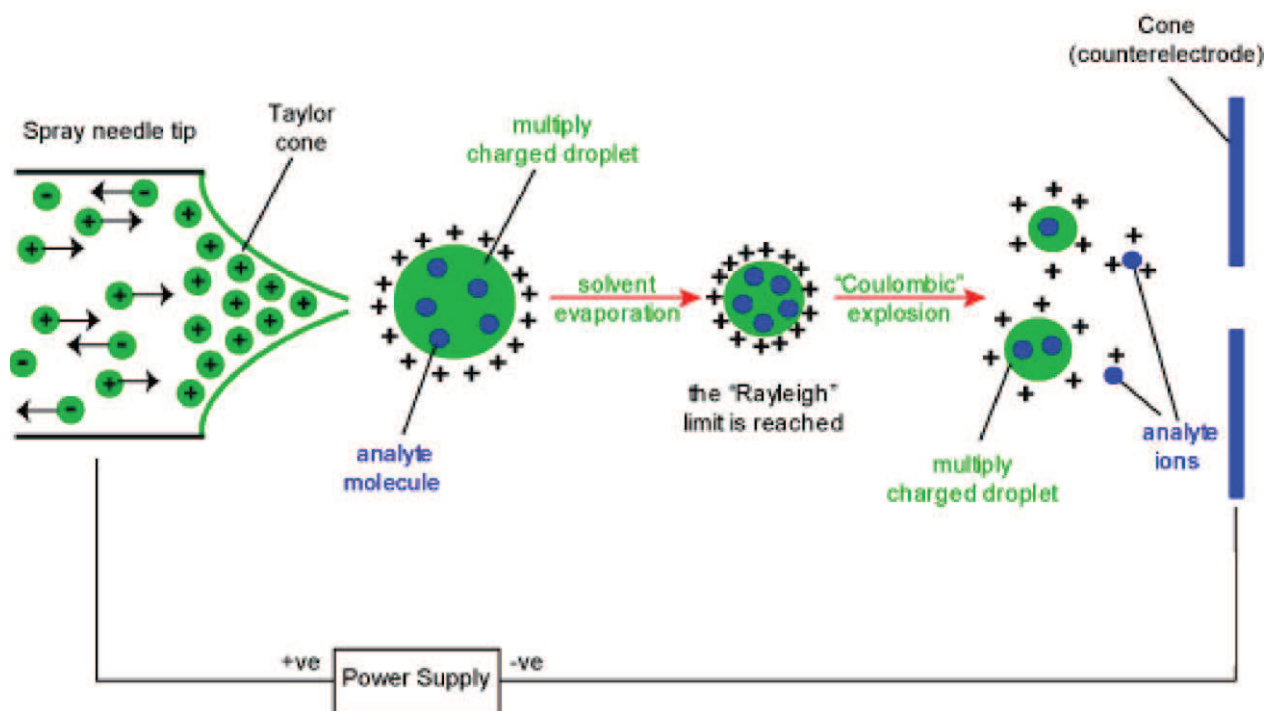


Figure 5. The electrospray ionization mechanism [53].

The ions' transfer is provided by difference in potential between capillary, which introduces liquid sample with zero potential, and heated inlet capillary, which possesses negative (in positive ionization mode) or positive potential (in negative ionization mode). Moreover, the inlet capillary is the component, which separates two parts under different pressure conditions. The atmospheric pressure exists in the ion source, however inside the mass spectrometer the high vacuum is applied. Therefore, both pressure and voltage differences lead to the ions transfer into the inlet capillary, followed by their acceleration and entrance to mass analyzer.

ESI is a soft ionization technique and is dedicated to non-volatile, polar and large molecular size compounds. The multicharging phenomenon that can appear during the ionization process allows to detect large molecules, because finally their m/z ratios are measured by mass analyzer. In practical point of view, when LC-ESI-MS is performed, the critical point is choice of proper eluents for chromatographic purposes. They should be characterized by low boiling-point as well as low surface tension. The addition of weak acid (for positive mode) or weak base (for negative mode) into the mobile phase is

recommended. Additionally, it is necessary to avoid solid and non-volatile substances (i.e. phosphate buffers) in eluents used during LC separation, due to possible ion suppression which in consequence can lead to insufficient ionization. To provide reliable ESI performance, all ion source parameters (nebulizing and drying gas flow and temperature) should be optimized. They will be strictly dependent on LC eluent flow rate and composition. Therefore, in LC-ESI-MS, the mobile phase flow rate (in relation to the column dimensions) is up to 1.0 ml/min. However, recently, the modification of classical ESI mode, termed as nanoelectrospray (nano-ESI), was designed [54]. In this approach, the sample is introduced into the ion source with much lower flow rate (below 1 μ l/min) though capillary dimension is 20 μ m. These improvements provide more efficient ionization process and reduce ion suppression problem.

d) Atmospheric pressure chemical ionization (APCI)

Although atmospheric pressure chemical ionization (APCI), from a technical point of view is very similar to ESI, the principle is different. Unlike ESI, no voltage is applied to the capillary, instead the heater for either analytes or eluent evaporation is employed. The liquid sample is introduced into the source at atmospheric pressure through heated nebulizer. Then corona discharge ionizes the solvent molecules similarly to CI manner and numerous reagent ions are produced. Ion-molecule interaction provides the ionization of compounds present in analyzed sample. Unlike ESI, in APCI process, ions are generated from neutral molecules which make this technique suitable for small (up to 1000 Da) analytes with low to medium polarity range. In comparison to ESI, APCI can deal with higher LC eluent flow rates, normally up to 2 ml/min.

e) Matrix-assisted laser desorption ionization (MALDI)

Matrix-assisted laser desorption ionization (MALDI) is capable to ionize large molecules from samples in solid state. In general, the sample is cocrystallized with a matrix on a stainless-steel plate. Next, the dried sample is illuminated with a pulse of laser light which is absorbed by the chromophore moieties from the analytes included in the matrix. Then,

the photon energy is transferred to the analyte, which provides its ionization and desorption from the matrix. Only single charged ions are generated. MALDI represents soft ionization technique and typically little fragmentation can appear. The parameters that should be considered during MALDI performance include proper matrix type, analyte:matrix ratio (as a starting point 1:10⁴ is often used) and power of the laser fluence.

3.2 Mass analyzers

Molecule ions, generated in various ionization modes, are transferred into the mass analyzer in which they are separated based on m/z ratio. There are numerous mass analyzers which employ magnetic or electric field as well as time of flight, to achieve reliable resolution of ions and their further detection. The main parameters of the mass analyzer include upper mass limit, transmission and resolution. The upper limit is defined as the highest m/z value that can be measured. The transmission determines the number of ions recorded by the detector in comparison to the number of ions generated in source. Finally, the resolution is the ability to separate signals from two ions with a similar m/z ratio. So far, among various types of mass analyzers, quadrupole (Q) analyzer, time of flight (TOF) analyzer, ion trap (IT) analyzer, ion mobility spectrometer (IMS) or Fourier transform ion cyclotron resonance (FT-ICR) have been used. However, in metabolomics research the Q and TOF are emerging and the most powerful mass analyzers.

The Q analyzer works in an oscillating field produced between four parallel rods of circular or hyperbolic cross section. The opposite rods make pairs that are characterized by the same potential value but with opposite polarity. Therefore, one rod pair is a specific filter for ions with high m/z ratio, whereas other for ions with low m/z ratio. The ion beam passes through the central axis of the rods in oscillating field. The ion mass and charge are the only factors that determine the ion trajectories. Only ions with narrow m/z ratio will be capable to cross, whereas others will undergo the unstable oscillation and will be rejected. The Q analyzer can operate in two modes, both, in scan mode when the narrow m/z ratio range will be measured and in SIM (single ion monitoring) mode which provide monitoring of only selected m/z ratio value. The advantages of the Q analyzer application are as follows: fast scan

of the ion beam, ability to monitor selected ion and possibility to use in tandem MS approach. However, the main drawback of this mass analyzer is its low resolving power.

In turn, TOF analyzer is characterized by much higher resolution relative to Q analyzer. In TOF analyzer, ions of the similar kinetic energy E_k but different m/z ratios need different time periods to pass a fixed distance. Therefore, lighter ions reach the detector faster than the heavier ones. There are different work modes in which TOF analyzer operates. In the first one, linear mode, the analyzer and detector are located in the same line. Due to the fact that ions of the same m/z value (isobaric ions) need to reach the detector simultaneously, the TOF analyzer in linear mode possesses high sensitivity but low resolution. The second work mode with the use of reflectron was developed to overcome this limitation. This is an electric field that initially slows the ions, and then accelerates or reflects them back out toward the detector. This results in a decrease of the difference between time of flight values for the same m/z ratios, therefore these ions reach the detector at the same time. As a consequence of reflectron application, increased resolution is observed (more than 10^4).

Recently, the Q and TOF analyzers have been combined in one instrumentation (Q-TOF) [55] which is useful in the context of metabolomics studies. In untargeted metabolic fingerprinting the Q-TOF application provides both qualitative detection of all compounds present in biological sample by TOF and the fragmentation pattern analysis of selected m/z ratios by Q analyzer. This helps in either known or unknown metabolites identification. In targeted metabolomics, mainly Q analyzer is employed for quantitative metabolite analysis.

3.3 Tandem mass spectrometry

Tandem mass spectrometry (MS/MS or MS^n), as a fragmentation technique, is important for metabolite analysis and facilitates the comparison of experimental fragmentation patterns with available standards or mass spectral databases to confirm structural identity of potential metabolites. Information on fragmentation can be derived from numerous and various combinations of mass analyzers, which provides the isolation and fragmentation of target ions and enables subsequent detection of the resulting fragments. The most commonly

applied tandem mass spectrometers include Q-TOF and triple quadrupole (QqQ). Q-TOF instruments possess high resolution, mass accuracy and scan rate as well as ensure both MS profiling and tandem MS/MS analysis during a single experiment. In this case, the first quadrupole isolates target ions, which are then fragmented in a collision cell and finally measured by a TOF mass analyzer.

The QqQ workflow contains three basic steps. First, the precursor ion is filtered in the first mass analyzer, then the precursor ion is fragmented in collision cell to generate fragment ions, which are filtered and measured in the third mass analyzer. The most commonly used fragmentation mode is so called tandem-in-space, which employs two analyzers separated by collision cell. First mass analyzer (Q1) acts as the mass filter and isolates the precursor ion with specific m/z value. Then precursor ion reaches to the collision cell (q2) where the collision with inert gas (helium, nitrogen or argon) occurs and fragment ions are generated. Finally, the fragment ions get to the second mass analyzer (Q3) where separation according to m/z value and fragmentation of spectra are recorded. The schematic construction of QqQ analyzer was shown in Figure 6 [56]. The QqQ analyzer provides high sensitivity often at the femtomol level. Additionally, in combination with TOF analyzer the high resolution and mass accuracy can be achieved. Q-TOF analyzer coupled with chromatographic or electrophoretic techniques are extensively used in untargeted metabolomics research.

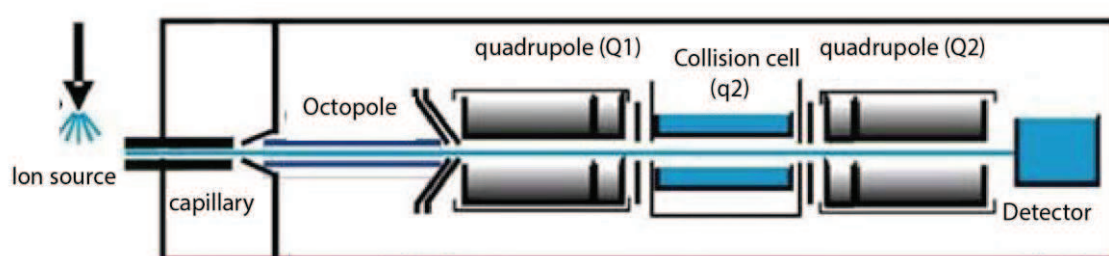


Figure 6. The schematic construction of QqQ mass analyzer [56].

4. Pulmonary arterial hypertension

4.1 Clinical definitions and epidemiology

Pulmonary arterial hypertension (PAH), as a subgroup of pulmonary hypertension (PH), has been defined as an average pulmonary arterial pressure (mPAP) above 25 mmHg at rest state by right heart catheterization (RHC) assessment [57]. Previous definition included also the exercise criterion (mPAP >30 mmHg as assessed by RHC). However, due to the fact that healthy individuals can develop much higher levels and no published data has supported this observation, the exercise criterion is no longer used in the clinical practice. PH is a haemodynamic, and pathophysiological condition, therefore various parameters such as pulmonary wedge pressure (PWP), pulmonary vascular resistance (PVR), and cardiac output (CO) are used in haemodynamic definitions (Table 4). There are numerous risk factors that can lead to PH development, so it is currently classified into few main clinical groups, which will be described in details in the next section. However, based on the haemodynamic criteria there are two main types of PH, termed as pre-capillary and post-capillary. Irrespective of clinical variant or various origin, there is a common fact that PH is a progressive disorder, which leads to right ventricle failure and thereby to life-threatening state.

Table 4. Haemodynamic definition of PH [57].

Definition	Haemodynamic characteristic	Clinical group
Pulmonary hypertension (PH)	$mPAP \geq 25$ mmHg	All
Pre-capillary PH	$mPAP \geq 25$ mmHg $PWP \leq 15$ mmHg CO normal or reduced	PAH PH due to lung diseases Chronic thromboembolic PH PH with unclear or multifactorial mechanisms
Post-capillary PH	$mPAP \geq 25$ mmHg $PWP \geq 15$ mmHg CO normal or reduced	PH due to the left heart disease

From an epidemiological point of view, it is still widely believed that PH is a rare disease [58]. However, numerous risk factors that are involved in PH development have been identified. Additionally, PH often appears as a condition associated with other physiological or pathophysiological alterations within human organism, such as pregnancy, lung diseases, HIV infection, heart and blood vessel diseases, lupus or scleroderma. For this reason, the true evidence of PH is largely underestimated and not fully known. In the last decade, only few epidemiological studies have been carried out to estimate accurately the PH burden. For instance, only in 2002, PH was a cause of 15 668 deaths and 260 000 hospitalizations in the United States [59]. Even though it is known, that PH can affect men and women of all ages, in this study, among all hospitalized individuals, 61% were women and 66% were in the age of 65 or older [59]. Another study was conducted on Scottish population in order to provide robust epidemiological data concerning PAH and the prevalence of 52 cases per million population were obtained [60]. The next epidemiological study, including 647 patients, with

strict PAH diagnosis, was performed in France [61]. As a result of this comparison, the prevalence ranging from 5-25 cases per million population was obtained [61]. Moreover, in developing world as Africa, South America or Asia, the frequently occurring diseases such as sickle cell disorders or schistosomiasis have been related to known risk factor of PH development [62]. To continue, hypoxia phenomenon is also a major worldwide factor, which predispose to PH progression [63]. In general, including all clinical variants of the disease, PH has been estimated to affect up to 100 million people worldwide [64]. Summarizing, PH is still underestimated either in developed or developing countries. The extensive well-designed epidemiological studies are required to estimate accurately the global burden of PH, especially in population exposed to various and complex risk factors.

4.2 Clinical classification

The clinical classification of PH aims to group together different variants of the disease, which are similar in terms of pathomechanisms, clinical manifestations and therapeutic approaches.

The classification of (PH) has gone through a number of changes since the first classification was proposed in 1973 and included only two categories such as primary and secondary PH based on the presence or absence of identifiable causes or risk factors [65]. As a result of many clinical improvements and modifications, the current classification of PH, was agreed upon at the 4th World Symposium on Pulmonary Hypertension in 2008, and expanded to five main clinical groups of the disease. Obviously, there are many subtypes among each category and they were summarized in Figure 7 [66]. Since, the pulmonary arterial hypertension (PAH) is a subject of this doctoral thesis, the main focus is devoted to it and this clinical group will be described in details. PAH represents the first category of PH which consists of five subtypes such as: idiopathic PAH, heritable PAH, drug- and toxin-induced PAH, associated with identified disease (APAH) and persistent pulmonary hypertension of newborns.

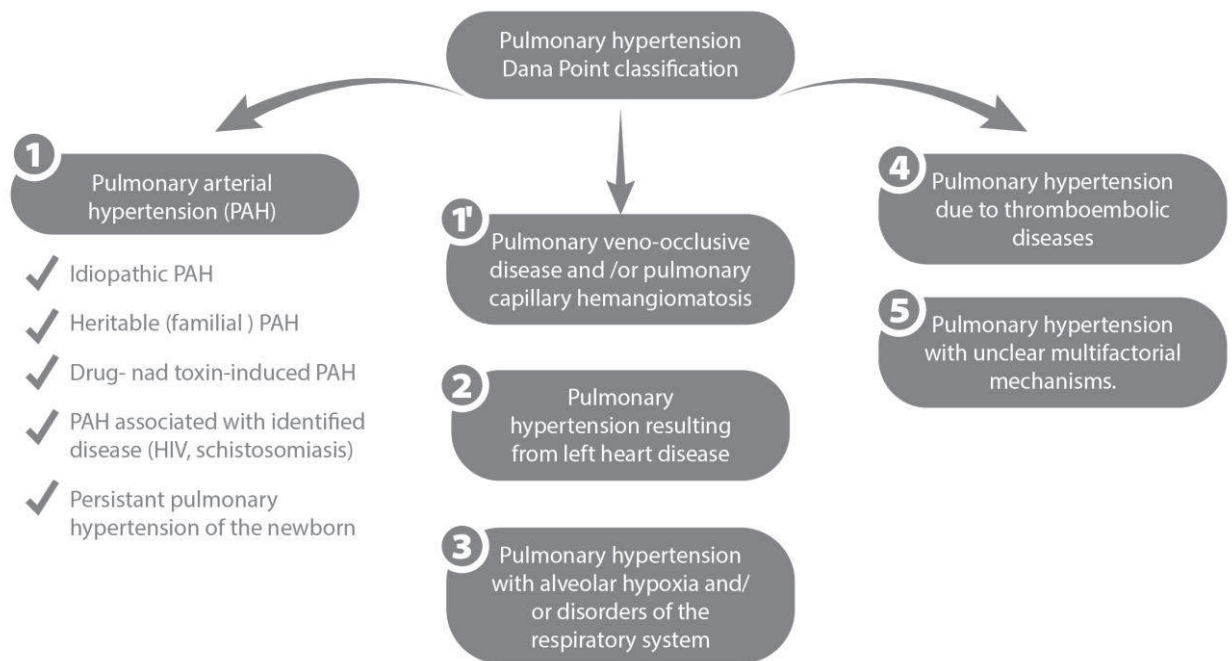


Figure 7. Clinical classification of pulmonary hypertension [66].

a) Idiopathic PAH

In contrast to PAH associated with other pathological conditions, the idiopathic PAH appear suddenly when neither the family history nor marked risk factor are observed. It is also termed as unexpected or sporadic pulmonary hypertension. The possible causes, pathomechanisms are unknown and therefore it is difficult to set effective therapy approach. However, in some patients with idiopathic PAH, mutations in bone morphogenetic protein receptor type 2 (*BMPR2*) gene were observed.

b) Heritable PAH

In previous clinical classifications it was defined as familial PAH. This PAH subtype is characterized by the presence of germline mutations in *BMPR2* gene, which is one of the

transforming growth factor β signaling family. Rarely the mutation occurs in activin receptor-like kinase type 1 or endoglin.

c) Drug- and toxin-induced PAH

Drugs, toxins, disorders or phenotype (age, gender) are well known risk factors, which means that they play a predisposing role in the disease development. The risk factors based on their strength of association with specific disease are classified as definite, very likely, possible, or unlikely. In case of PAH, the *Surveillance of Pulmonary Hypertension in America* study (SOPHIA) was conducted to investigate the effect of appetite suppressants intake, nonselective monoamine reuptake inhibitors, selective serotonin reuptake inhibitors, antidepressants, and anxiolytics on this type of PAH development. The results of SOPHIA study were summarized in Table 5.

Table 5. Updated risk factors for PAH development [66].

Risk factor category	Risk factor
Definite	Aminorex, Fenfluramine, Dexfenfluramine, Toxic rapessed oil
Likely	Amphetamines, L-tryptophan, Methamphetamines
Possible	Cocaine, Phenylpropanolamine, St. John's Wort, Chemotherapeutic agents
Unlikely	Oral contraceptives, Estrogen, Cigarette smoking

The above-mentioned three subcategories of PAH are related to the development of isolated pulmonary arterial diseases. Next PAH subtype occurs as a result of the association with other diseases and so is defined as associated with PAH (APAH). APAH includes PAH associated with connective tissue diseases, HIV infection, portal hypertension, congenital heart diseases, schistosomiasis or chronic hemolytic anemia.

a) PAH associated with connective tissue diseases

This is an important clinical subgroup. Patients with systemic sclerosis, lung fibrosis, systemic lupus, erythematosus, mixed connective tissue disease, Sjögren syndrome, polymyositis or rheumatoid arthritis can be more susceptible to PAH development. In these patients the right heart catheterization should be considered to detect or exclude possible PAH. The highest PAH prevalence, around 20% was confirmed in case of systemic sclerosis [67].

b) PAH associated with HIV

Human immunodeficiency virus (HIV) associated with PAH has a stable prevalence of 0.5% and has been described by clinical, hemodynamic, and histologic characteristics similar to PAH. Thus the mechanism for PAH development during HIV infection is still unclear due to the fact that neither the virus nor viral DNA has been presented in pulmonary endothelial cells. Therefore, an indirect mechanism of the virus influence by employing secondary messengers as cytokines, growth factors, endothelin, or viral proteins can be involved in PAH progression.

c) Portopulmonary hypertension

The development of PAH in association with elevated pressure in the portal circulation is known as portopulmonary hypertension (POPH) [68]. The hemodynamic studies have revealed that from 2% to 6% of patients with portal hypertension develop PH [69]. However, the right heart catheterization is required to confirm POPH diagnosis, due to the fact that numerous factors can increase mPAP in the presence of advanced liver disease. Some recent

case-control studies confirmed that female gender and autoimmune hepatitis are important risk factors of POPH development.

d) PAH associated with congenital heart diseases

Many patients with congenital heart diseases (CHD) if not treated, can develop PAH. The main reasons of increased blood flow and pressure can cause pulmonary arteriopathy. The most advanced variant of PAH associated with CHD is defined as Eisenmenger syndrome. The pathophysiological and histopathologic hallmarks of PAH associated with CHD include endothelial dysfunction in pulmonary vasculature.

e) PAH associated with schistosomiasis

The multifactorial pathomechanisms of PAH in patients with schistosomiasis are probable. They contain POPH as a frequent consequence of this disease and vascular inflammation as an effect of impacted schistosoma eggs. PAH associated with schistosomiasis represents a frequent subtype of PAH, mainly in countries where the infection is endemic. The prevalence of PAH associated with schistosomiasis has been estimated at 4.6% [70].

f) PAH associated with chronic hemolytic anemia

The evidence that PAH occurs as a consequence of hemolytic anemias including sickle cell disease (SCD), thalassemia, hereditary spherocytosis, stomatocytosis and microangiopathic hemolytic anemia has recently increased [66]. PAH has been observed most frequently in patients with SCD characterized by plexiform lesions. However, the pathomechanism of PAH in SCD is still uncertain. The possible hypothesis is that chronic hemolysis leads to higher nitric oxide consumption and subsequent resistance to nitric oxide bioactivity [71]. Finally, the smooth muscle guanosine which acts as vasodilator and has antiproliferative properties, is inactivated. The fifth PAH subcategory is represented by persistent pulmonary hypertension of newborns (PPHN). It develops when the normal cardiopulmonary transition fails to occur [72]. PPHN may be generally caused by the abnormally constricted pulmonary vasculature

due to lung parenchymal diseases. It can also develop when lungs possess normal parenchyma and remodeled pulmonary vasculature, and therefore is defined as an idiopathic PPHN.

4.3 Pathomechanisms of pulmonary arterial hypertension

Recently updated PAH subtypes are classified based on underlying causes. However, the excessive pulmonary vasoconstriction and abnormal vascular remodeling of all vascular layers (intima, media, adventitia) are common pathological processes in each PAH subcategory. Intimal changes include endothelial injury and cell proliferation, fibroblasts infusion, intimal fibrosis or rarely obstruction by unique plexiform lesions [73]. Additionally, the vascular smooth muscle cell (SMC) proliferation is another dominant hallmark in PAH pathomechanism. Altogether structural changes characterize apoptosis-resistant and proliferative cellular phenotype. Recently, the role of chronic inflammatory events or progenitor cells has been under extensive research.

The imbalance in vasoactive mediators is the prominent perturbation in PAH pathomechanism. The reduced production of vasodilatory mediators including prostaglandin I₂, nitric oxide (NO; product of NO synthases), and cyclic guanosine monophosphate (the second messenger downstream of NO) is well described in PAH patients [74,75]. Increased levels of asymmetric dimethylarginine, which acts as an endogenous inhibitor of NO synthase, might also be a relevant indicator of PAH development [76]. Additionally, the generation of potent vasoconstrictors such as thromboxane, endothelin 1 or 5-hydroxytryptamine (5-HT) was observed to be increased both in PAH patient and mouse model of hypoxia-induced pulmonary hypertension [77,78]. To continue, also an abnormal activity of both K⁺ and Ca²⁺ channels have been linked with pulmonary vascular tone dysregulation, disturbance of cellular homeostasis and induced fibroproliferation, mainly in SMC cells.

In view of cell proliferation and vascular remodeling, some vasoconstrictors enhance the proliferative events. For instance, endothelin 1 and 5-HT were reported to stimulate SMC proliferation [79, 80]. The constant Ca²⁺ flux from both extracellular and intracellular space might also enhance the SMC proliferation. The remodeling activity concerns either large or smaller distal arteries of pulmonary circulation. The collagen excess may mainly contribute to

remodeling phenotype, which was confirmed based on the mice or rats hypoxic pulmonary hypertension models [81]. However, there are other numerous factors involved in PAH vascular remodeling and they are summarized below:

a) Growth factors

Trough activation of tyrosine kinase receptors, various growth factors act as chemoattractants for fibroblasts, SMC cells or endothelial cells. As a result, the intracellular cascade signaling involved in migration, cell proliferation and resistance to apoptosis, are activated. The most relevant growth factors, that are strongly implicated in PAH pathomechanism, include vascular endothelial growth factor (VEGF) and VEGF receptor 2 (VEGFR-2), basic fibroblast growth factor (bFGF), platelet-derived growth factor (PDGF), hepatocyte growth factor (HGF) and transforming growth factor- β (TGF- β). Altogether, growth factors, are involved in numerous cellular functions such as proliferation, migration or differentiation and their role in PAH pathological hallmarks has been reported in various animal models [82].

b) Proteases and elastases

Proteases and elastases are the members of matrix metalloproteinases (MMPs) and they modulate the extracellular matrix (ECM) proteins. Up-regulation of MMPs and endogenous vascular elastase activity have been observed in remodeled lung vasculature in experimental and clinical PAH models [83].

c) Bone morphogenetic protein receptor type 2 (*BMPR2*)

The mutations in *BMPR2* gene have been observed mainly in heritable and idiopathic PAH subtypes. However, the mechanisms by which *BMPR2* mutations deregulate intracellular signaling are not completely understood and their action may differ between various cell types. The potential mechanisms proposed as a result of *in vitro* experiments contain up-regulation of proliferative pathways involving p38 mitogen-activated protein kinase [84] or reduced activation of the transcription factor Smad 1 [85]. Therefore the hypotheses that

BMPR2 mutations may be involved in excessive endothelial cell proliferation, growth of SMCs or pulmonary vasculopathy in PAH, requires further extensive investigations.

d) Notch signaling

Notch signaling is essential for cell-fate determination during embryonic stage [82]. It plays a role in multiple processes of vascular development such as vasculogenesis, angiogenesis, and differentiation of vascular SMCs. Notch 3 and its target, *HES5* gene, were observed to be expressed in lung biopsies from non-familial PAH patients, and in the lungs of two PAH rodent models [86]. These results underline, that up-regulation of the Notch 3 signaling is associated with PAH development either in humans or in rodent models of PAH.

e) Peroxisome proliferator-activated receptor γ (PPAR γ)

The physiological processes regulated by peroxisome proliferator-activated receptors (PPARs) range from lipogenesis to inflammation. PPAR γ is expressed in many tissues, such as vascular endothelial cells, vascular SMCs, and macrophages [87] and is implicated in cell growth, inflammation and angiogenesis [88], so it has a potential role in PAH pathology. Many reports suggested, that reduced PPAR γ in cells of the pulmonary vascular wall leads to PAH development, so that the activation of PPAR γ might inhibit PAH progression [82]. Altogether, the PAH pathomechanisms involving the vasoactive mediators imbalance, cell proliferation and vascular remodeling were summarized in Figure 8 [82].

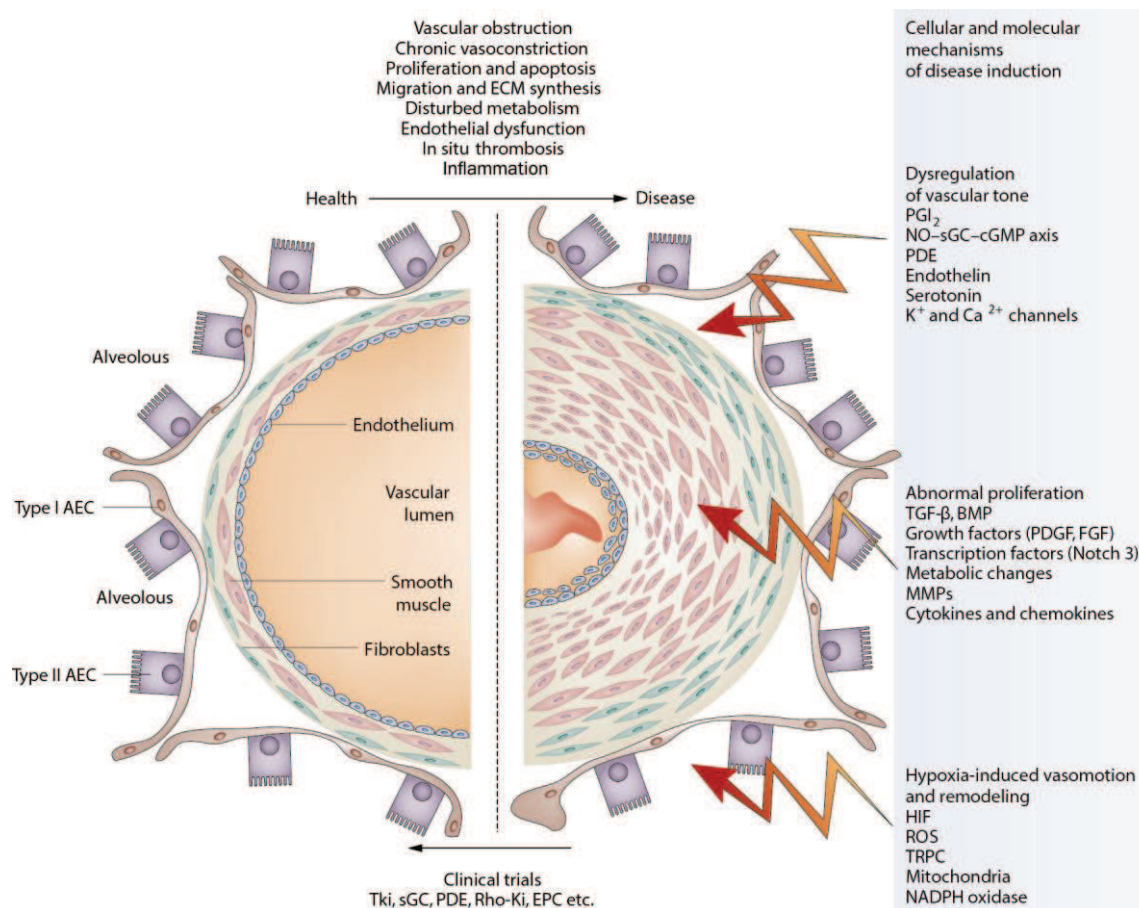


Figure 8. The major mechanisms in PAH pathogenesis [82].

The endothelial repair and angiogenesis might be another pathological hallmark of PAH pathology and development. Bone marrow derived endothelial progenitor cells (EPCs) circulate in adult peripheral blood and are recruited in the endothelial integrity maintenance and repair of endothelial injury [89]. The EPCs also play a relevant role in vasculogenesis and angiogenesis in vascular system. During the last two decades, it has been reported that plexiform lesions might occur as a result of EPCs growth deregulation and moreover the VEGF and VEGFR-2 expression were demonstrated in plexiform lesions of PAH patients, which might confirm the contribution of the lesions to angiogenesis alteration [90]. The recent study confirmed that elevated level of circulating proangiogenic progenitor cells was observed in idiopathic PAH patients in comparison to control group [91]. Although the accurate mechanism of angiogenesis deregulation in PAH pathogenesis still remains unclear.

The inflammation has also been suggested as a crucial pathological process in PAH development. Monocytes, macrophages, T lymphocytes and dendritic cells are observed in both plexiform lesions and other vascular lesions of PAH-affected human lungs [92]. The inflammation plays a relevant role in PAH associated especially with infectious diseases (HIV, schistosomiasis). In this pathological process numerous cytokines and chemokines are employed. Among cytokines group, increased circulating levels of monocyte chemoattractant protein 1, tumor necrosis factor, IL-1 β , and IL-6 were reported in patients with idiopathic PAH [93]. Chemokines are involved in various activities of leukocyte cells, including activation and adherence. Therefore, the chemokine-dependent mechanisms providing inflammatory cell recruitment in the lungs of PAH patients have been analyzed and have revealed the crucial role of FKN (also known as C-X3-C motif chemokine 1), RANTES (Regulated upon Activation, Normally T cell Expressed and Secreted) and chemokine ligand 2 (CCL-2), particularly [94,95].

What is more, the thrombosis is another common hallmark of PAH and investigations with the use of calibrated automated thrombography confirmed, that idiopathic PAH patients have a hypercoagulable phenotype [96]. As a result of this research, the increased level of fibrinopeptide A (marker of fibrin synthesis), elevated activity of von Willebrand factor, thromboxane A₂ increased (proaggregatory factor), and decreased level of NO and prostacyclin (aggregation inhibiting factor) were observed in PAH patients as compared to healthy individuals.

Recently, the role of some metabolic pathways in mitochondria have been suggested to be involved in PAH mechanism and pathogenesis [97]. The metabolic perturbations concern mainly, the imbalance between glycolysis and oxidative phosphorylation which are the main pathways providing the energy production at the cellular level (Figure 9). The shift of glucose metabolism from oxidative phosphorylation to glycolysis, especially in hypoxic condition, is termed as Warburg effect [98]. The abnormal cellular metabolism and mitochondrial dysfunction can provide new targets in therapeutic process of PAH, however the impact of metabolic alterations on disease pathogenesis requires further investigation, especially based on clinical trials.

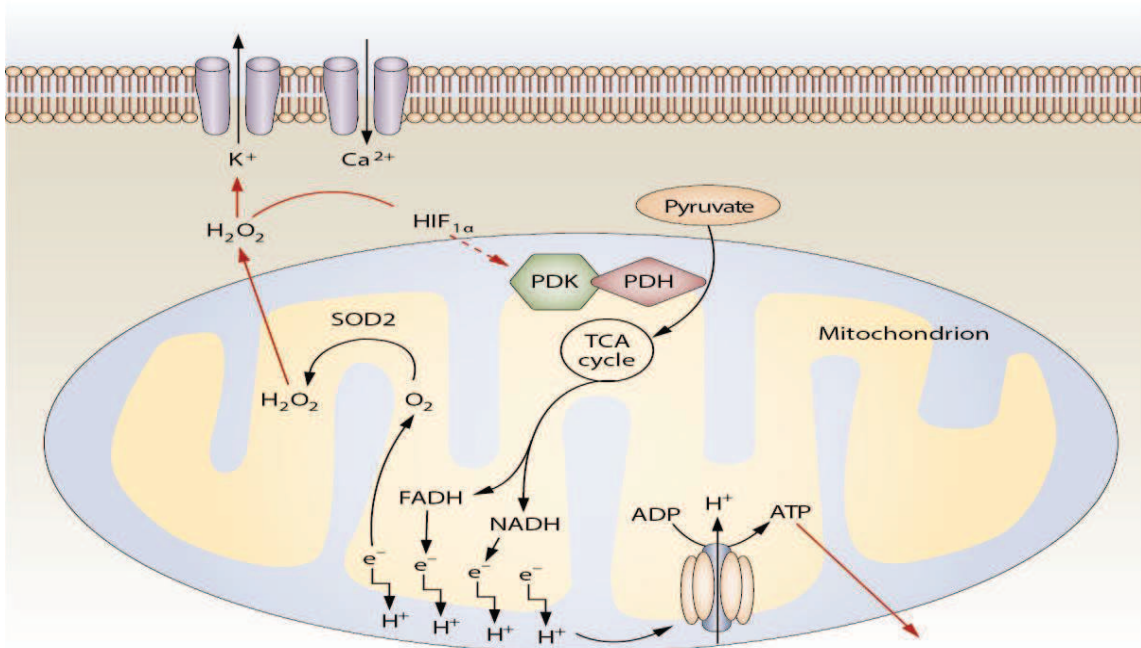


Figure 9. The metabolic pathways in mitochondrion involved in energy production [82].

4.4 Current diagnosis and treatment in pulmonary arterial hypertension

The current diagnosis of PAH is still a big challenge due to the lack of specific clinical manifestation, mainly at the early stages of the disease, which leads to relatively high mortality. Additionally, the PAH can be caused by multifactorial etiologies, the range of which has still been updated and expanded. To continue, there are numerous complex pathomechanisms suggested to be potentially involved in PAH pathogenesis, however they are mainly based on animal models. Therefore, to sum up, the above-mentioned factors, as well as the diagnosis of PAH is still poor and inaccurate. Although, there are several blood tests that might be performed routinely in PAH patients. However, none of these tests specifically diagnose PAH development. The routine blood tests performed in PAH patients are listed as follows.

a) BNP- B-type Natriuretic Peptide

The increased level of BNP is useful to diagnose heart failure. If the levels are elevated in the blood, the heart is under strain and fails, which is relevant for PAH patients. If the level is elevated, some additional tests, such as an echocardiogram are recommended.

b) BMP-Basic Metabolic Panel

The BMP panel includes some basic electrolytes and compounds representing basic kidney function, such as glucose, calcium, sodium, potassium, chloride, BUN (blood urea nitrogen), and creatinine. This test is used in PAH patients under the diuretic treatment, which can lead to losses of important electrolytes or to renal damage if not monitored properly.

c) CMP-Complete Metabolic Panel

The CMP contains all parameters measured by BMP and additionally albumin, total protein, ALP (alkaline phosphatase), ALT (alanine amino transferase), AST (aspartate amino transferase), and bilirubin. This test is useful in PAH patients for the same reason as BMP, however provides additional liver function monitoring. It is recommended to control liver function in PAH case, because the increased pressure in the pulmonary arteries leads to dysfunction of the right side of the heart and consequently to liver damage.

d) D-dimer

Plasma D-dimer, as a specific degradation product of crosslinked fibrin, can be altered in a numerous conditions including cancer, necrosis, infection or inflammation. Thus, for the confirmation of PAH diagnosis is very poor. However, very often the absence of D-dimer can clearly exclude the presence of PAH which provides high negative predictive value of this biochemical parameters.

The ventilation-perfusion scintigraphy, computed tomography or pulmonary angiography are the imaging techniques frequently applied in PAH diagnostic process. Pulmonary angiography represents an invasive and resource-demanding procedure, however is characterized by high diagnostic accuracy [99]. Computed tomography and ventilation/perfusion scanning are low invasive techniques that are used in PAH diagnosis but

are also time-consuming with limited sensitivity when employing contrast agent administration and radiation [98]. To sum up, there is still lack of specific, sensitive, cost-effective, accurate and safe diagnostic tool for early PAH detection.

Although, no effective treatment for PAH patients is available, improvements in understanding the pathomechanisms of this disorder have provided the development of target therapies towards specific pathways. Drugs and agents that regulate abnormalities in the prostacyclin, endothelin, and nitric oxide signaling have been tested in randomized, controlled studies and revealed benefits in functional status, pulmonary hemodynamics, and disease progression [100]. The target pathways for currently recommended therapies were shown in Figure 10.

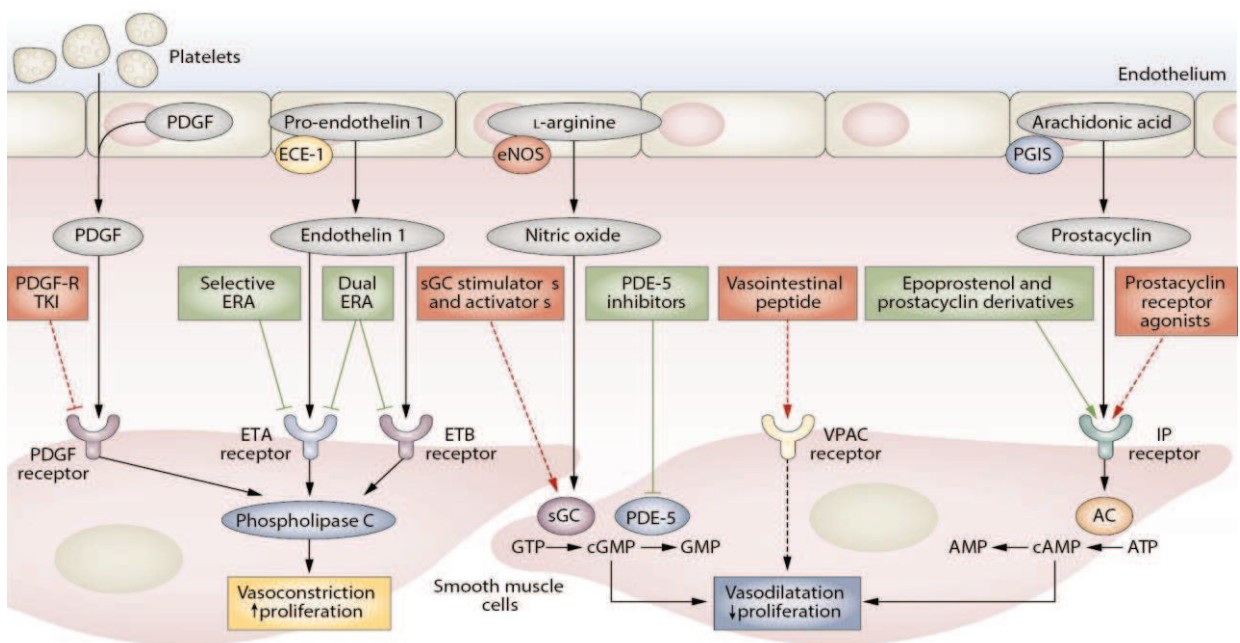


Figure 10. Current and emerging therapies and their targets in PAH treatment [100].

The modern-day licensed therapies include the stable prostacyclin analogs termed as prostanoids, endothelin receptor antagonists (ERA) and phosphodiesterase type 5 (PDE-5) inhibitors. The common agents and drugs that can be used in each targeted treatment were presented in Table 6.

Table 6. The drugs and agents used in the currently licensed therapies [100].

Targeted therapy	Drugs and agents used
Prostanoids	Epoprostenol Iloprost (<i>inhalation</i>) Iloprost (<i>intra venous</i>) Treprostinil (<i>inhalation</i>) Treprostinil (<i>sub cutaneous</i>) Treprostinil (<i>intra venous</i>)
Endothelin receptor antagonists	Bosentan Ambrisentan Sitaxentan Macitentan
Phosphodiesterase type 5 inhibitors	Sildenafil Tadalafil

Due to the fact that after application of above-mentioned specific treatments, the PAH progression is often observed, employment of multidrug therapy to target different deregulated pathways simultaneously, seems to be a promising approach. Accordingly, combined therapies using two or more agents from different drug classes are now recommended [101]. Recently, other potential therapeutic concepts including prostacyclin receptor agonists, vasoactive intestinal polypeptide (VIP), soluble guanylate cyclase (sGC) activators and stimulators, tyrosine kinase inhibitors or bone-marrow derived endothelial progenitor cells (EPCs) have been proposed, and subjected to continuous and intensive research [100]. Thus, incessant development and progress in basic and clinical research within PAH population can result in better understanding of its pathogenesis, and identification of novel therapeutic targets which may consequently lead to effective drug discovery and design.

II. THE OBJECTIVE OF THE DOCTORAL THESIS

The objective of the doctoral thesis was to study plasma untargeted metabolic fingerprints during an acute and chronic phase of pulmonary arterial hypertension (PAH) in an animal and human model. To reveal as many metabolite changes as possible in the whole metabolome, two complementary analytical platforms such as liquid chromatography coupled with quadrupole time of flight MS detector (LC-QTOF-MS) and gas chromatography coupled with single quadrupole MS detector (GC-Q-MS) were chosen and applied in this study. To study plasma metabolite changes in an acute phase, the pig model, in which the severe and stable PAH was induced by polydextrane microspheres injection, was proposed. Then, the human model based on the comparison between healthy and PAH patients was used to analyze plasma metabolite fingerprints in chronic stage of the disease.

Based on available literature, PAH diagnosis and pathogenesis is still incomplete and not clearly understood, especially, due to the lack of specific clinical symptoms at the initial stage of the PAH progression. There is a constant need to search early markers, that might indicate the disease initiation and to improve knowledge on mechanisms involved in PAH development. Metabolic alterations at molecular level may be associated with PAH pathogenesis and occur before marked clinical manifestation. Therefore, untargeted plasma metabolic fingerprinting was applied in this doctoral thesis to reveal global metabolites changes related to disease development. To select potential metabolic markers of PAH, the main research steps involved in untargeted metabolomics workflow included:

- 1) Experimental design, sample collection and metabolite extraction;
- 2) Plasma metabolic fingerprinting with LC-QTOF-MS and GC-Q-MS;
- 3) Data extraction and processing;
- 4) Univariate and multivariate discriminant statistical analysis;
- 5) Metabolite identification;
- 6) Biochemical pathway analysis and biological interpretation.

III. EXPERIMENTAL PART

5. Materials and methods

5.1. Instrumentation

- High-performance liquid chromatography (HPLC) system equipped with degasser, two binary pumps, and thermostatted autosampler (1200 series, Agilent Technologies, Waldbronn, Germany) coupled with quadrupole and time of flight mass spectrometry detector (QTOF 6520, Agilent Technologies, Waldbronn, Germany).
- Ultra high-performance liquid chromatography (UHPLC) system equipped with degasser, two binary pumps, and thermostatted autosampler (1290 Infinity series, Agilent Technologies, Waldbronn, Germany) coupled with quadrupole and time of flight mass spectrometry detector (QTOF 6520, Agilent Technologies, Waldbronn, Germany).
- Gas chromatography (GC) instrument (7890A, Agilent Technologies, Waldbronn, Germany) interfaced to inert single quadrupole (Q) mass spectrometer with triple-Axix detector (5975C, Agilent Technologies, Waldbronn, Germany).

HPLC-QTOF-MS and UHPLC-QTOF-MS instruments were connected with personal computer (PC) with Mass Hunter Workstation B.05.00, Mass Hunter Qualitative Analysis B.05.00 (Agilent Technologies, Waldbronn, Germany), DA Reprocessor B.05.00 (Agilent Technologies, Waldbronn, Germany) and Molecular Structure Correlator (MSC) B.05.00 software (Agilent Technologies, Waldbronn, Germany) for data acquisition, data extraction and compound identification.

GC-Q-MS instrument was connected with PC equipped with Agilent MSD Chemstation E.02.00.493 Software (Agilent Technologies, Waldbronn, Germany) for data acquisition.

- PC with Windows 7 operating system Microsoft Office software equipped with Mass Profiler Professional B.12.01 (Agilent Technologies, Waldbronn, Germany) for data processing and treatment.
- PC with Windows 7 operating system Microsoft Office software equipped with MATLAB 2007b (Mathworks, Natick, MA, USA) and SIMCA P+ 13.03. (Umetrics, Umea, Sweden) software for univariate and multivariate statistical data analysis and plotting.
- PC with Windows 7 operating system Microsoft Office software equipped with AMDIS 2.17 and MS Search 2.0 software (<http://chemdata.nist.gov/mass-spc/amdis/>) for data deconvolution and compound identification.
- Microcentrifuge Eppendorf 5415R (Eppendorf AG, Hamburg, Germany).
- Milli-Q Plus 185 Water Purification System (Millipore, Bedford, USA).
- Speedvac Concentrator (Thermo Fisher Scientific, Waltham, MA, USA).
- Refrigerated Vapor Trap (RUT4104, Thermo Scientific, Waltham, Massachusetts, USA).
- Oil pump (E-LAB2, Edwards, Crawley, England, United Kingdom).
- Automatic pipettes Eppendorf Research (Eppendorf, Hamburg, Germany).
- Ultrasonic baths 3000513, Selecta P.
- Vortex mixer (TopMix FB15024 Fisher Scientific, Thermo Scientific, Waltham, Massachusetts, USA).
- Stove (Digitheat 80L Selecta, Barcelona, Spain).
- Analytical weight-machine: Explorer, OHAUS.
- Freezer (-80°C): FORMA 88000 series (Thermo Scientific, Waltham, MA, USA).
- Fridge (-20°C): Space plus, Electrolux.

5.2 Disposable materials and reagents

5.2.1 Disposable materials

- HPLC amber vials 1.5 ml (Agilent Technologies, Waldbronn, Germany).
- Glass inserts with polymer feet 250 μ l (Agilent Technologies, Waldbronn, Germany).
- Clear vials fused with 200 μ l glass inserts (Chromacol, Welwyn Garden City, UK).
- Open top short screw caps for clear vials fused with 200 μ l glass inserts (Chromacol, Welwyn Garden City, UK).
- Screw caps for amber vials 1.5 ml (Agilent Technologies, Waldbronn, Germany).
- Crimp, aluminum silver caps with, 4mm hole (Chromacol, Welwyn Garden City, UK).
- 4 mm nylon syringe filters 0.22 μ m (Thermo Scientific, Waltham, Massachusetts, USA).
- Pipette tips (Eppendorf, Hamburg, Germany).
- Eppendorf polypropylene tubes 1.5 ml (Eppendorf, Hamburg, Germany).
- LC reversed phase column Zorbax Extend RRH+ C18, 2.1x5.0 mm, 1.8 μ m (Agilent Technologies, Waldbronn, Germany).
- LC reversed-phase column Discovery HS C18 15 cm \times 2.1 mm, 3 μ m (Supelco, Bellefonte, Pennsylvania, USA).
- Guard column (Discovery HS C18 2 cm \times 2.1 mm, 3 μ m (Supelco, Bellefonte, Pennsylvania, USA).
- GC-Column DB5-MS, 30 m length, 0.25 mm i.d., 0.25 μ m film 95% dimethyl/ 5% diphenylpolysiloxane, (Agilent Technologies, Waldbronn, Germany).
- GC- pre-column (10 m J&W) (Agilent Technologies, Waldbronn, Germany).
- Septa for GC injection port (Agilent Technologies, Waldbronn, Germany).
- Liners for GC injection port Restek 20782 (Bellefonte, PA USA).
- Electrospray nebulizer needle (Agilent Technologies, Waldbronn, Germany).

- Micro-Grit Paper MESH 4000 for shield of ion transfer capillary cleaning (Agilent Technologies, Waldbronn, Germany).
- Purification filters for Milli-Q Plus 185 Water Purification System (Millipore, Bedford, USA).

5.2.2 Reagents

- LC-MS grade acetonitrile, Fluka Analytical, Chemie Gmbh (Steinheim, Germany)
- LC-MS grade water, Fluka Analytical, Chemie Gmbh (Steinheim, Germany)
- LC-MS grade isopropanol, Fluka Analytical, Chemie Gmbh (Steinheim, Germany)
- HPLC grade heptane 98%, Fluka Analytical, Chemie Gmbh (Steinheim, Germany)
- LC-MS Ultra formic acid 98%, Fluka Analytical, Chemie Gmbh (Steinheim, Germany)
- Silylation grade pyridine 99%, Sigma-Aldrich (St. Louis. MO, USA)
- O-methoxyamine hydrochloride, Sigma-Aldrich (St. Louis. MO, USA)
- N,O-Bis(trimethylsilyl)trifluoroacetamide with 1% trimethylchlorosilane (BSTFA+1% TMCS, vol/vol) Pierce Chemical Co. (Rockford, IL, USA)
- n-fatty acid methyl ester mixture (n-FAMES C8-C22) - retention index marker, Supelco (Bellefonte, PA, USA)
- Methyl stearate C18:0 in heptane (1000 ppm) Sigma-Aldrich (St. Louis. MO, USA)
- Creatine, arginine, α -tocopherol, Sigma Aldrich (St. Louis. MO, USA)
- Protonated purine (Agilent Technologies, Waldbronn, Germany)
- Protonated hexakis (1H, 1H, 3H-tetrafluoropropoxy) phosphazine (or HP-921) (Agilent Technologies, Waldbronn, Germany)
- Trifluoroacetic acid (TFANH₄) ammonium anion (Agilent Technologies, Waldbronn, Germany)
- Hexakis (1H, 1H, 3H-tetrafluoropropoxy) phosphazine (or HP-0921) (Agilent Technologies, Waldbronn, Germany)
- Reverse-osmosed purified water from Milli-Q Plus 185 (Millipore, Bedford, USA)

5.2.3 Solutions

- Methanol: ethanol mixture 50:50 (v/v) for plasma deproteinization before LC-MS metabolic fingerprinting analysis. The solution was prepared by mixing the equal volume of methanol and ethanol (i.e., 50 ml), then ultrasonicated for 15 min and kept at temperature of -20°C in the fridge prior to analysis.
- 0.1 % formic acid solution in water. The solution was used as a mobile phase in LC-MS metabolic fingerprinting analysis. 1 mL of 99% formic acid was measured by automatic pipette and added to 100 mL volumetric flask filled in half by purified water, and then filled with purified water to the volume of 1000 mL.
- 0.1 % formic acid solution in acetonitrile. The solution was used as a mobile phase in LC-MS metabolic fingerprinting analysis. 1 mL of 99% formic acid was measured by automatic pipette and added to 100 mL volumetric flask, filled in half with acetonitrile, and then to the volume of 1000 mL.
- 20% isopropanol solution in water. The solution was used for electrospray nebulizer needle and capillary shield cleaning. 20 mL of isopropanol was mixed with 80 mL of purified water, then ultrasonicated for 15 min and kept at room temperature for one week.
- ESI-LOW tuning mix. The solution was used for Q-TOF-MS calibration (Agilent Technologies, Waldbronn, Germany)
- Reference mass solution for LC-QTOF-MS. The solution was continuously introduced by calibrant delivery system during analysis to ensure mass accuracy measurement. In 1000ml bottle, the 950 mL of LC-MS grade acetonitrile and 50 mL of LC-MS grade water were mixed and then 2.0 mL of purine, 0.9 ml of HP-0921 and 1.0 ml of TFANH₄ were added. The solution was mixed by shaking and kept in the fridge at a temperature of 4°C before LC-QTOF-MS analysis.
- O-methoxyamine hydrochloride solution in pyridine (15 mg/mL). The solution was used for derivatization before GC-Q-MS metabolic fingerprinting analysis. 225 mg of O-methoxyamine hydrochloride were dissolved in 15 mL of 99% pyridine and then ultrasonicated for 30 min and kept in the fridge at temperature of 4°C before GC-Q-MS analysis.

- Bistrimethylsilyltrifluoroacetamide with 1% trimethylchlorosilane (BSTFA+1% TMCS) (Supelco, Bellefonte, Pennsylvania, USA). The solution was used for the second derivatization step before GC-Q-MS metabolic fingerprinting analysis.
- Methyl stearate (10 ppm in heptane). The solution was used as internal standard (IS) in plasma pretreatment step before GC-Q-MS metabolic fingerprinting analysis. 100 μ l of stock solution (methyl stearate 1000 ppm in heptane) was pipetted into glass 10 ml tube and 9900 μ l of heptane was added. Then, the solution was ultrasonicated for 15 min and kept in the fridge at temperature of 4°C prior to GC-Q-MS analysis.
- Quality control (QC) samples. The solutions were used to control LC-QTOF-MS and GC-Q-MS system stability and method reproducibility. QC samples were prepared as a pool of equal volume of each plasma samples used in the experiment. Then the pool was vortex mixed and divided into the equal volume as plasma sample used for metabolic fingerprinting analysis (50 μ l). The QC samples were prepared with the same sample pretreatment procedure as the real plasma samples.

5.3 Biological samples

5.3.1. Animal model

The animal experimental model consisted of 2–3 month old castrated-male Large-White pigs. The investigation was approved by the Institutional Animal Research Committee no ES280790000176 and performed in accordance with the Guide for the Care and Use of Laboratory Animals. At the beginning of the experiment, anesthesia was evoked by intramuscular injection of ketamine (20 mg/kg), xylazine (2 mg/kg), and midazolam (0.5 mg/kg), with buprenorphine (0.3 mg/kg) for analgesia. Next animals were intubated. Hemodynamic parameters were measured under mechanical ventilation (Fi O₂ 35%) and anesthesia was continued with intravenous midazolam (0.2 mg/kg/h). Simultaneously, the electrocardiographic and oxymetric parameters were monitored. To continuously control the systemic arterial pressure and pulmonary arterial pressure using Swan-Ganz catheter, the right femoral artery and vein were percutaneously cannulated. Hemodynamic parameters covered mean pulmonary arterial pressure (mPAP), cardiac output (CO) assessed by thermodilution, mean systemic blood pressure (mSBP), oxygen saturation (O₂ sat), heart rate (HR) and pulmonary vascular resistance (PVR). The PVR value was calculated as the difference between mPAP pulmonary capillary wedge pressure (PCWP) and divided by the CO in Wood units (WU). The acute pulmonary hypertension (PH) was induced in 8 pigs by through the femoral vein injection of polydextrane microspheres with a bead diameter of 100– 300 µm (Sephadex G50 Coarse dry, Pharmacia Biotech GmbH). Animals were exposed to several doses of a suspension of 2.5 mg of microspheres per mL as far as the mPAP increased above 40 mmHg which was kept for at least 20 min, what confirmed the acute severe and stable PH due to pulmonary embolism (PE).

The animal blood was collected in two time points: immediately before the microspheres injection (baseline) and in the stable phase of acute PH (1h after the first microspheres injection). The hemodynamic characteristics of baseline and acute PH stage were presented in Table 7 and Table 8. Blood samples were taken from the femoral vein and collected into tubes with lithium heparin. To obtain plasma samples the vein blood was

centrifuged (30 min, 2000 x g, 4 °C) and 500 µL of supernatants were frozen at -80°C until metabolic fingerprinting analysis.

Table 7. Hemodynamic parameters of animals at baseline state.

Animal ID Baseline	HR (bpm)	O ₂ sat (%)	mSBP (mmHg)	mPAP (mmHg)	CO (L/min)	PVR (WU)
Pig 1	77	100	100	22	5.15	2.52
Pig 2	70	100	101	25	4.95	3.27
Pig 3	106	100	91	19	6.55	1.52
Pig 4	101	100	90	24	4.92	2.43
Pig 5	66	100	67	17	2.43	1.23
Pig 6	80	100	125	25	4.29	3.03
Pig 7	55	100	85	15	2.76	1.09
Pig 8	75	100	94	15	3.63	1.65

Table 8. Hemodynamic parameters of animals at acute pulmonary hypertension (PH) state.

Animal ID Acute PH	HR (bpm)	O ₂ sat (%)	mSBP (mmHg)	mPAP (mmHg)	CO (L/min)	PVR (WU)
Pig 1	91	98	94	40	3.59	8.9
Pig 2	98	94	78	40	3.70	8.6
Pig 3	108	87	95	45	4.70	7.7
Pig 4	99	83	73	42	3.42	9.4
Pig 5	96	85	64	45	2.29	17.5
Pig 6	90	87	98	40	3.03	10.6
Pig 7	79	91	78	41	2.42	14.4
Pig 8	80	94	76	43	2.46	14.6

HR-heart rate, O₂ sat- oxygen saturation, mSBP- mean systemic blood pressure, mPAP-mean pulmonary arterial pressure, CO-cardiac output, PVC- pulmonary vascular resistance

The PH occurrence in all animals was confirmed by both hemodynamic parameter measurements and observation of histopathological changes in lung parenchyma including capillary vessel obstruction, inflammatory infiltration, and intraalveolar edema and hemorrhage [102] which were similar to those observed in patients with PH due to PE (Fig. 11).

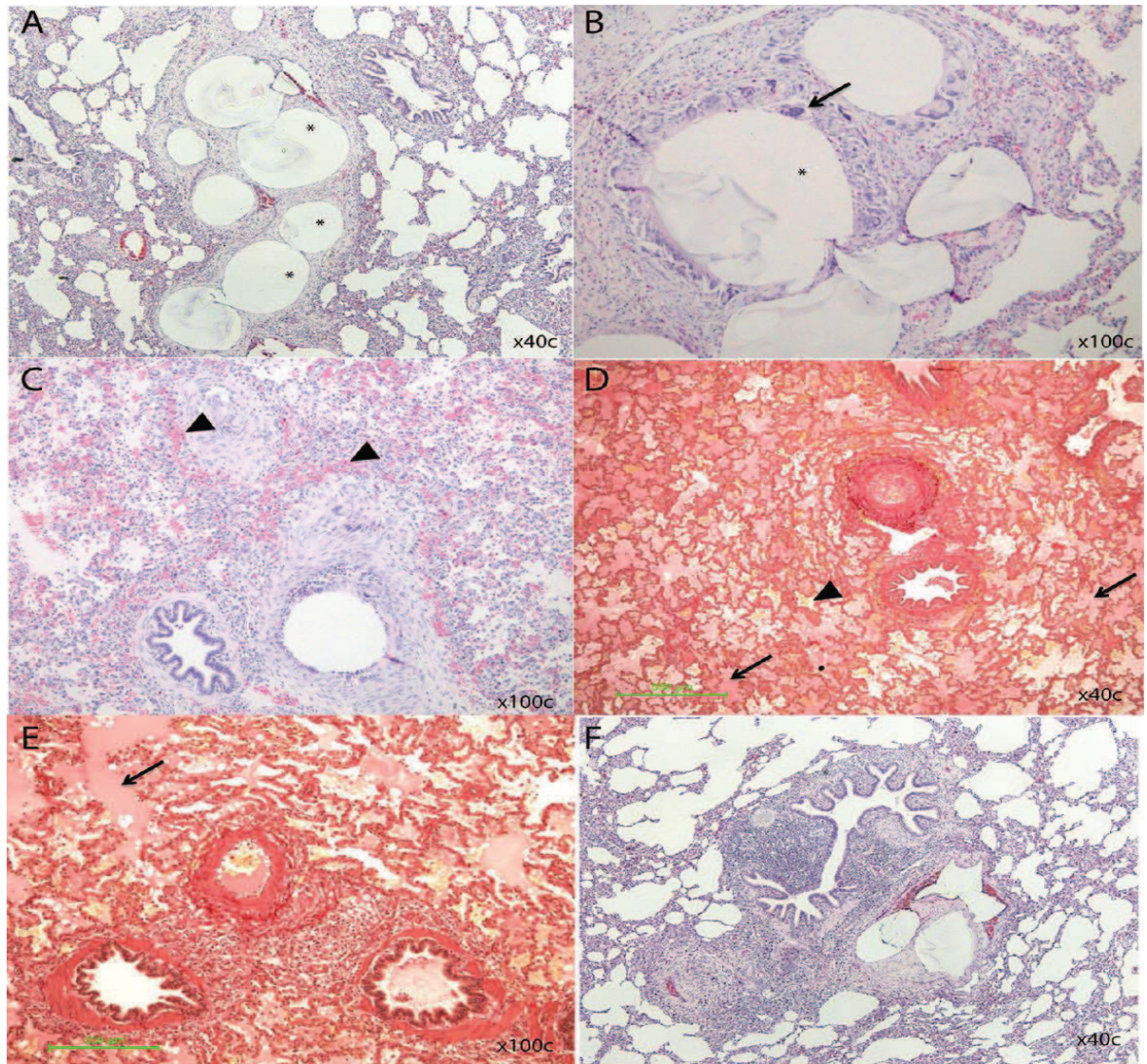


Figure 11. The histopathological changes in lung parenchyma of a pig that underwent euthanasia 3h after acute PH induction by PE procedure. (A) Vessel obstruction by several microspheres marked as asterisk. (B) Macrophages infiltration around the microsphere obstructing the vessel marked as asterisk. (C) The hemorrhage pointed with arrowheads. (D) The hemorrhage marked as arrowhead and intraalveolar edema pointed with arrows. (E) The example of intraalveolar edema marked as arrow. (F) The severe perivascular and peribronchial inflammatory infiltration [102].

5.3.2. Human model

The human model of pulmonary arterial hypertension (PAH) comprised of 40 patients divided into two patient groups. The 20 healthy individuals and 20 patients with confirmed PAH derived from CLINIC University Hospital in Barcelona were included in this study. The investigation was carried out in accordance with approval of The Ethical Committee of Clinical Investigations in Barcelona (CEIC, the approval number CIF-G-08431173) and the informed consent was signed by each participant of the study. The studied groups were matched according to age, BMI and gender (15 women and 5 men both in control and PAH group). The U Mann-Whitney test was used to study the age and BMI difference between control and PAH patients. The results of statistical analysis confirmed that analyzed groups are uniform regarding to these criteria. The detailed data concerns the mean and standard deviation (SD) of the age and BMI values within the studied groups and statistical analysis of the difference between them were collected in Table 9. Additionally the clinical characteristics of each individual of studied groups including age, gender, BMI, PAH etiology and associated diseases were presented in Table 10. The careful design of this study concerning all: age, BMI, gender matching and associated diseases occurrence was provided to avoid significant differences that are not related to the biological aim of the study and consequently ensure reliable metabolomics results. The blood samples for metabolic fingerprinting analysis were obtained from cubital vein and drawn into lithium heparin-containing tubes. Then, after the centrifugation step (30 min, 2000 x g, 4°C), the obtained plasma samples (200 µl) were frozen at -80°C and stored until metabolomics experiment.

Table 9. Statistical analysis of age and BMI difference in the studied groups.

Studied group	Age (Mean ±SD)	BMI (Mean ± SD)
Control group	50.30 (±14.84)	25.17 (±3.65)
PAH group	50.75 (±15.22)	25.36 (±3.73)
U Mann-Whitney test	<i>p</i>=0.957 (>0.05)	<i>p</i>= 0.871 (>0.05)

Table 10. Clinical characteristics of individual participant included into the metabolomics study.

Patient ID	Age	Gender	BMI	PAH etiology	Hepatitis	HIV infection	DM	Nephritis	IHC	AVC
PAH 1	22	F	19.7	1	0	0	0	0	0	0
PAH 2	38	F	21.9	1	0	0	0	0	0	0
PAH 3	66	F	25.4	2	0	0	0	1	0	0
PAH 4	67	F	31.4	2	0	0	0	0	0	0
PAH 5	60	M	27.1	2	0	0	0	0	1	0
PAH 6	30	F	25.0	1	0	0	0	0	0	0
PAH 7	59	F	27.0	2	0	0	0	0	0	0
PAH 8	57	M	29.0	1	0	0	0	0	0	0
PAH 9	24	F	27.0	3	0	0	0	0	0	0
PAH 10	62	F	31.6	2	0	0	0	0	0	0
PAH 11	70	F	25.5	2	0	0	0	0	0	0
PAH 12	47	F	22.6	5	1	1	0	0	0	0
PAH 13	45	F	23.8	2	0	0	0	0	0	0
PAH 14	58	F	20.7	4	0	0	0	0	0	0
PAH 15	57	M	30.1	6	0	0	1	0	0	0
PAH 16	44	M	22.2	1	0	0	0	0	0	0
PAH 17	31	F	19.6	1	0	0	0	0	0	0
PAH 18	51	F	25.0	1	0	0	0	0	0	0
PAH 19	73	M	29.7	1	0	0	0	0	0	0
PAH 20	54	F	22.9	1	0	0	0	1	1	0
CONTROL 1	23	F	21.4	0	0	0	0	0	0	0
CONTROL 2	36	F	20.0	0	0	0	0	0	0	0
CONTROL 3	63	F	26.0	0	0	0	0	0	0	0
CONTROL 4	67	F	31.2	0	0	0	1	0	0	0
CONTROL 5	60	M	27.3	0	0	0	0	0	0	0
CONTROL 6	31	F	22.7	0	0	0	0	0	0	0
CONTROL 7	57	F	28.2	0	0	0	0	0	0	0
CONTROL 8	57	M	28.6	0	0	0	0	0	0	0
CONTROL 9	23	F	25.0	0	0	0	0	0	0	0
CONTROL 10	58	M	31.8	0	0	0	0	0	0	0
CONTROL 11	69	F	24.5	0	0	0	0	0	0	0
CONTROL 12	49	F	23.7	0	0	0	0	0	0	0
CONTROL 13	45	F	23.9	0	0	0	0	0	0	0
CONTROL 14	60	F	22.4	0	0	0	1	0	0	0
CONTROL 15	59	M	28.4	0	0	0	0	0	0	0
CONTROL 16	44	F	20.8	0	0	0	0	0	0	0
CONTROL 17	31	F	19.6	0	0	0	0	0	0	0
CONTROL 18	51	F	24.1	0	0	0	0	0	0	0
CONTROL 19	72	M	30.0	0	0	0	0	0	0	0
CONTROL 20	51	F	23.7	0	0	0	0	0	0	0

In case of gender: M means man, F means woman.

In case of PAH etiology: 0-control, 1-idiopathic, 2-PAH due to systemic sclerosis, 3-PAH due to other connective tissue diseases, 4-PAH due to congenital heart diseases, 5-PAH due to HIV infection, 6-portopulmonary hypertension (POPH), 7-PAH due to schistosomiasis.

In other cases: 1 means presence and 0 means absence of the disease, DM-diabetes mellitus, IHC- ischemic heart disease, AVC- atrioventricular canal defect.

5.4 Biological sample preparation

5.4.1. Plasma sample pretreatment for LC-QTOF-MS metabolic fingerprinting

Both pig and human plasma samples were prepared with the same sample pretreatment procedure prior to LC-QTOF-MS metabolic fingerprinting. Plasma samples were thawed in ice for 120 min. Then plasma samples were vortexed for 30 s and 50 μ l were pipetted into eppendorf 1.5 ml tubes. The 150 μ l cold (-20°C) mixture of methanol and ethanol (1:1, v/v) was added into the tubes. Subsequently, samples were mixed for 1 min and then kept for 5 min at 4°C and vortexed for a few seconds. Then samples were centrifuged at $15400 \times g$ for 20 min at 4°C , and the obtained supernatant was filtered through a $0.22 \mu\text{m}$ syringe nylon filter. The simplified workflow of plasma preparation procedure was presented in Figure 12. Simultaneously with plasma samples, the quality control (QC) samples were prepared. The QCs were a pool of equal volume (20 μ l) of each plasma sample used in particular experiment. The QCs were prepared with the same sample pretreatment procedure as pig or human plasma samples.

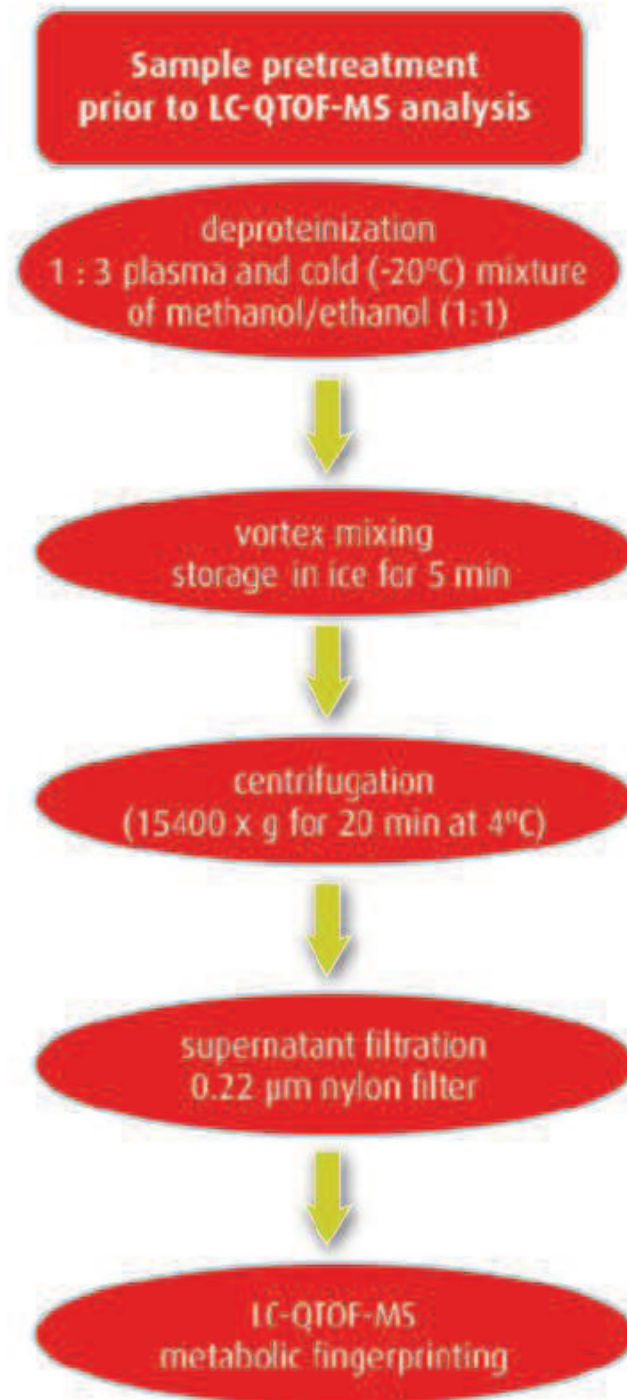


Figure 12. The simplified workflow of plasma sample pretreatment before LC-QTOF-MS metabolic fingerprinting.

5.4.2. Plasma sample pretreatment for GC-Q-MS metabolic fingerprinting

Plasma samples included in both animal and human model were treated with the same procedure before GC-Q-MS metabolic fingerprinting experiment. At the beginning, plasma samples were thawed in ice for 120 min and then mixed by vortex mixer for 30 s. 50 μ l of each plasma sample were pipetted into 1.5 ml eppendorf tubes and 150 μ l of cold acetonitrile (-20°C) were added. Then, samples were mixed by vortex mixer for 2 min and kept at the temperature of 4°C for 5 min. Afterwards, samples were centrifuged with the microcentrifuge at $15400 \times g$ for 10 min at 4°C . Next, 100 μ l of each supernatant were transferred to GC glass vial equipped with 200 μ l insert and evaporated to dryness (about 150 min) by speedvac concentrator at 30°C . Afterwards, the 2-step derivatization procedure was conducted. The first step, termed as methoxymation provides the carbonyl functional groups conversion to oximes what eliminates an undesirable slow and reversible silylation with carbonyl groups whose products can be thermally labile. Subsequently, the second step named silylation is performed to replace exchangeable protons with trimethylsilyl (TMS) groups as well as to form the TMS esters of metabolites to make them suitable for GC-Q-MS analysis. During the methoxymation step, 10 μ l of o-methoxyamine hydrochloride in pyridine (15 mg/ml) were added to each dried sample and thoroughly mixed for 1 min with the vortex mixer. Then, the samples were ultrasonicated three times for 10 s and vortexed again for 2 min. Afterwards, all samples were covered by aluminum foil and incubated at the room temperature in the dark place for 16 h. Next, the silylation step was employed: 10 μ l of bistrimethylsilyltrifluoroacetamide with 1% trimethylchlorosilane (BSTFA+1% TMCS) were rapidly added into each sample and vigorously mixed for 5 min. Afterwards, all samples were incubated in the stove for 1 h at 70°C . Then, the samples were cooled down for 1 h in the dark place and 100 μ l of methyl stearate internal standard (IS) (10 ppm) was added to each sample and vigorously mixed with vortex mixer for 2 min. The IS addition was performed to control the instrument performance during the samples sequence analysis. Similar to LC-QTOF-MS methodology, the QC samples were simultaneously prepared as a pool of all plasma samples and underwent the same sample pretreatment procedure. The simplified scheme of plasma sample preparation to GC-Q-MS metabolic fingerprinting analysis was shown in Figure 13.

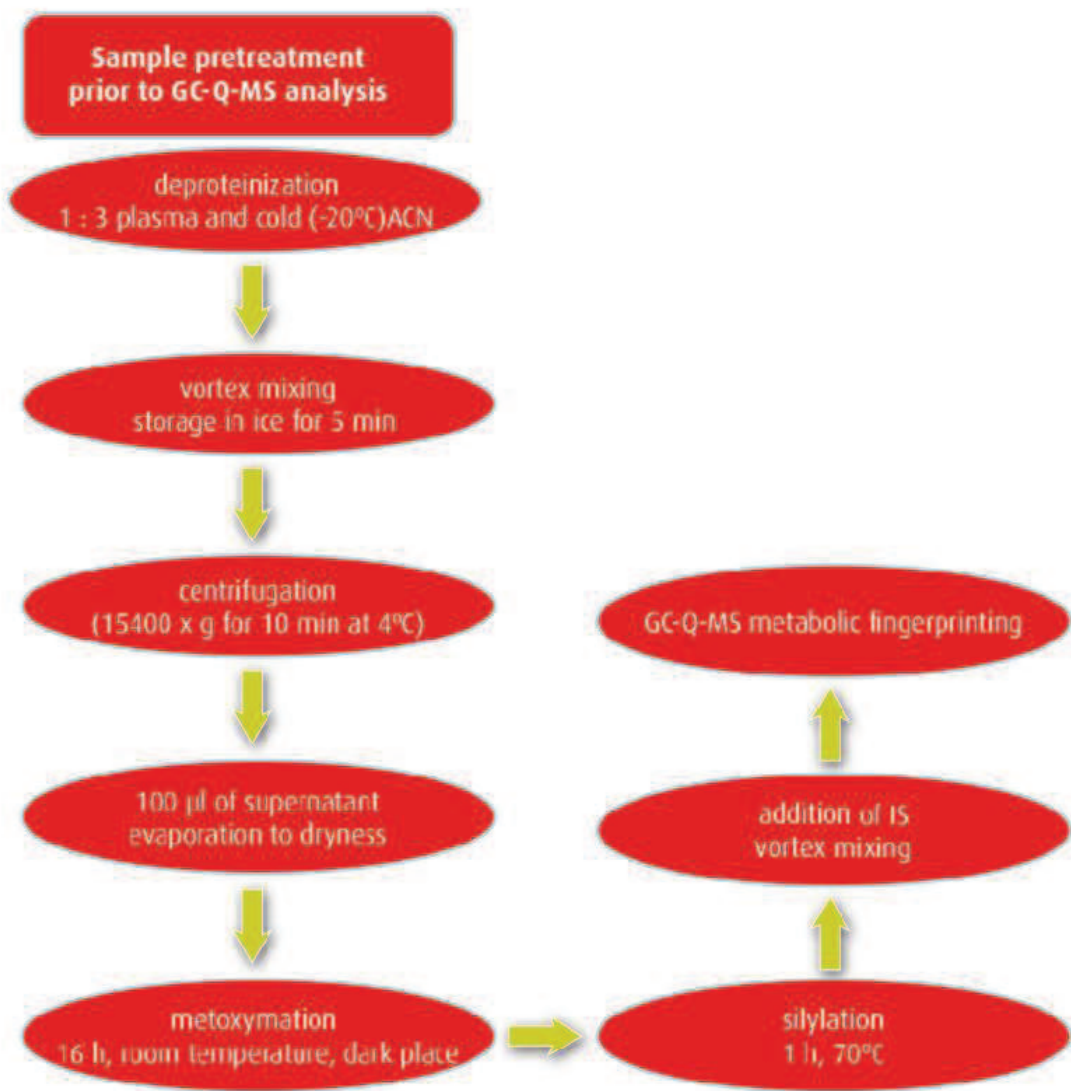


Figure 13. The simplified scheme of plasma sample pretreatment prior to GC-Q-MS metabolic fingerprinting.

5.5 Analytical platforms used in plasma metabolic fingerprinting

5.5.1. Plasma metabolic fingerprinting with LC-ESI-QTOF-MS

All analytical methods used in this doctoral thesis were developed and optimized in the Centre of Metabolomics and Bioanalysis (CEMBIO) of San Pablo University in Madrid. Plasma metabolic fingerprinting in an animal-based experiment was performed with UHPLC-ESI-QTOF-MS (UHPLC 1290 series, QTOF 6550, Agilent Technologies) system and the optimized parameters of chromatographic separation and ESI ion source and Q-TOF spectrometer were collected in Table 11. Human plasma samples were fingerprinted by use of HPLC-ESI-QTOF-MS apparatus (HPLC 1200 series, QTOF 6520, Agilent Technologies) and the optimized method parameters were shown in Table 12. Both experiments based on an animal and human model were performed in scan mode to detect as many as possible metabolites present in plasma samples. Additionally, due to the fact that, there are chemically diverse compounds in metabolome, which can create positive or negative ions, the plasma metabolic fingerprinting with LC-ESI-QTOF-MS was performed in both (positive ESI+ and negative ESI-) ionization modes in separate runs. Before each experiment, the nebulizer needle and shield of the capillary in the LC-ESI-QTOF-MS system were cleaned with 20% isopropanol solution in water. The LC-ESI-QTOF-MS instrument was calibrated with the use of tuning mixture including reference masses (ESI-LOW tuning mix) before plasma sample analyses. At the beginning of each sequence run 8 QC sample injections were performed to provide the column and system equilibration. To avoid analytical bias the plasma samples were analyzed in randomized order during the metabolic fingerprinting analyses. To monitor system stability, method reproducibility the regular (after every 5 plasma samples) injection of QC samples was performed. To provide mass measurement accuracy, the reference masses at m/z 121.0509 and m/z 922.0098 in positive ion mode; and m/z 112.9856 and m/z 1033.9881 in negative ion mode were continuously introduced by means of automated calibrant solution delivery system, during the plasma sample analyses.

Table 11. The parameters of optimized method for UHPLC-ESI-QTOF-MS based plasma metabolic fingerprinting.

Method parameter	ESI +	ESI (-)																																										
Chromatographic conditions																																												
Mobile phase	A: 0.1% formic acid in water B: 0.1% formic acid in acetonitrile	A: 0.1% formic acid in water B: 0.1% formic acid in acetonitrile																																										
Chromatographic column	Zorbax Extend RRH+ C18, 2.1 x 5.0 mm, 1.8 μ m	Zorbax Extend RRH+ C18, 2.1 x 5.0 mm, 1.8 μ m																																										
Mobile phase flow rate	0.6 mL/min	0.6 mL/min																																										
Mobile phase gradient	<table border="1"> <thead> <tr> <th>Time</th> <th>A %</th> <th>B%</th> </tr> </thead> <tbody> <tr> <td>0.0 min</td> <td>95</td> <td>5</td> </tr> <tr> <td>1.0 min</td> <td>95</td> <td>5</td> </tr> <tr> <td>7.0 min</td> <td>20</td> <td>80</td> </tr> <tr> <td>11.5 min</td> <td>0.0</td> <td>100</td> </tr> <tr> <td>12.0 min</td> <td>95</td> <td>5</td> </tr> <tr> <td>15.0 min</td> <td>95</td> <td>5</td> </tr> </tbody> </table>	Time	A %	B%	0.0 min	95	5	1.0 min	95	5	7.0 min	20	80	11.5 min	0.0	100	12.0 min	95	5	15.0 min	95	5	<table border="1"> <thead> <tr> <th>Time</th> <th>A %</th> <th>B%</th> </tr> </thead> <tbody> <tr> <td>0.0 min</td> <td>95</td> <td>5</td> </tr> <tr> <td>1.0 min</td> <td>95</td> <td>5</td> </tr> <tr> <td>7.0 min</td> <td>20</td> <td>80</td> </tr> <tr> <td>11.5 min</td> <td>0.0</td> <td>100</td> </tr> <tr> <td>12.0 min</td> <td>95</td> <td>5</td> </tr> <tr> <td>15.0 min</td> <td>95</td> <td>5</td> </tr> </tbody> </table>	Time	A %	B%	0.0 min	95	5	1.0 min	95	5	7.0 min	20	80	11.5 min	0.0	100	12.0 min	95	5	15.0 min	95	5
Time	A %	B%																																										
0.0 min	95	5																																										
1.0 min	95	5																																										
7.0 min	20	80																																										
11.5 min	0.0	100																																										
12.0 min	95	5																																										
15.0 min	95	5																																										
Time	A %	B%																																										
0.0 min	95	5																																										
1.0 min	95	5																																										
7.0 min	20	80																																										
11.5 min	0.0	100																																										
12.0 min	95	5																																										
15.0 min	95	5																																										
Time of analysis	15 min	15 min																																										
Column temperature	60°C	60°C																																										
Injection volume	0.5 μ l	0.5 μ l																																										
Ion source parameters																																												
Gas temperature	250°C	250°C																																										
Drying gas flow	12 L/min	12 L/min																																										
Nebulizer pressure	52 psig	52 psig																																										
Mass spectrometer parameters																																												
Capillary voltage	3000 V	3000 V																																										
Skimmer	65 V	65 V																																										
Fragmentor	175 V	250 V																																										
Octopole radio frequency voltage (OCT RF Vpp)	750 V	750 V																																										
Mass range (<i>m/z</i>)	50-1000	50-1100																																										
Scan rate	1 spectrum/1 second	1 spectrum/1 second																																										

Table 12. The parameters of optimized method for HPLC-ESI-QTOF-MS based plasma metabolic fingerprinting.

Method parameter	ESI +	ESI (-)																														
Chromatographic conditions																																
Mobile phase	A: 0.1% formic acid in water B: 0.1% formic acid in acetonitrile	A: 0.1% formic acid in water B: 0.1% formic acid in acetonitrile																														
Chromatographic column	Discovery HS C18 150 × 2.1 mm, 3 µm with guard column Discovery HS C18 20 × 2.1 mm, 3 µm	Discovery HS C18 150 × 2.1 mm, 3 µm with guard column Discovery HS C18 20 × 2.1 mm, 3 µm																														
Mobile phase flow rate	0.6 mL/min	0.6 mL/min																														
Mobile phase gradient	<table border="1" style="display: inline-table; border-collapse: collapse;"> <thead> <tr> <th>Time</th> <th>A %</th> <th>B%</th> </tr> </thead> <tbody> <tr> <td>0.0 min</td> <td>75</td> <td>25</td> </tr> <tr> <td>35.0 min</td> <td>5</td> <td>95</td> </tr> <tr> <td>36.0 min</td> <td>75</td> <td>25</td> </tr> <tr> <td>45.0 min</td> <td>75</td> <td>25</td> </tr> </tbody> </table>	Time	A %	B%	0.0 min	75	25	35.0 min	5	95	36.0 min	75	25	45.0 min	75	25	<table border="1" style="display: inline-table; border-collapse: collapse;"> <thead> <tr> <th>Time</th> <th>A %</th> <th>B%</th> </tr> </thead> <tbody> <tr> <td>0.0 min</td> <td>75</td> <td>25</td> </tr> <tr> <td>35.0 min</td> <td>5</td> <td>95</td> </tr> <tr> <td>36.0 min</td> <td>75</td> <td>25</td> </tr> <tr> <td>45.0 min</td> <td>75</td> <td>25</td> </tr> </tbody> </table>	Time	A %	B%	0.0 min	75	25	35.0 min	5	95	36.0 min	75	25	45.0 min	75	25
Time	A %	B%																														
0.0 min	75	25																														
35.0 min	5	95																														
36.0 min	75	25																														
45.0 min	75	25																														
Time	A %	B%																														
0.0 min	75	25																														
35.0 min	5	95																														
36.0 min	75	25																														
45.0 min	75	25																														
Time of analysis	45 min	45 min																														
Column temperature	60°C	60°C																														
Injection volume	10 µl	10 µl																														
Ion source parameters																																
Gas temperature	330°C	330°C																														
Drying gas flow	10.5 L/min	10.5 L/min																														
Nebulizer pressure	52 psig	52 psig																														
Mass spectrometer parameters																																
Capillary voltage	3000 V	4000 V																														
Skimmer	65 V	65 V																														
Fragmentor	175 V	175 V																														
Octopole radio frequency voltage (OCT RF Vpp)	750 V	750 V																														
Mass range (<i>m/z</i>)	50-1000	50-1100																														
Scan rate	1 spectrum/1 second	1 spectrum/1 second																														

5.5.2. Plasma metabolic fingerprinting with GC-Q-MS

The GC-Q-MS based plasma metabolic fingerprinting method applied in the doctoral thesis was developed and optimized in the Centre of Metabolomics and Bioanalysis (CEMBIO) of San Pablo University in Madrid. The optimized method was used for plasma metabolic fingerprinting both in an animal and human based experiment. To obtain global metabolites profile, 2 μ l of previously derivatized plasma samples were injected in split mode onto a GC-Column DB5-MS (30 m length, 0.25 mm i.d., 0.25 μ m film 95% dimethyl/ 5% diphenylpolysiloxane) with an integrated pre-column (10 m J&W) from Agilent Technologies. The optimized carrier gas (He) flow rate and injector temperature were 1 mL/min and 250 °C, respectively. Split ratio was set from 1:5 to 1:10 with 3 to 10 mL/min He flow into deactivated glass-wool split liner. Temperature gradient was programmed as follows: the initial oven temperature was set at 60 °C (held for 1 min), then increased to 325 °C at 10 °C/min, finally a cool-down period was used for 10 min before the next plasma sample injection. Total analysis time was 37.5 min. Detector transfer line, filament source and quadrupole temperatures were optimized at 290 °C, 230 °C and 150 °C, respectively. Voltage for electron impact (EI) ionization source was 70 eV. Mass spectrometer operated in scan mode over a mass range of 50-600 m/z at 2 spectra/s. Before each metabolomics experiment the calibration and tune of GC-Q-MS system was performed. Additionally, the injection needle was cleaned with LC-MS grade isopropanol and heptane. The septum and liner in the injection port were changed after 100 and 250 injections, respectively. Before plasma samples analyses, the n-fatty acid methyl ester mixture (n-FAMES C8-C22) analysis was performed for further retention indices calculation. Both, in an animal and human based experiment, the derivatized plasma samples were fingerprinted in the randomized order and the regular injection of QC samples (after every 6 plasma samples) was performed to control sample pretreatment reproducibility and system's stability.

5.6 The data extraction and processing methods

5.6.1. Data acquired with LC-ESI-QTOF-MS plasma metabolic fingerprinting

The raw data obtained in both animal and human based study was reprocessed with DA reprocessor software (B.05.00, Agilent Technologies) to extract all compounds detected in plasma metabolic fingerprints. The data extraction method was created with the use of the molecular feature extraction (MFE) algorithm available in MassHunter Qualitative Analysis B.05.00 software (Agilent Technologies). The MFE tool groups ions based on their charge-state, isotopic distribution, the adducts or dimers presence and creates a list of all possible compounds occurred in the full TOF mass scan range. The MFE algorithm allows to clean up the obtained raw data from background noise and artifacts. The background noise threshold was 200 counts and possible adducts included: +H, +Na, +K for positive ionization mode, and: -H, +HCOO for negative ionization mode. Neutral loss of water was considered in both ionization modes. After data extraction, for each plasma sample, the list of all detected components described by monoisotopic mass, retention time and intensity was obtained. Next, due to mass accuracy and retention time shift (because of analytical variation or matrix effect) during the analyses of all plasma samples in particular experiment, the peak alignment is required to ensure that the same component (ideally metabolite) is pointed as the same entity in all samples. Thus, the data extracted for all plasma samples were multialigned by means of MassProfiler Professional Software (B.12.01, Agilent Technologies). The alignment parameters for data acquired with UHPLC-ESI-QTOF-MS platform in an animal based experiment were 0.5% and 20 ppm for retention time and mass correction, respectively. For data obtained in human based study with using HPLC-ESI-QTOF-MS system, the alignment parameters were set to 1.0% and 20 ppm for retention time and mass correction, respectively. Then, prior to statistical analysis, a compound filtration was employed to remove random signals from the data matrix and select only metabolic variables that may represent biological meaning. Therefore the aligned data matrices were filtered to remain only these potential compounds that were present in all or most (at least 90%) of the samples in one of the compared groups (in the control or pulmonary arterial hypertension group).

5.6.2. Data acquired with GC-Q-MS plasma metabolic fingerprinting

During either animal or human plasma metabolic fingerprinting study with GC-Q-MS platform, the data was acquired with Agilent MSD ChemStation Software (E.02.00.493, Agilent Technologies). The raw data deconvolution and compound identification were automatically performed with Automated Mass Spectral Deconvolution and Identification System (AMDIS) software. The first data reprocessing aims to retention index (RI) calculations based on RI calibration file containing information about retention time (RT) and RI of the fatty acid methyl esters present in standard mixture which was analyzed at the beginning of the plasma samples sequence. The proper selection of compounds used for RI calculation should be considered to cover total time of plasma metabolic fingerprinting analysis. The composition of RI calibration file used in both animal and human based experiment was shown in Table 13. RI for each detected compound was calculated based on the RT and RI of the closest eluting fatty acid methyl ester. RI of particular compound represents the constant which in relative to its RT is less sensitive to analytical variation. Therefore, all the deconvoluted compounds were identified based on retention time, retention index and mass spectrum. According to mass spectrum and RI similarity to those presented in the Fiehn RTL library, the list of identified compounds for each plasma sample was obtained. Additionally, mass spectra of possible compounds, which were not available in the Fiehn RTL library, were searched through NIST mass spectral library. Based on data including RT, target and qualifier m/z values, the in-house target library was created and used in second data processing. Then, the multialignment was performed with the use of Mass Profiler Professional software (B.12.01., Agilent Technologies). Subsequently, the obtained data matrix was filtered according to compound frequency and compounds presented in at least 75% of all samples in the one of compared groups were remained. During the data normalization step, the intensities of these compounds were divided by intensity of the IS in particular plasma sample. The normalization step was performed before further statistical analysis.

Table 13. The characteristics of compounds included in the RI calibration file used for GC-Q-MS data processing.

Compound	RI value	RT value (min)
[C8] Methyl caprylate	800	7.745
[C10] Methyl caprate	1000	10.579
[C12] Methyl laurate	1200	13.193
[C14] Methyl myristate	1400	15.552
[C16] Methyl palmitate	1600	17.967
[C18] Methyl stearate	1800	19.649
[C20] Methyl eicosonoate	2000	21.444
[C22] Methyl docosonate	2200	23.102

5.7 Univariate and multivariate statistical data analysis

To find the statistically significant differences between control and pulmonary hypertension groups either in animal or human model, first, an univariate statistical analysis was applied. In case of the variables selected after processing and filtration steps in the animal study, normality of distribution was checked with Shapiro-Wilk test. The group variances homogeneity was assessed with Levene's test. For normally distributed data paired standard t test (homogeneity of group variances) or paired Welch's t test (heterogeneity of group variances) were applied. For variables without normal distribution, the nonparametric U Mann-Whitney test was used. In case of data obtained in human based experiment, instead of paired t tests, the unpaired standard or Welch's t tests were applied. The univariate statistical calculations were performed with Matlab 2007b (Mathworks, Natick, MA, USA) and Mass Profiler Professional B.12.01. (Agilent Technologies) software. Subsequently, the multivariate statistical analysis was performed. As a first approach, the Principal Component Analysis (PCA) was applied. PCA, as an unsupervised exploratory method was employed to check the quality of the analysis. For this purpose all the aligned variables detected both in LC-ESI-

QTOF-MS or GC-Q-MS were treated with quality assurance requirements [103], filtered according to their presence in QC samples. The compounds with frequency <50% in all QC samples were removed. Then, the variation of these variables responses in QC samples was also considered and expressed as coefficient of variation (CV). Thus, the compounds with CV<30% for LC-ESI-QTOF-MS data or CV<40% for GC-Q-MS data were used for PCA model plotting. The QC samples grouping in PCA plot confirms the system stability during sample analyses and ensures that group separation is related to biological, not analytical variation. All multivariate models were built with SIMCA P+ 13.03. software (Umetrics, Umea, Sweden). PCA as a classification method was applied to detect group classification and to reveal potential outliers by using Hotelling's T² range plot.

Afterwards, the supervised partial least squares discriminant analysis (PLS-DA) was applied to select potential metabolites that contributed the most into group discrimination which were assessed with jackknife (JK) confidence intervals. In the case of LC-ESI-QTOF-MS data only the statistically significant variables selected in an univariate analysis were used to build PLS-DA model. Then the JK method was applied to reduce the false positive results. Therefore, only variables that passed through both univariate and multivariate statistical analysis were considered for further compound identification. Since, in the case of GC-Q-MS data, the metabolites were firstly identified by Fiehn RTL, in-house target or NIST libraries, all compounds after data deconvolution, processing, normalization and filtration were applied to PLS-DA plotting. Therefore, the metabolites that were statistically significant in univariate test or JK criteria were included in biochemical interpretation. The intensities of selected variables were log-transformed and Pareto scaled before building independent multivariate PCA or PLS-DA models. The obtained multivariate models were described by R² and Q² parameters, which correspond to explained and predicted variance, respectively. Additionally, the obtained PLS-DA models were validated by leave-one-out cross validation (LOOCV) approach with the use of Matlab 2007b software. The datasets obtained in each metabolic fingerprinting experiment were divided into training (70% of all samples) and test sets (30% of all samples) using the Kennard and Stone algorithm and the percentages of samples which were correctly classified by each PLS-DA model were calculated. In addition, the sensitivity and specificity of the obtained discriminant models were also assessed. The training set was

used for validation procedure whereas the predictive value of the previously built classification models were determined using the test set.

5.8 Metabolite identification and biochemical interpretation

The identification of metabolites selected in both univariate and multivariate statistical analysis is strictly related to the analytical platform applied for plasma metabolic fingerprinting experiment. In the case of GC-Q-MS data, due to standardization (70 eV) and reproducibility of EI mode there are some universal mass spectral libraries containing fragmentation patterns of numerous chemical compounds. In both an animal and human models of pulmonary hypertension, the metabolites which differentiated the compared groups were identified based on comparison of their RT, RI and mass spectra with those available both in Fiehn RTL library, in-house target plasma library and NIST library. For each metabolite detected in plasma metabolic fingerprints with the use of GC-Q-MS platform, the target and three qualifier ions were chosen to provide the reliable identification. In the case of data obtained with LC-ESI-QTOF-MS technique, the accurate masses of variables represented the significant differences between compared groups were firstly searched through publicly available databases including:

- HMDB (www.hmdb.ca),
- METLIN (www.metlin.scripps.edu),
- KEGG (www.genome.jp/kegg),
- LIPIDMAPS (www.lipidmaps.org).

Moreover, the in-house developed search browser: CEU MassMediator (ceumass.eps.uspceu.es/mediator) was used for simultaneous searching through all commercially available databases listed above. However, the databases searching provided only the putative metabolites identification.

Therefore, the identity of metabolites found in databases was confirmed with fragments obtained in LC-MS/MS analysis with use of the same QTOF in single ion monitoring (SIM) mode. The fragmentation experiments were conducted with the same chromatographic conditions as the first plasma metabolic fingerprinting analysis in scan mode.

The selected ions were targeted to collision-induced dissociation (CID) and the fragmentation was performed based on previously assessed accurate masses and retention times. The collision energy used for fragmentation of particular compound was calculated by following formula:

$$\text{Collision energy} = [(\text{slope}) \times (\text{m/z})] / 100 + \text{offset}$$

where slope=3.6, offset=4.8

The comparison of fragmentation patterns obtained in plasma samples with those presented in databases provided the metabolites identification. In this case, the METLIN database is especially useful for identity confirmation due to the fact that mass spectra presented in this database were obtained in fragmentation experiments performed with the QTOF manufactured by the Agilent company. In the case of standards availability, the metabolites identification was confirmed by comparison of RT, isotopic distribution, and fragments of commercially available reagents with those detected in plasma samples either in an animal or human model of pulmonary hypertension.

Afterwards, the biochemical interpretation was performed for altogether identified metabolites with both LC-ESI-QTOF and GC-Q-MS platforms. Therefore, the main aim was to find connections between biochemical pathways and statistically significant metabolites are involved. The KEGG and ExPASy databases were used for biochemical pathways analysis and interpretation. The connections between various and distant biochemical pathways provided the global insight into metabolites changes that can be involved in pathological processes of pulmonary hypertension.

IV. RESULTS AND DISCUSSION

6. Plasma metabolic fingerprinting with LC-ESI-QTOF-MS and GC-Q-MS in an animal model of acute pulmonary hypertension

Sixteen pig plasma samples were divided into two compared groups: a baseline group before PE induction (n=8) and acute (1h after PE induction) PE group (n=8) with the confirmed pulmonary hypertension (PH). The pig plasma samples were analyzed by metabolic fingerprinting approach with the use of UHPLC-ESI-QTOF-MS platform in positive (ESI+) and negative (ESI-) ionization modes. As a complementary technique, GC-Q-MS was applied. The examples of chromatograms representing the pig plasma metabolic fingerprints obtained in both analytical platforms were displayed in Figures 14, 15 and 16 [102].

To check the quality of the analysis and method reproducibility all pig plasma samples and QC samples were plotted in PCA models. For datasets obtained in UHPLC-ESI(+)-QTOF-MS, UHPLC-ESI(-)-QTOF-MS and GC-Q-MS, the separate multivariate models were built. The datasets used in PCA plotting were filtered in accordance to quality assurance requirements described in section 5.7. and consisted of 1252, 1099 and 69 variables for UHPLC-ESI(+)-QTOF-MS, UHPLC-ESI(-)-QTOF-MS and GC-Q-MS data, respectively. The close clustering of the QC samples in all multivariate models confirmed the system stability and method reproducibility during each metabolic fingerprinting experiment (Figure 17). In addition, no significant outliers according to Hotelling's T² range plot were observed. The outlier detection is crucial before the further discriminant multivariate analysis, because they can lead to model destabilization and affect the final statistical results. The cluster of QC group confirmed that groups separation is caused by sample biological content not analytical variation.

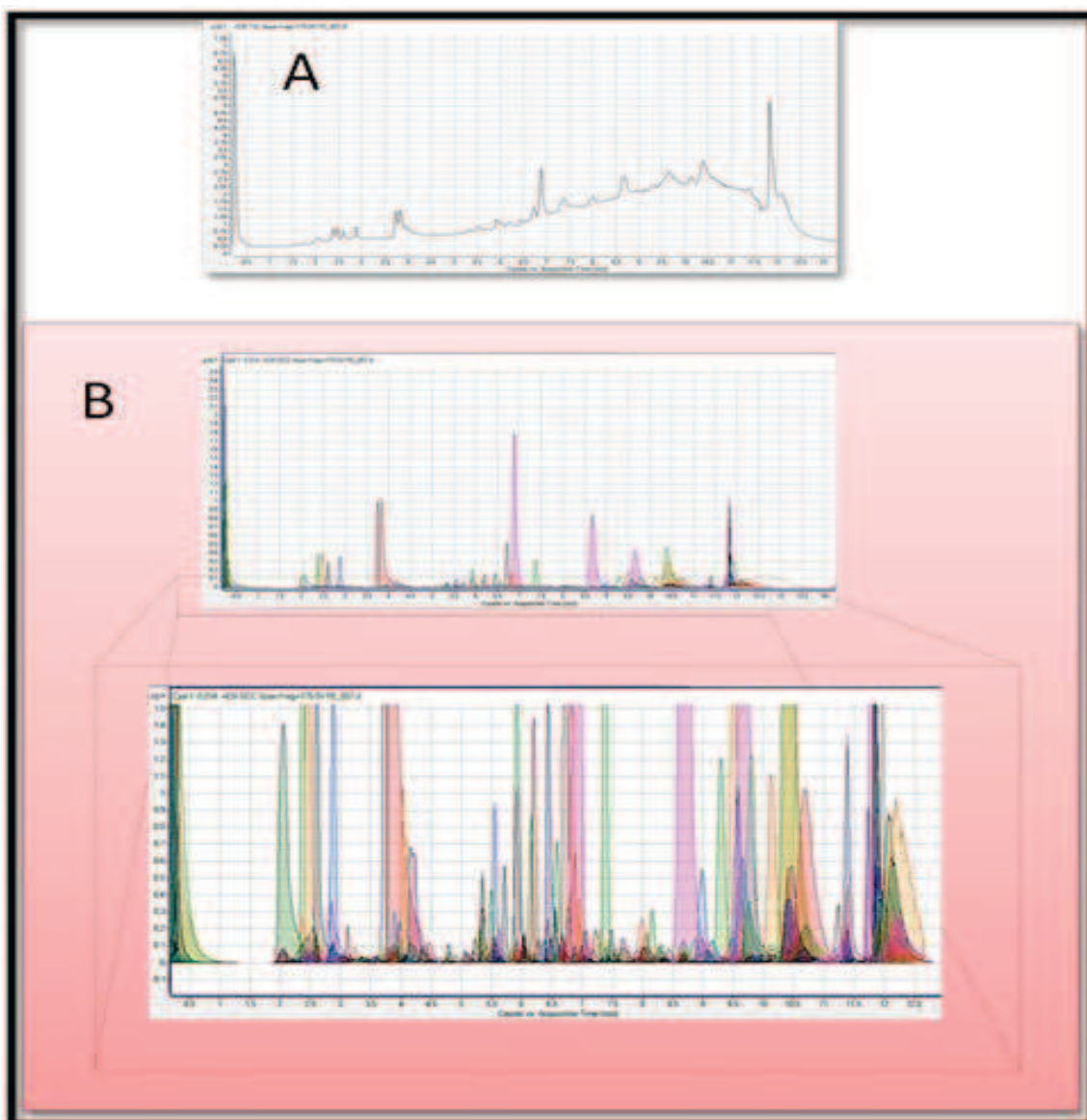


Figure 14. Representative UHPLC-ESI(+)-QTOF-MS chromatogram of pig plasma metabolic fingerprint from one pig plasma extract. A: Total Ion Chromatogram (TIC); B: overlay of all the individual features obtained after Molecular Feature Extraction (MFE) represented as extracted compound chromatogram (ECC) [102].

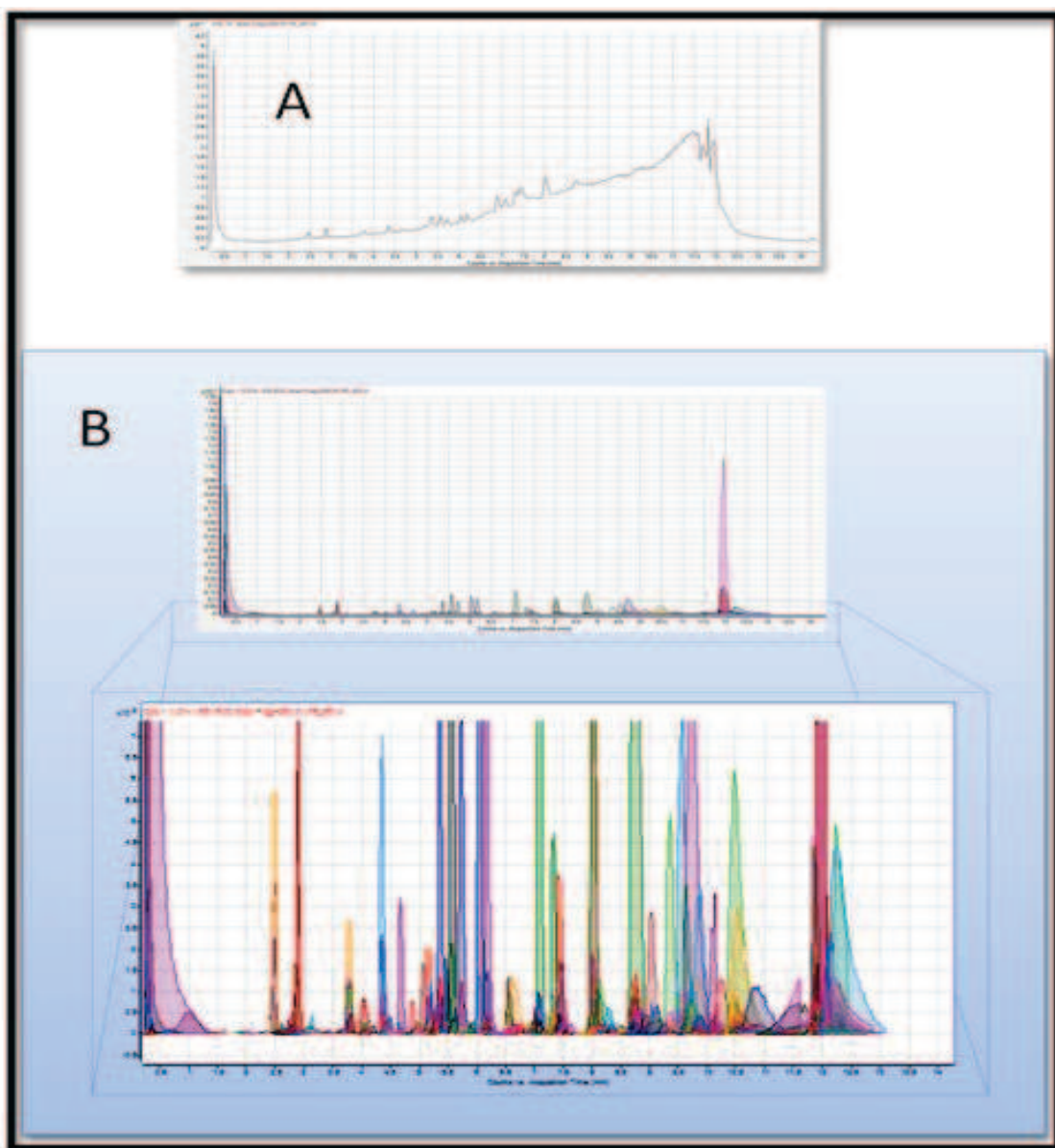


Figure 15. Representative UHPLC-ESI(-)-QTOF-MS chromatogram of pig plasma metabolic fingerprint form one pig plasma extract. A: Total Ion Chromatogram (TIC);

B: overlay of all the individual features obtained after Molecular Feature Extraction (MFE) represented as extracted compound chromatogram (ECC) [102].

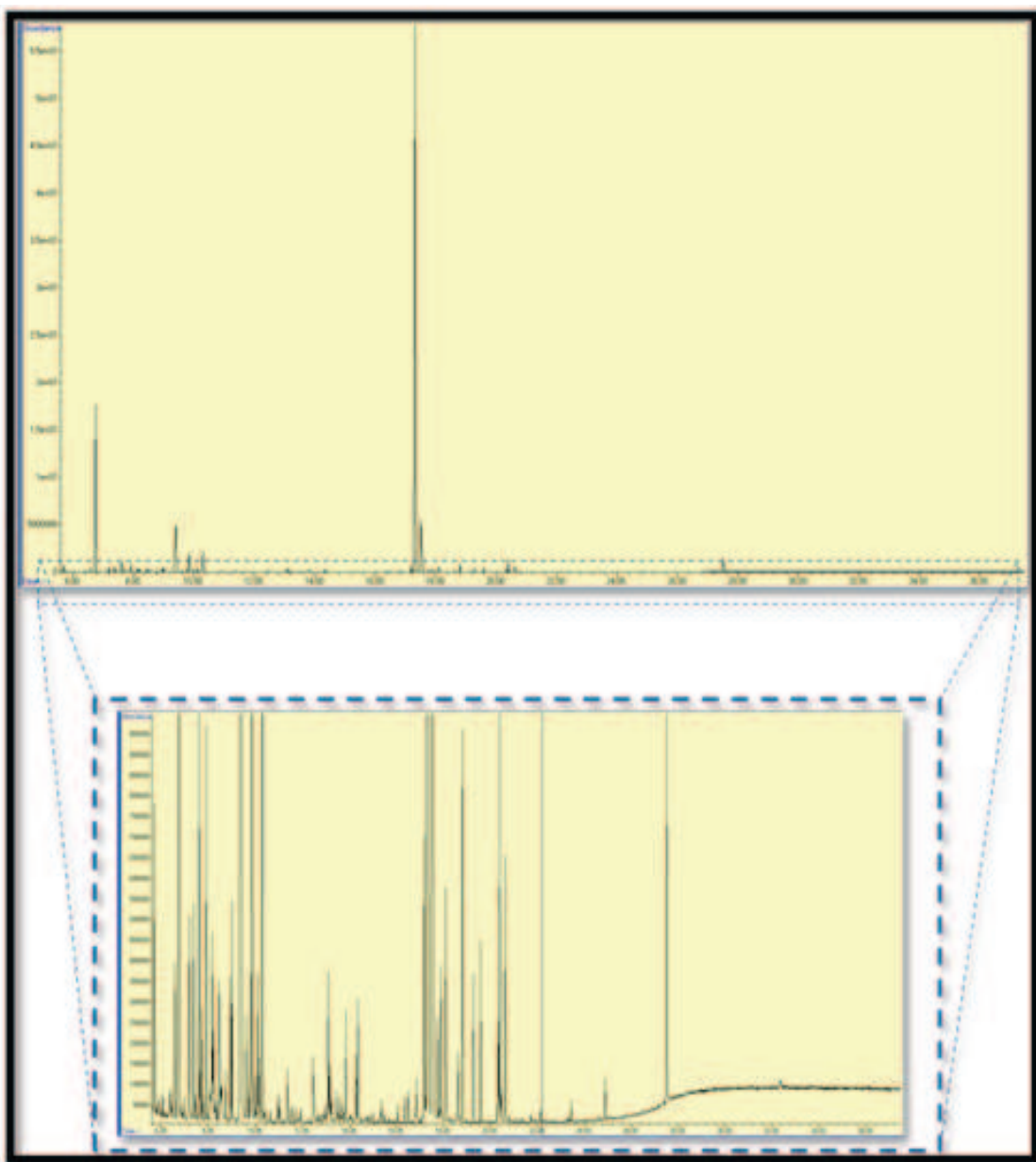
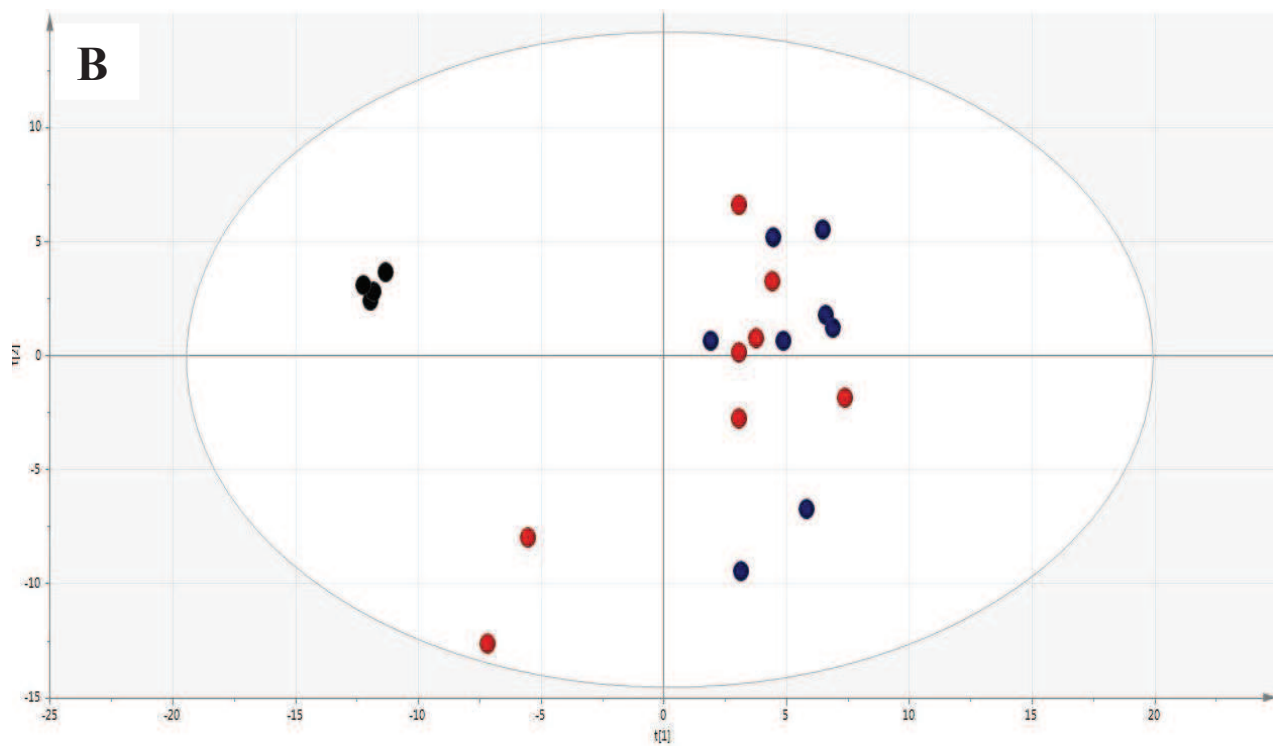
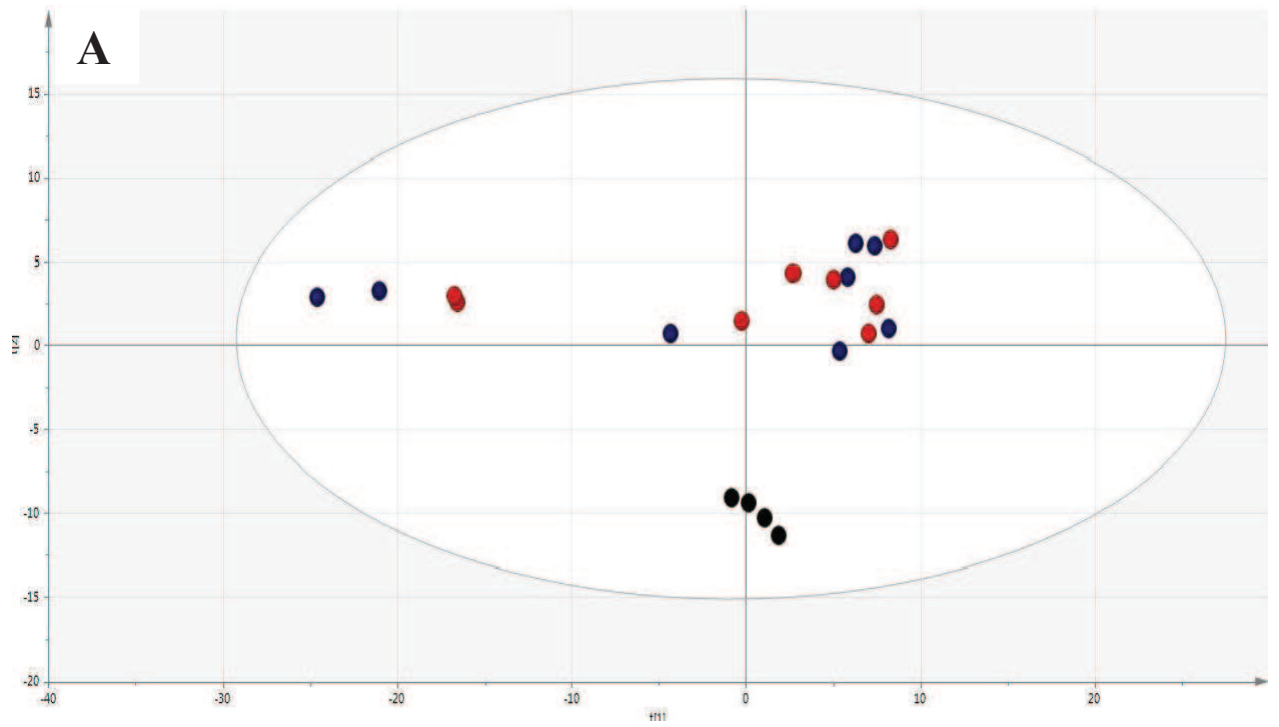


Figure 16. Representative GC-Q-MS Total Ion Chromatogram (TIC) of pig plasma metabolic fingerprint form one pig plasma extract [102].



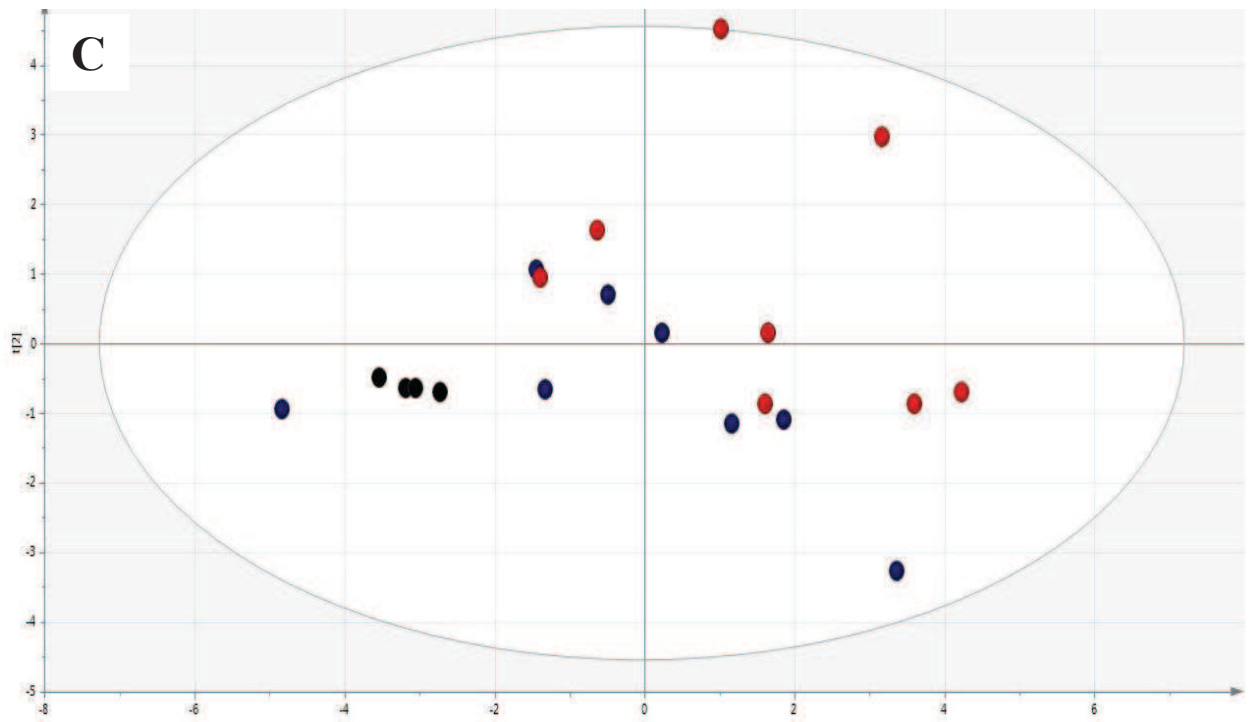


Figure 17. Principal Component Analysis to verify quality of chromatographic analysis in all plasma metabolic fingerprinting experiments.

A) Scores plot for a PCA model built with the data set obtained in UHPLC-ESI(+)-QTOF-MS. Quality parameters for the model: explained variance $R^2 = 0.569$, predicted variance $Q^2 = 0.451$.

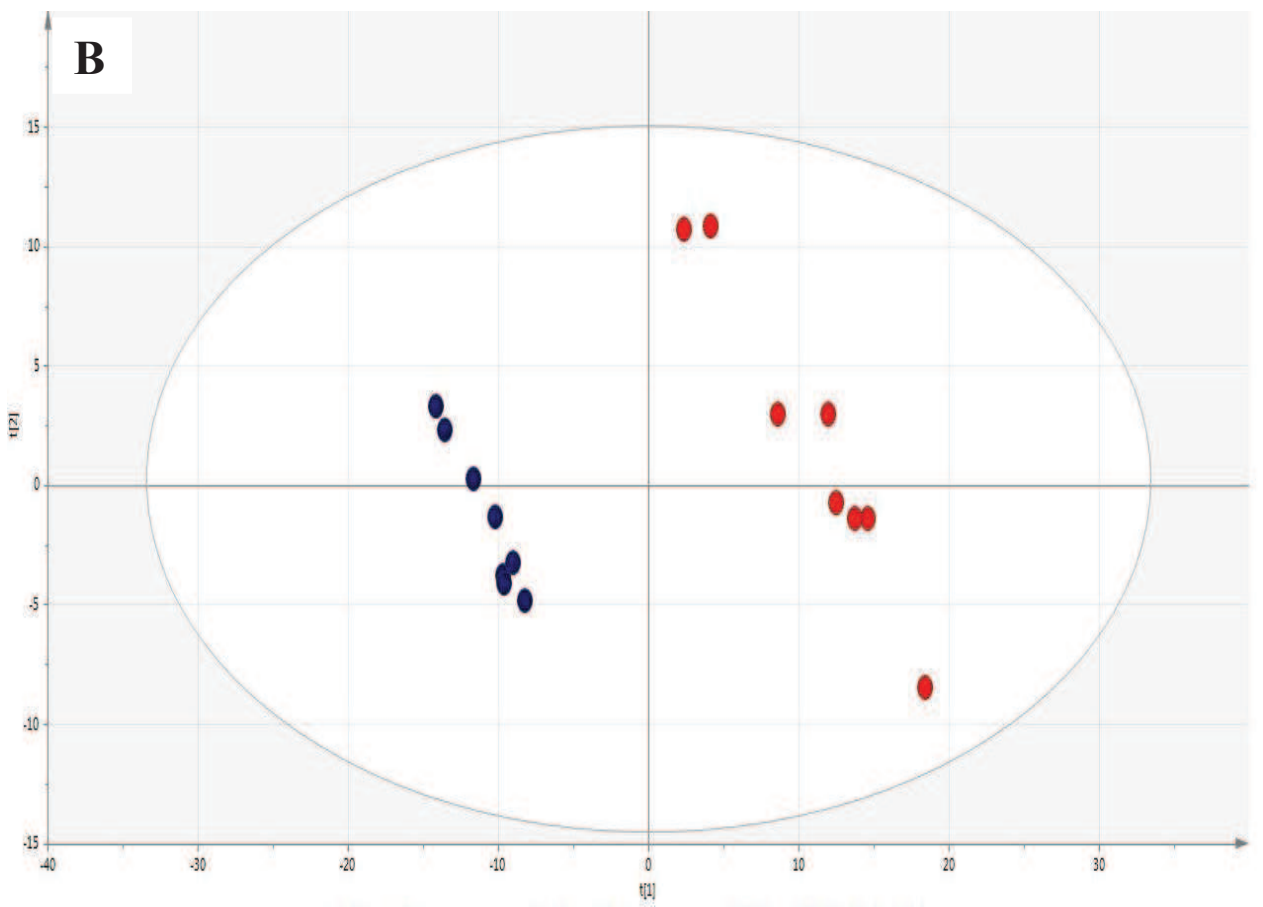
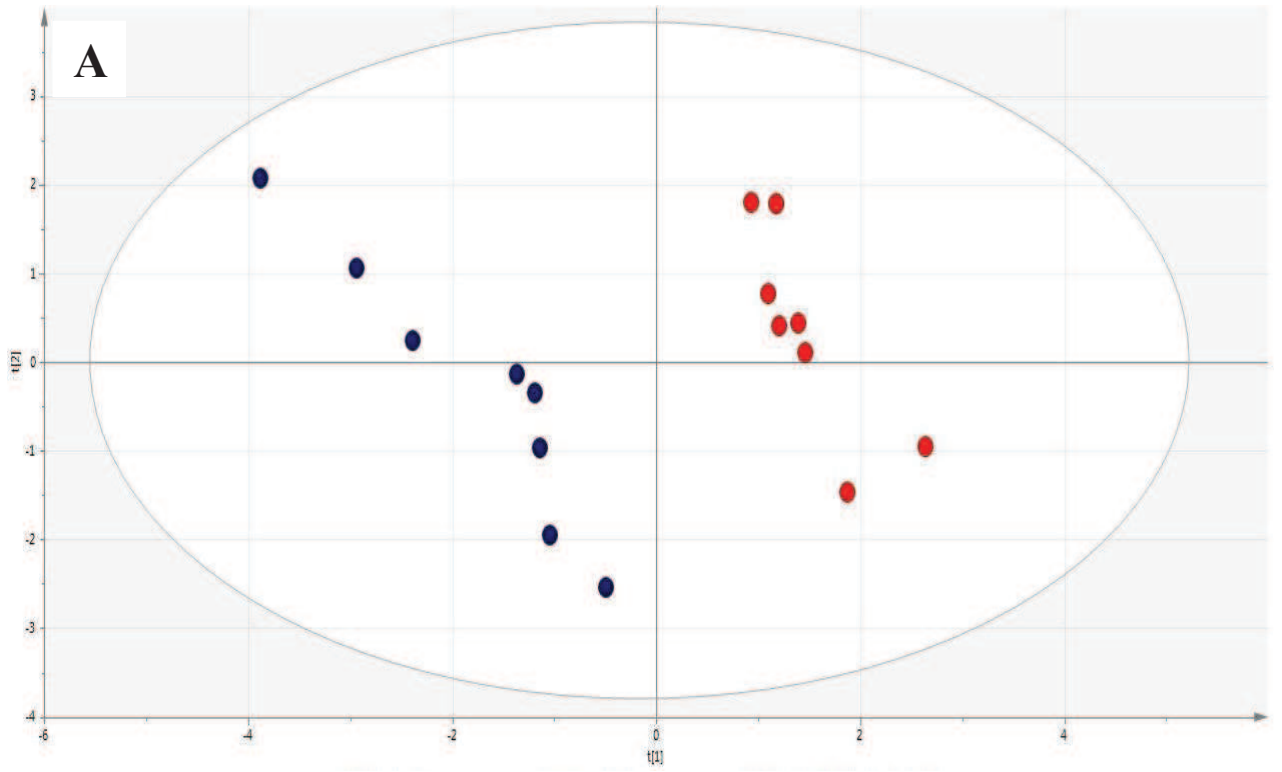
(B) Scores plot for a PCA model built with the data set obtained in UHPLC-ESI(-)-QTOF-MS. $R^2 = 0.556$, $Q^2 = 0.308$.

(C) Scores plot for a PCA model built with the data set obtained in GC-Q-MS. $R^2 = 0.649$, $Q^2 = 0.368$.

QC samples have been marked as black spots. Animal groups before and after acute PE induction have been marked as blue spots or red spots, respectively.

6.1 Univariate and multivariate statistical analysis

After data reprocessing and multialignment the obtained datasets consisted of 30191 or 13696 features for UHPLC-ESI(+)-QTOF-MS and UHPLC-ESI(-)-QTOF-MS, respectively. In the case of GC-Q-MS data, 144 compounds were aligned in all pig plasma samples. Then, to clean up the obtained datasets from random signals, the filtration step was applied. For either UHPLC-ESI(+)-QTOF-MS or UHPLC-ESI(-)-QTOF-MS datasets, the 100% filtration limit was used what meant that only features presented in all samples in at least one of the group (i.e. in all samples before or in all samples after acute PE) were included in univariate statistical analysis. In the case of GC-Q-MS data matrix, the 75% frequency criterion was applied due to complexity of derivatization process which can produce various derivatives of the same compound. After filtration step the datasets were reduced to 1482 and 842 features for UHPLC-ESI(+)-QTOF-MS and UHPLC-ESI(-)-QTOF-MS, respectively as well as 94 compounds for GC-Q-MS. Subsequently, the univariate statistical analysis employed both paired *t* test and paired U Mann-Whitney test. As a result 68 and 78 variables as well as 8 compounds, in the case of UHPLC-ESI(+)-QTOF-MS, UHPLC-ESI(-)-QTOF-MS and GC-Q-MS data, respectively, were selected as significantly changed between compared groups. Then, only significant variables were used to build multivariate supervised PLS-DA models for UHPLC-QTOF-MS data from both polarity modes. Subsequently, the JK confidence interval criteria were applied as a multivariate statistical test to select variables which are mainly involved in group separation. Therefore, only variables that passed through both univariate and multivariate statistical criteria were included in the metabolite identification. In the case of GC-Q-MS, all variables after data filtration step were used to build the PLS-DA models and then the metabolites that were statistically significant according to univariate tests or JK criteria were considered in biochemical interpretation. The PLS-DA models for three independent datasets were built with SIMCA P+ 13.03 software and were presented in Figure 18.



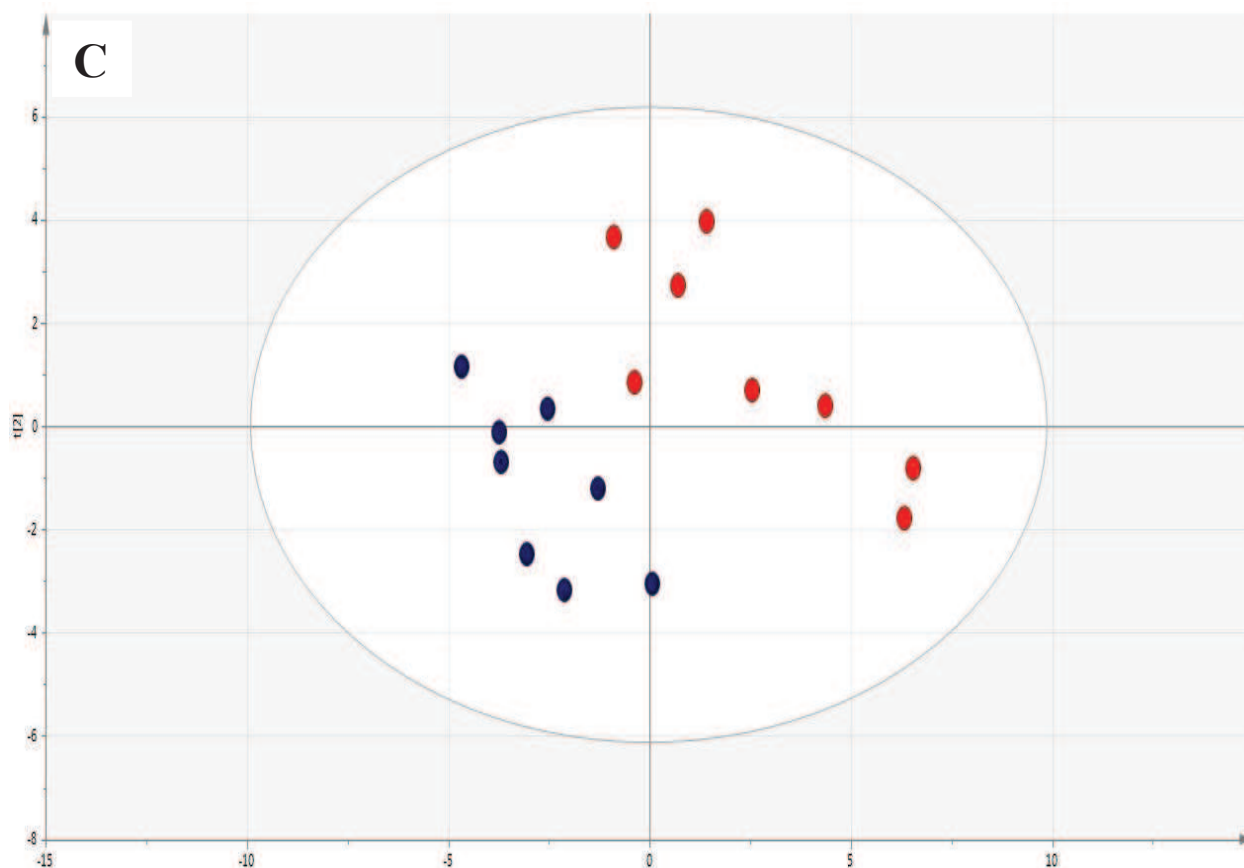


Figure 18. PLS-DA plots for plasma metabolic fingerprints obtained before and after acute PE induction.

(A) PLS-DA model ($R^2 = 0.959$, $Q^2 = 0.713$) for significantly changed variables detected in pig plasma with UHPLC-ESI(+)-QTOF-MS.

(B) PLS-DA model ($R^2 = 0.999$, $Q^2 = 0.984$) for significantly changed variables detected in pig plasma with UHPLC-ESI(-)-QTOF-MS.

(C) PLS-DA model ($R^2 = 0.924$, $Q^2 = 0.402$) for compounds detected in pig plasma with GC-Q-MS, after data filtration.

The animal groups before and after acute PE have been marked as blue or red spots, respectively.

6.2 Discriminant models validation

To avoid overfitting and to check the predictive value of the obtained PLS-DA models, the leave-one-out cross-validation (LOOCV) method was applied with the use of Matlab 2007b software. The procedure of LOOCV approach was in detail described in section 5.7. The correct classification rate (CCR) for training and test sets was calculated for each PLS-DA model. The sensitivity and specificity of particular independent discriminant model were also calculated based on confusion matrices. The predictive value (Q) of each PLS-DA model was assessed based on test sets prediction by the model built on training sets. The results of prediction and LOOCV procedure for three independent PLS-DA models were collected in Table 14.

Table. 14. The results of prediction and LOOCV procedure for independent discriminant models obtained for data from pig plasma metabolic fingerprinting experiments.

PLS-DA models	LV	CCR_training set	CCR_test set	Q
UHPLC-ESI(+)-QTOF-MS data	2	82%	100%	100%
UHPLC-ESI(-)-QTOF-MS data	2	100%	100%	100%
GC-Q-MS data	2	64%	80%	75%

LV=latent variables used in PLS-DA construction

Based on LOOCV results the confusion matrix of each PLS-DA model was built. Then, the sensitivity and specificity were calculated with the use of following formulas:

$$\text{Sensitivity} = \text{TP} / (\text{TP} + \text{FN})$$

$$\text{Specificity} = \text{TN} / (\text{TN} + \text{FP})$$

$$\text{Positive Predictive Value (PPV)} = \text{TP}/(\text{TP}+\text{FP})$$

$$\text{Negative Predictive Value (NPV)} = \text{TN}/(\text{TN}+\text{FN})$$

In the formulas presented above the shortcuts as TP, TN, FN, FP mean:

- TP (true positive) – the objects belonging to pulmonary hypertension (PH) group and were correctly classified to this group;
- TN (true negative) – the objects belonging to baseline (B) group and were correctly classified to this group;
- FN (false negative) – the objects belonging to pulmonary hypertension (PH) group and were incorrectly classified to B group;
- FP (false positive) – the objects belonging to baseline (B) group and were incorrectly classified to PH group.

The confusion matrices, sensitivities and specificities of each discriminant model were presented in Tables 15, 16 and 17.

Table 15. The confusion matrix, sensitivity and specificity of PLS-DA model based on UHPLC-ESI(+)-QTOF-MS data set.

		Predicted		Sensitivity	Specificity	PPV	NPV
		B	PH				
Actual	B	8	0	0.75	1.0	1.0	0.8
	PH	2	6				

Table 16. The confusion matrix, sensitivity and specificity of PLS-DA model based on UHPLC-ESI(-)-QTOF-MS data set.

		Predicted		Sensitivity	Specificity	PPV	NPV
		B	PH				
Actual	B	8	0	1.0	1.0	1.0	1.0
	PH	0	8				

Table 17. The confusion matrix, sensitivity and specificity of PLS-DA model based on GC-Q-MS data set.

		Predicted		Sensitivity	Specificity	PPV	NPV
		B	PH				
Actual	B	5	3	0.75	0.63	0.67	0.71
	PH	2	6				

6.3 Metabolite identification

The information about the metabolites, significantly changed in pig plasma during the acute phase of PH, which were identified either in UHPLC-(ESI+)-QTOF-MS or UHPLC-(ESI-)-QTOF-MS were collected in Table 18. For each particular metabolite, the RT, the measured monoisotopic mass, mass found in database, mass error, detection mode, formula, *p*-value, percentage of change in PH group, coefficient of variation (CV) for QC samples and identification based on fragments analysis, were included. The mass error was calculated with the following formula:

$$\text{Mass error (ppm)} = [(M_{\text{DB}} - M_{\text{EXP}}) / M_{\text{EXP}}] \times 1000000$$

Where: M_{DB} means mass found in database, M_{EXP} means experimental mass.

In turn, the percentage of change in PH group in comparison to baseline (B) group was calculated with the following formula:

$$\% \text{ change} = [(\text{Average PH} - \text{Average B}) / \text{Average B}] \times 100$$

Where the average PH and average B correspond to average of metabolite intensity in PH and B group, respectively.

In the case of metabolites identified in GC-Q-MS and significantly changed in pig plasma in acute phase of PH, the information concerning RT, RI, target ion, qualifier ions, *p*-value, percentage of change in PH group and CV for QC samples were presented in Table 19.

Table 18. Metabolites significantly changed in pig plasma during acute phase of PH, identified during UHPLC-QTOF-MS metabolic fingerprinting experiment.

Name	Formula	Mass (DB)	RT (min)	Ionization mode	Measured mass	Mass error (ppm)	p-value	change PH vs B [%]	QCs CV [%]	Identification
docosatetraenoic acid	C22H36O2	332.2715	7.4	negative	332.2719	-1.0	0.0442	-56	7	331.2641, 313.2063, 285.1474, 265.1416, 196.8666, 112.9835
docosapentaenoic acid	C22H34O2	330.2559	7.1	negative	330.2562	-1.0	0.0341	-50	7	329.2484, 311.2605, 285.1487, 183.0122, 79.9588, 61.9881
leukotriene C4	C30H47N3O9S	625.3033	6.1	positive	625.2949	-3.5	0.0002	38	15	Database, isotopic distribution
hydroxy-oxo-hexadecanoic acid	C16H30O4	286.2144	5.0	negative	286.2148	-1.4	0.0003	-25	9	285.207, 267.207, 223.2373, 160.8399
dihydroxyoctadecadienoic acid (dHODE)	C18H32O4	312.2300	5.3	negative	312.2308	-2.4	0.0073	-106	2	367.2617, 311.1687, 183.0120, 119.0503
hydroxy-octadecenoic acid (HOME)	C18H34O3	298.2509	5.7	negative	298.2516	-3.0	0.0235	-189	5	297.2420, 279.2270, 252.3270, 183.1352, 101.0628
oxo-heptadecatrienoic acid	C17H26O3	278.1882	5.1	negative	278.1888	-2.2	0.0081	-97	20	277.181, 259.181, 233.8374, 215.0941, 166.8653, 99.9252
dodecadienoic acid	C12H20O2	196.1463	4.5	negative	196.1467	-2.0	0.0043	-54	6	195.1386, 176.9294, 150.8409, 136.3264, 61.9880
methyl-tridecanedioic acid	C14H26O4	258.1831	4.4	negative	258.1839	-3.0	0.0002	-42	9	257.8169, 239.8047, 221.8410, 193.8308, 165.8647, 99.9248
sphingosine	C18H33NO2	295.2511	5.0	positive	295.2526	-5.0	0.0001	79	8	296.2604, 265.0220, 207.0349 109.1016, 95.0858
Cer(d18:1/22:0)-1P	C46H90NO11P	863.6252	9.1	positive	863.6156	9.0	0.0192	-33	19	Database, isotopic distribution
SM(d18:1/23:0)	C46H93N2O6P	800.6771	7.8	positive	800.6811	-5.0	0.0002	-60	19	801.6889, 617.6882, 225.1303, 184.0758
PC(O-40:4)	C48H90NO7P	823.6455	10.3	positive	823.6340	14.0	0.0003	48	26	824.6418, 639.634, 184.0761, 104.1083, 86.0609

Name	Formula	Mass (DB)	RT (min)	Ionization mode	Measured mass	Mass error (ppm)	p-value	change PH vs B [%]	CV in QCs[%]	Identification
PS(36:2)	C42H78NO10P	787.5363	11.4	positive	787.5386	-3.0	0.0002	-174	7	788.4817, 770.4817, 649.5179, 603.4817, 133.0878
PI(21:0/10:0)	C40H77O13P	796.5102	8.7	negative	796.5075	3.3	0.0092	-154	10	795.4894, 535.6918, 325.1822 283.2637, 241.0375 239.8673, 212.0283, 170.9851 116.9283
PI(21:0/13:1)	C43H81O13P	836.5414	8.0	negative	836.5386	3.3	0.0002	-87	10	835.526, 575.526, 383.1867, 325.1815, 241.1342, 211.1816,61.9879
LPE(16:0)	C21H44NO7P	453.2855	5.5	positive	453.2864	-2.0	0.0051	-45	6	454.2932,436.3392,313.2734, 133.0866, 71.0860
LPE(20:4)	C25H44NO7P	501.2855	5.3	negative	501.2888	-6.5	0.0126	-122	2	500.2750, 359.1942, 311.1664, 303.8052, 279.2308, 195.9859, 152.9990
LPI(20:1)	C29H55O12P	626.3431	9.6	negative	626.3381	8.0	0.0074	-170	8	625.3371,365.2993,339.1993, 311.1649, 152.9269
LPA(12:0)	C15H31O7P	354.1808	6.5	negative	354.1838	-9.0	0.0035	-56	6	353.1723, 254.1499, 199.0060, 181.0060, 155.0125, 119.0495
PA(18:0/18:3)	C39H71O8P	698.4886	9.7	negative	698.4925	-5.5	0.0315	-156	5	697.4763, 597.4763, 283.2680,265.8536, 278.2083, 78.8820
creatine	C4H9N3O2	131.0695	0.2	positive	131.0690	3.6	0.0157	-47	6	standard, 132.0768, 90.1426, 87.0557
arginine	C6H14N4O2	174.1117	0.2	positive	174.1126	-5.0	0.0423	-36	16	standard, 175.1187, 130.0983, 60.0563
alpha-tocopherol	C29H50O2	430.3817	7.2	positive	430.3812	-0.3	0.0255	39	19	standard, 431.3919, 226.9544, 165.0922,
didesmethyl tocotrienol	C25H36O2	368.2715	7.3	negative	368.2728	-3.4	0.0002	-76	6	Database, isotopic distribution
desmosine	C24H39N5O8	525.2798	5.3	negative	525.2880	-4.7	0.0021	-79	6	524.2746, 466.2871, 303.2290, 241.2146

Table 19. Metabolites significantly changed in pig plasma during acute phase of PH, identified during GC-Q-MS metabolic fingerprinting experiment.

Name	T (target ion)	Q (qualifier ion)	RT (min)	RI	p- value	change PH vs B [%]	CV for QCs [%]
pyruvic acid	174	89, 73, 59	6.584	721	0.025	71	19
lactic acid	117	191, 147, 73	6.749	733	0.042	123	10
glycerol	205	147, 117, 73	9.857	945	0.006	175	14
palmitic acid	313	129, 117, 73	18.813	1720	0.037	49	36
oleic acid	339	129, 117, 75	20.403	1892	0.021	82	35
3- hydroxybutyric acid	233	147, 117, 78	8.208	774	0.044	53	26
acetoacetate	89	202, 186, 59	7.806	787	JK	81	17
citric acid	273	347, 147, 73	16.519	1494	JK	116	16
α -ketoglutaric acid	198	156, 147, 75	13.742	1250	JK	85	34
fumaric acid	245	147, 75, 73	10.857	1025	JK	114	14
malic acid	233	245, 133, 147	12.681	1164	JK	179	28
2- hydroxybutyric acid	131	205, 147, 73	7.721	773	JK	105	17
pyroglutamic acid	156	230, 147, 73	13.099	1196	JK	53	*
phenylalanine	120	146, 91, 75	13.466	1226	JK	76	*
tryptophan	202	291, 117, 73	20.535	1888	JK	128	*
2- ketoisocaproic acid	200	147, 99, 73	8.951	851	0.009	79	36
hypoxanthine	265	280, 206, 73	16.359	1480	JK	96	*
galacturonic acid	333	292, 160, 103	17.786	1638	0.002	229	14
β -alanine	248	248, 147, 73	11.931	1107	JK	72	*

*CV not available, JK-jackknife confidence interval

6.4 Biochemical interpretation and discussion

The metabolites found as significantly different among compared groups can be connected by various and numerous metabolic pathways, as graphically represented in Figure 19. The metabolite changes herein revealed, can be involved in the pathophysiological processes of acute PH due to PE. This can be explained by disturbed gas exchange which leads to oxygen deficiency and hypoxia state called hypoxic pulmonary vasoconstriction [104].

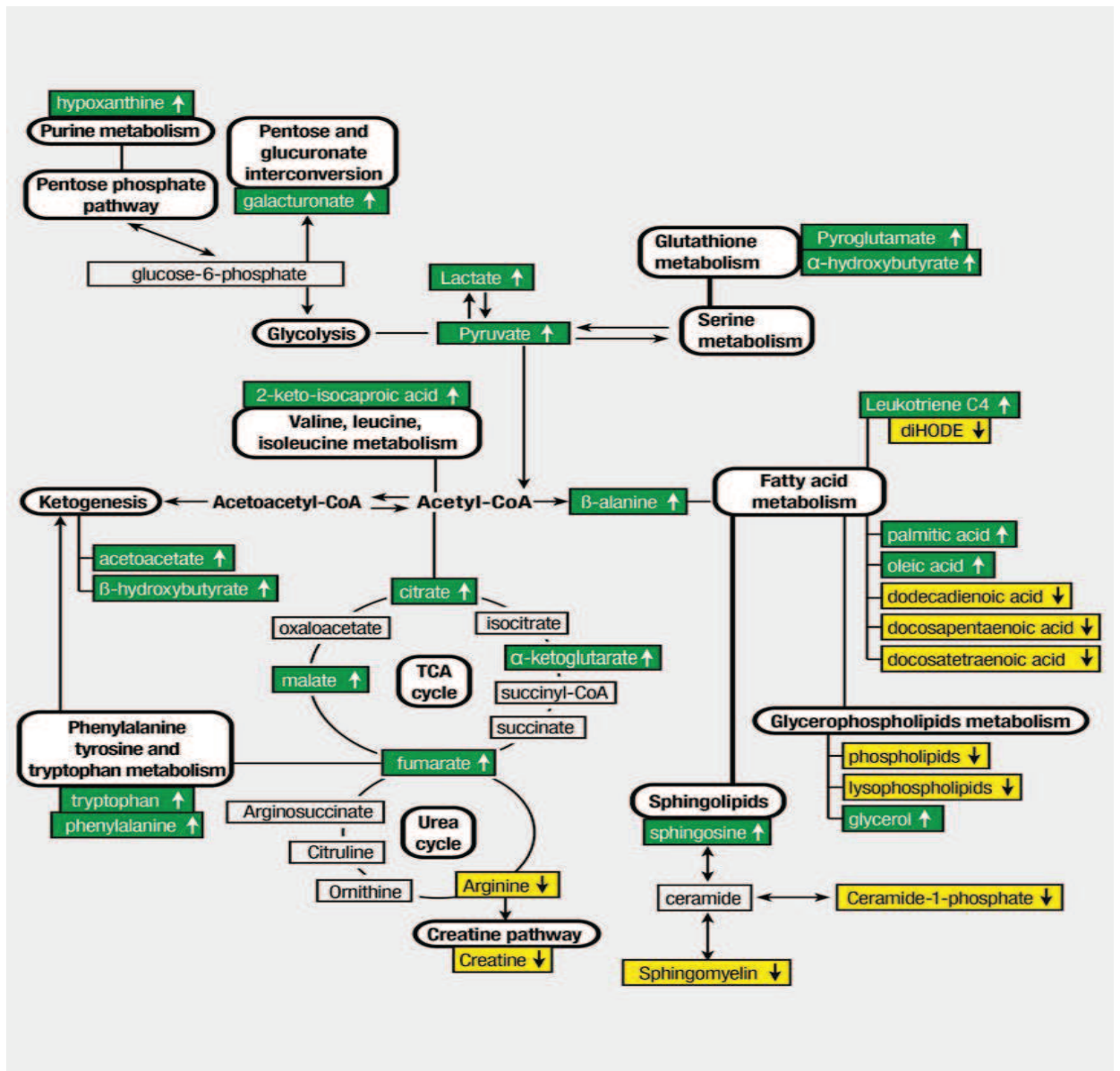


Figure 19. Metabolic changes in pig plasma during acute PH. Colored metabolites were detected using a GC-Q-MS or UHPLC-QTOF-MS platform. Those metabolites whose levels were increased in acute PH are highlighted in green and those that decreased in yellow boxes [102].

As can be seen in Tables 18 and 19 or in Figure 4, numerous of the significantly changed metabolites in pig plasma during acute PH are employed in the glycolysis and the tricarboxylic acid (TCA) cycle, involved in the energy production and the creation of primary blocks of other metabolic pathways. The TCA cycle transforms acetyl-CoA into few intermediates and produces CO₂, the reduced form of nicotinamide adenine dinucleotide (NADH + H⁺) and flavin-adenine dinucleotide (FADH + H⁺). These reduced coenzyme groups and cell oxygen are subsequently utilized by mitochondria in oxidative phosphorylation, which provides the main source for ATP production. In hypoxic state, the oxidative phosphorylation rate is limited due to the lack of oxygen, what results in the TCA cycle intermediates accumulation. This can be termed as an adaptive response to hypoxic stress, maximizing cellular energy production while protecting from adverse reactive oxygen species (ROS) accumulation. The observed increase in citrate, malate, fumarate and α -ketoglutarate in pig plasma during acute PH, could be related to a reduced TCA cycle turnover [102]. There are some recent reports suggesting that either the mitochondrial metabolism under hypoxia, the metabolism in the right ventricle or pulmonary vasculature can be characterized by impaired TCA cycle flux with succinate dehydrogenase dysfunction and activation of pyruvate dehydrogenase kinase, what consequently results in decreased energy production from both oxidative phosphorylation and TCA cycle [105, 106].

In addition the limited turnover of the TCA cycle might lead to acetyl-CoA accumulation. In the case of the reduced TCA cycle capability, acetyl-CoA is rather prompt to be used in ketogenesis pathway. In accordance to this, the increased levels of β -hydroxybutyrate (β -HB) and acetoacetate (ketone bodies) in acute PH group were observed. The overproduction of β -HB is typical for conditions, in which the redox state of hepatic mitochondria is altered in order to increase NADH level. The obtained herein results showed that ketone bodies could be involved in acute PH development, probably due to hypoxia-mediated alterations, what can help to explain and understand the PH pathogenesis. Furthermore, it has been reported that β -HB may protect the brain during hypoxic conditions by reducing glucose uptake and consumption rather than by acting as an alternative energy substrate [107].

A similar insight could be concluded from the differences found with pyruvate and lactate, which were also observed to be significantly different between compared groups. The increased levels of these metabolites in pig plasma during acute PH due to PE could also indicate the shift in glucose metabolism which is beneficial for ATP production and prevents from mitochondrial ROS generation. Oxygen level is a central regulator of the balance between glycolysis and oxidative phosphorylation in the energy metabolism[102]. Previous reports [108-110] confirmed that during hypoxic conditions ATP production was shifted toward glycolysis (Warburg effect) and led to cytosolic pyruvate accumulation that could be converted to lactate by lactate dehydrogenase [111,112].

Still, the oxygen deficiency during hypoxic stress in acute PH might result in incomplete oxidation, free radicals overproduction and the glutathione overconsumption, which are the major intracellular antioxidants [102]. As a result of this consumption the increased levels of α -hydroxybutyrate (α -HB) and pyroglutamate were found in animals with acute PH. α -HB is a byproduct of glutathione formation, and the relationship between the high level of this metabolite and the excess of glutathione demand, mitochondrial energy metabolism, or increased oxidative stress has been previously reported [113]. Pyroglutamate is another metabolite involved in glutathione metabolism and its increase in hypoxic cells has been recently reported [114].

Additionally, the observed herein energy imbalance is clearly associated with the lipid metabolism abnormalities. The increased levels of glycerol and free fatty acids (FFA), such as docosatetraenoic and docosapentaenoic acids as well as palmitic and oleic acids in pig plasma during acute phase of PH confirmed the increased rate of lipolysis. Related to this, the recent report suggested that hypoxia is related to lipolysis induction in adipose tissue [115]. Moreover, these metabolic changes can be associated with the phospholipase A2 (PLA2) activity which hydrolyzes phospholipids to free fatty acids, eicosanoids and lysophospholipids. In the animal group with acute PH, four lysophospholipids, four phospholipids and one phosphatidic acid were observed to be lower, what indicates the regulation of PLA2 activity, which isoforms were reported to be modified by hypoxia [116].

FFA can deliver the energetic and biosynthetic substrates for signaling molecules such as oxylipins, which are the cyclooxygenase- (COX), lipoxygenase (LOX), and

cytochrome P450- (CYP) derived oxidized metabolites of polyunsaturated fatty acids (PUFA). PUFA play a crucial role in cell proliferation, apoptosis, tissue repair, blood clotting and inflammation [102]. The best described oxylipins included prostaglandins and leukotrienes, the potent eicosanoid lipid mediators which derived mainly from arachidonic acid released by PLA2 [117]. The few oxylipins were significantly different between herein compared animal groups. However, the obtained results did not demonstrate the same trend for oxylipin compounds, while an increase of leukotriene C4 and a decrease in dihydroxyoctadecadienoic acid, hydroxyoctadecenoic acid and oxo-heptadecatrienoic acid were observed in pig plasma during acute PH. The initial idea that cysteinyl leukotrienes are involved in PH pathomechanism was performed by activity assessment of 5-lipoxygenase non-selective inhibitors or receptor's agonists [118], however this suggestion was not confirmed by further investigations [119,120].

In addition to oxylipins, changes in the levels of sphingolipids were also found between animal groups: lower sphingomyelin and ceramide-1-phosphate (Cer-1-P) as well as higher sphingosine in pig group with acute PH were observed [102]. Sphingolipids are a major class of lipids employed in eukaryotes membranes composition. However, the intensive investigations concerning their function and metabolism revealed that, for instance, sphingosine, sphingosine-1-phosphate, ceramide and Cer-1-P are bioactive signaling molecules, playing crucial role in cell growth, apoptosis, signal transduction and recognition [121]. In accordance to previously reported [122] results that showed the activation of neutral sphingomyelinase (nSMase) in isolated rat pulmonary artery smooth muscle cells (PASMC) during hypoxic pulmonary vasoconstriction, the observed herein decreased level of sphingomyelin can be related to nSMase activity. Cer-1-P is produced by direct phosphorylation of ceramide by ceramide kinase (CERK), and its role in cell growth and survival was previously suggested [123]. Moreover, it is worth to note that Cer-1-P by induction of cytosolic phospholipase A2 (cPLA2) plays important role in inflammatory response [121].

The decreased level of desmosine was also observed in pig plasma during acute phase of PH. Desmosine is an amino acid involved in elastin cross-linking and it is made by condensation of four molecules of lysine into pyridinium ring [102]. The previous reports

revealed that the desmosine and isodesmosine determination in biological matrices (urine, plasma, sputum) can indicate the elastin degradation in chronic pulmonary diseases [124,125]. However, the desmosine alteration has not been previously reported to be related to hypoxic condition, PE or PH. Although, it should be underlined that changes in desmosine level were herein observed in an acute, not chronic phase of PH that occurred only one hour after polydextrane microspheres injection.

PH is a multifactorial and complex vascular disease whose pathogenesis is not completely explained yet. Although, there are few suggested pathological processes associated with PH, such as vasoconstriction, increased vascular cells proliferation and resistance to apoptosis [82]. These hallmarks can be regulated by the stabilization of the hypoxia-inducible factor (HIF). HIF as main transcriptional regulator of the hypoxic response, has a predominant role in the PH induction [126]. HIF-1 α regulates activity of numerous enzymes, mainly employed in glycolysis pathway what lead to pyruvate dehydrogenase inhibition and lactate dehydrogenase induction [127,128]. These enzymatic perturbations result in glycolytic shift as was revealed in the present study (increase in pyruvate and lactate levels in animal group with acute PH). Additionally, the TCA itself is also involved in the HIF stabilization, as the prolyl hydroxylases which lead to its degradation in normoxia are regulated by TCA cycle intermediates [126]. Moreover, the recent studies suggested the abnormal cellular metabolism, notably of glycolytic shift, the potential role of HIF-1 α in these reactions, and alterations in mitochondrial function, as either key pathological hallmarks of PH progression or new therapeutic targets in PH treatment [82, 109].

In addition, HIF-1 α inhibits voltage-gated potassium (Kv) channels, what consequently leads to membrane depolarization and Ca²⁺ flux into the cells what in pulmonary circulation results in hypoxic vasoconstriction and subsequently to PH initiation [82, 129]. Moreover, HIF-1 α is controlled at the transcriptional and translational level by mammalian target of rapamycin (mTOR) signaling [130]. mTOR was suggested to be involved in cell growth and regulate both anabolic or catabolic pathways in lipid metabolism [131]. The oxylipins and lipid mediators observed to be significantly different between compared groups in the present animal model are associated with cell proliferation, cell survival, apoptosis and cell-cycle arrest [132]. The inflammation, resistance to apoptosis and increased cell

proliferation as suggested pathological reactions in PH development [133] can be regulated by both HIF and mTOR signaling. In addition, the recent report suggested the potential requirement of mTOR pathway in cell proliferation during hypoxia-induced PH [134].

To conclude, similarly to tumor cells, the imbalance between glycolysis and oxidative phosphorylation could play a crucial role in cell response in acute phase of PH and could be helpful to expand the knowledge about PH pathogenesis and may offer new insight into therapeutic targets to prevent or reverse disease progression.

To sum up, our results were obtained based on an animal model in which pigs were selected as experimental animals what was justified by the fact, that cardiovascular physiology, size, anatomy, and blood perfusion distributions are very similar in humans and pigs. However, the animal model proposed in present study possesses some limitations. The PH was generated by injection of polydextrane-microspheres while in human the most common cause is thrombi. Thus, either diffuse or segmental occlusion of pulmonary arteries could occur. In addition, the composition of the microspheres could have had influence on obtained results. However, the most of the acute metabolite changes during PH such as hypoxic vasoconstriction are common to various PH etiologies. Therefore our results can be useful in disease diagnosis from different causes. Simultaneously, it should be underlined that potential metabolic markers, selected in our study, should be validated in human population to check diagnostic power and reliability.

7. Plasma metabolic fingerprinting with LC-ESI-QTOF-MS and GC-Q-MS in a human model of pulmonary arterial hypertension

Forty human plasma samples were divided into two experimental groups: a control group consisting of 20 healthy individuals and disease group including 20 patients with the confirmed pulmonary arterial hypertension (PAH). The clinical characteristics of both studied group was described in section 5.3.2. The plasma samples were analyzed by metabolic fingerprinting approach with the use of HPLC-ESI-QTOF-MS technique in both positive (ESI+) and negative (ESI-) ionization modes. As a complementary platform the GC-Q-MS was applied. The examples of chromatograms obtained for plasma metabolic fingerprints with both analytical platforms were displayed in Figures 20, 21 and 22.

To check the robustness of analytical procedure of each plasma metabolic fingerprinting experiments, all human plasma and QC samples were plotted in PCA graphs. The data matrices obtained in HPLC-ESI(+)-QTOF-MS, HPLC-ESI(-)-QTOF-MS and GC-Q-MS were used to build separate multivariate models. The datasets before PCA plotting were filtered based on quality assurance requirements described in section 5.7. and consisted of 1950, 1114 and 49 variables for HPLC-ESI(+)-QTOF-MS, HPLC-ESI(-)-QTOF-MS and GC-Q-MS data, respectively. The appropriate clustering of the QC samples into group in each multivariate model confirmed the system stability and method reproducibility during metabolic fingerprinting experiments (Figure 23). The grouping of QC samples confirmed that compared experimental groups separation is due to biological and not to analytical variability. In addition, PCA plotting allowed to reveal one outlier according to Hotelling's T² range observed for GC-Q-MS data. The outlier detection is crucial before the further discriminant multivariate analysis, because they can lead to model destabilization and affect the final statistical results. Therefore the detected outlier (sample C_3) was not included in further statistical analysis.

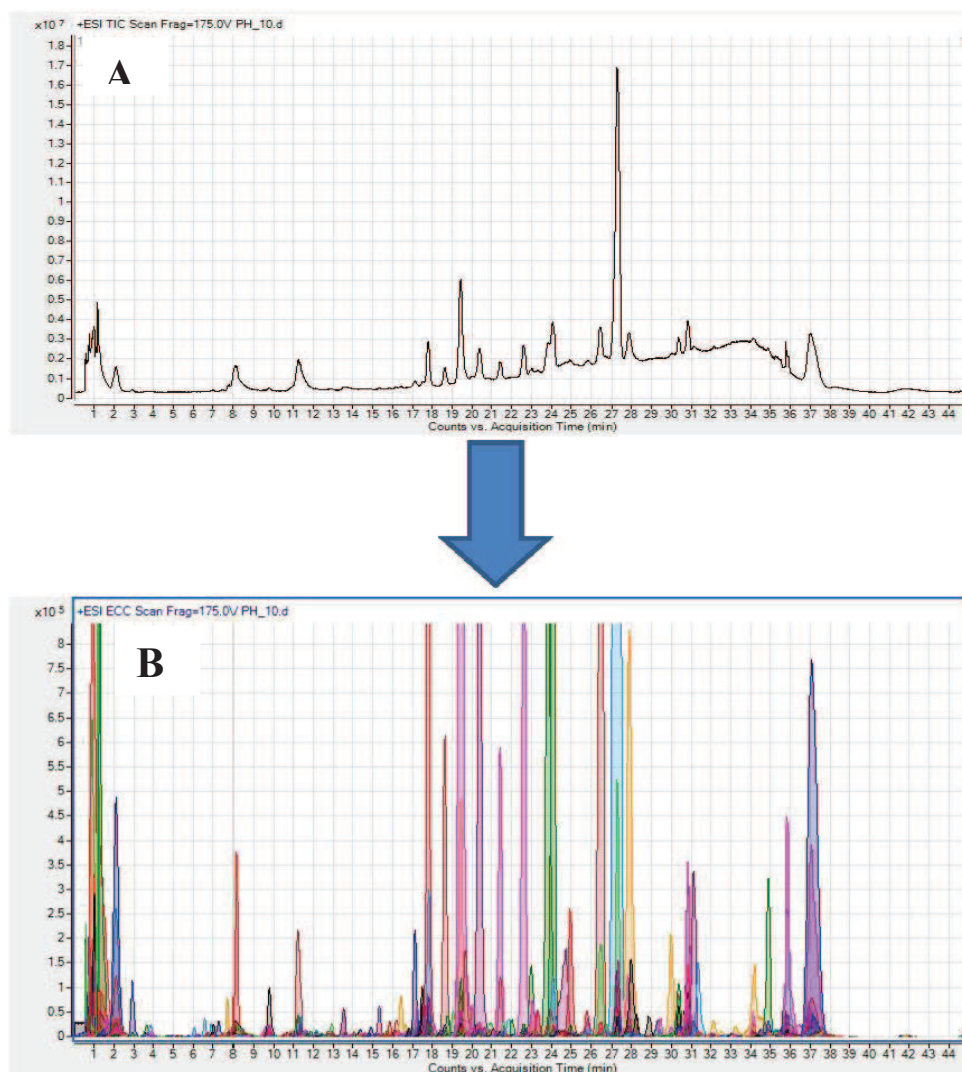


Figure 20. Representative HPLC-ESI(+)-QTOF-MS chromatogram of plasma metabolic fingerprint from exemplary human plasma extract. A: Total Ion Chromatogram (TIC).

B: overlay of all the individual features obtained after Molecular Feature Extraction (MFE) represented as extracted compound chromatogram (ECC).

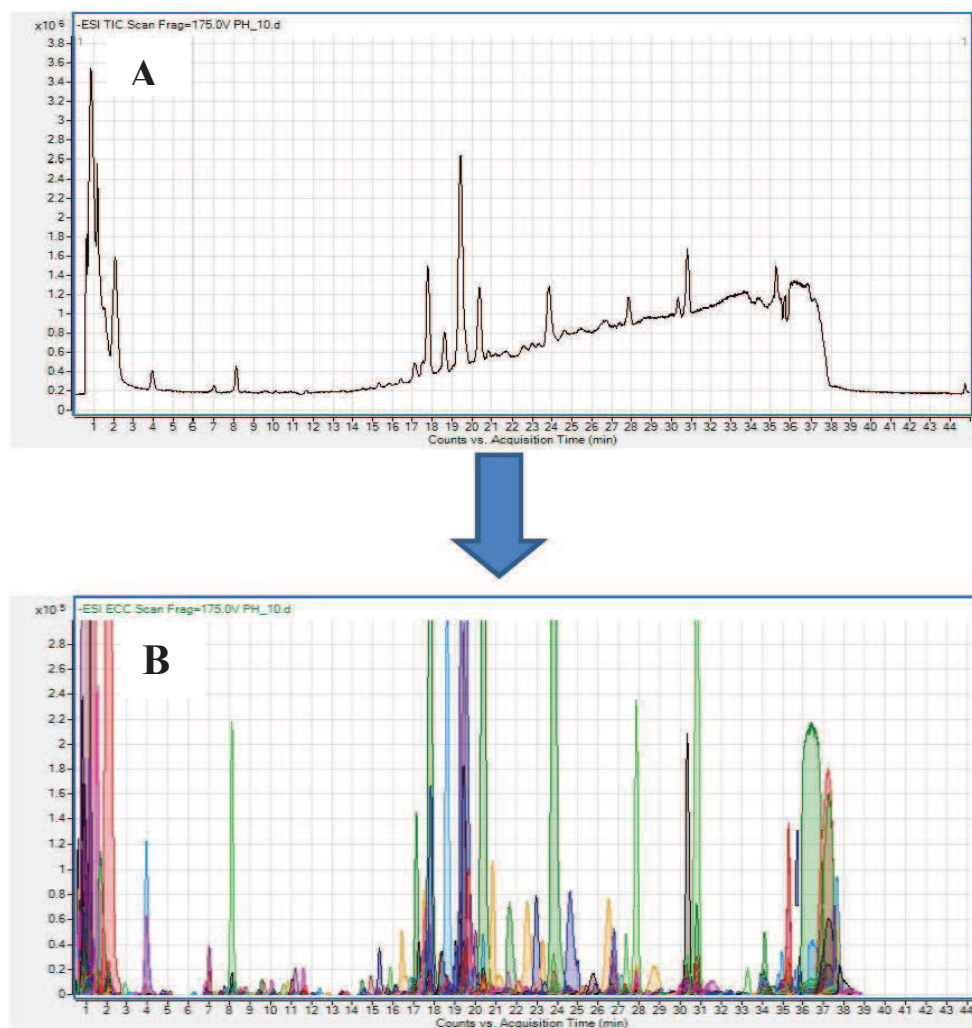


Figure 21. Representative HPLC-ESI(-) - QTOF-MS chromatogram of plasma metabolic fingerprint from exemplary human plasma extract. A: Total Ion Chromatogram (TIC).

B: overlay of all the individual features obtained after Molecular Feature Extraction (MFE) represented as extracted compound chromatogram (ECC).

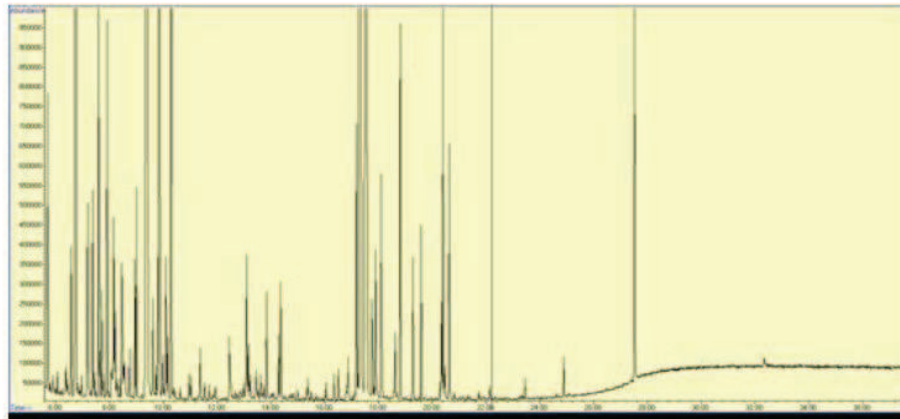
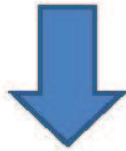
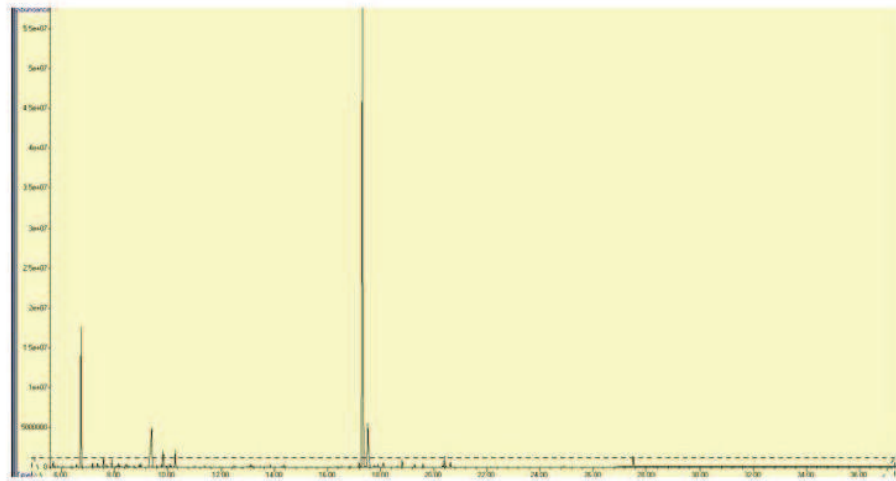
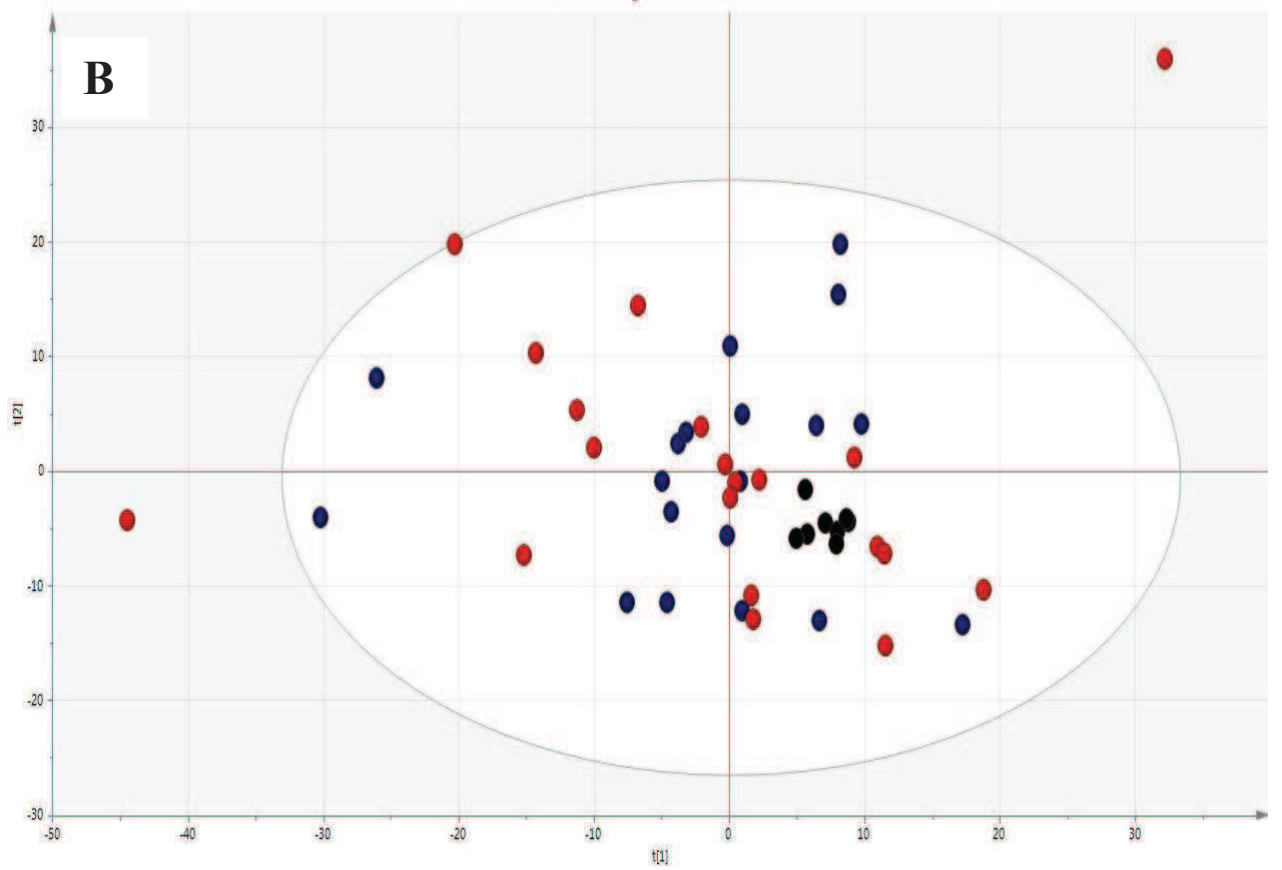
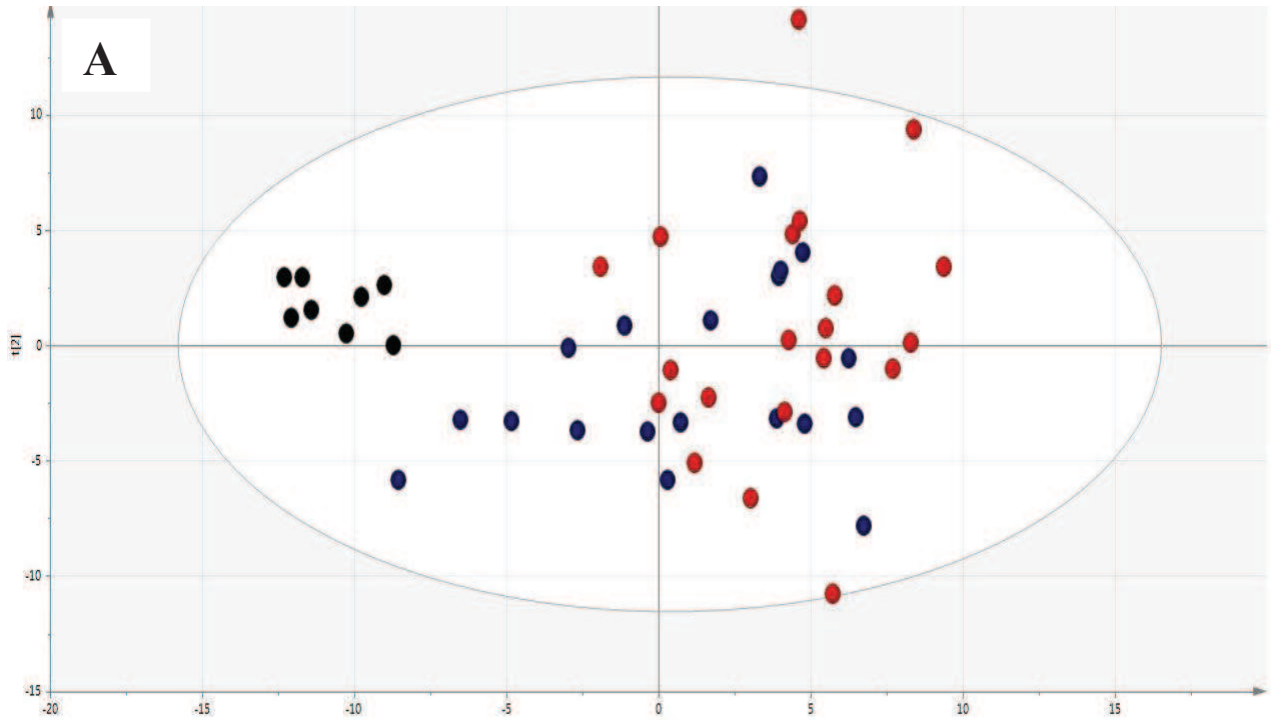


Figure 22. Representative GC-Q-MS Total Ion Chromatogram (TIC) of plasma metabolic fingerprint from exemplary human plasma extract.



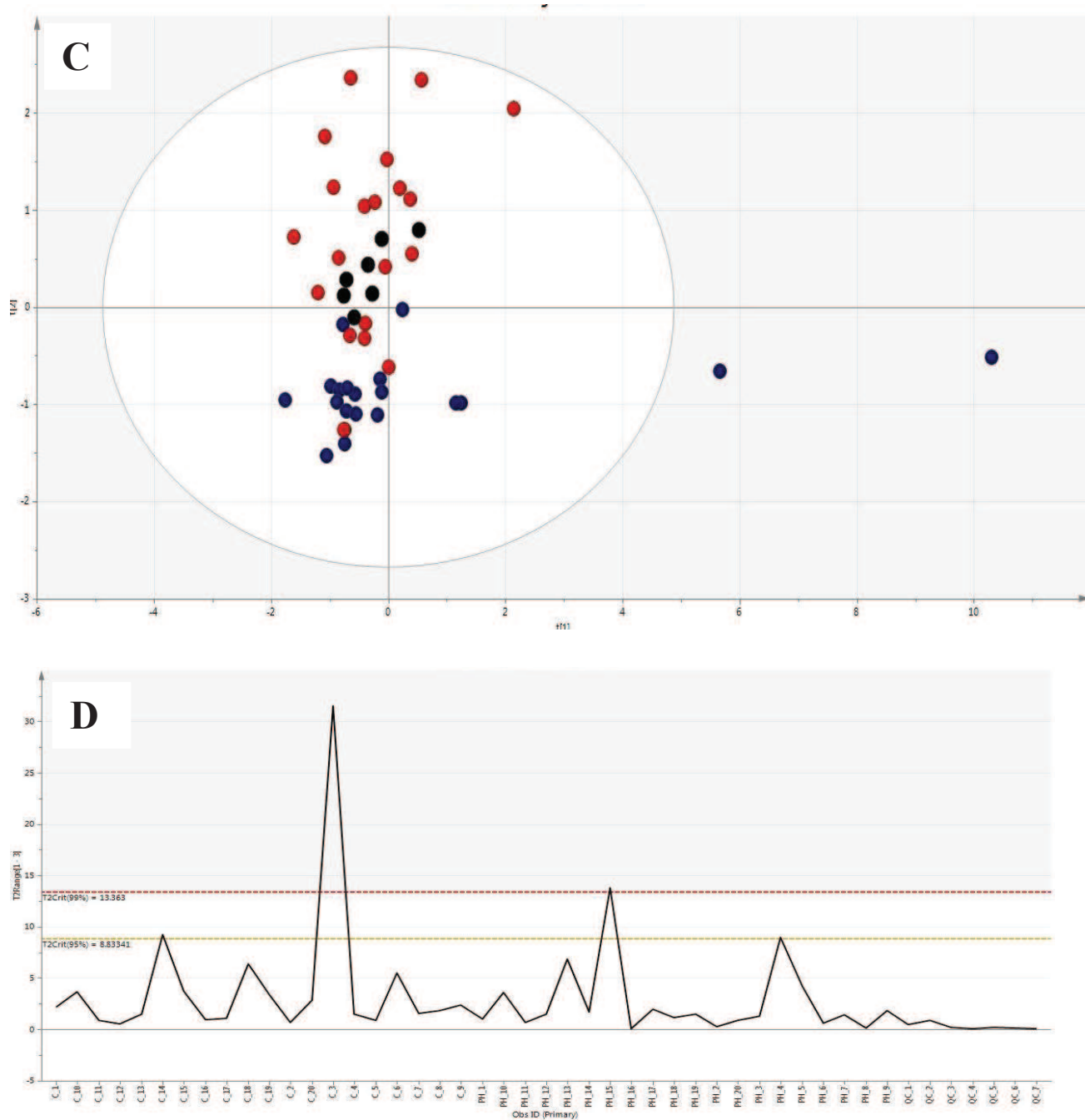


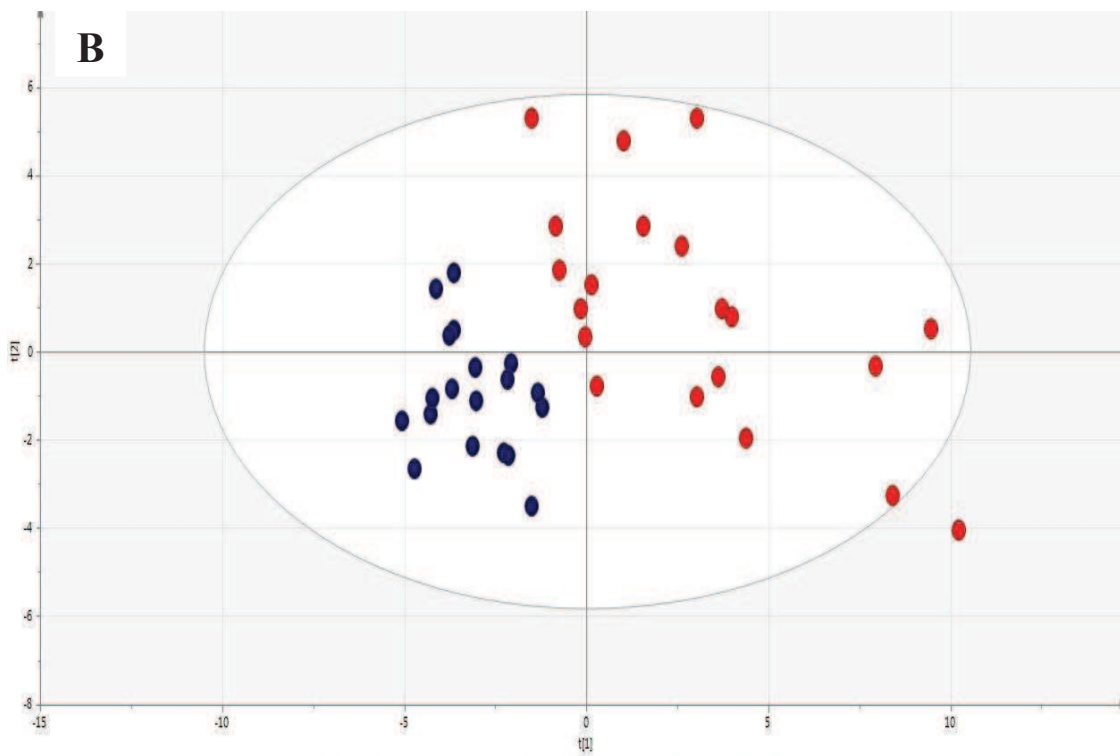
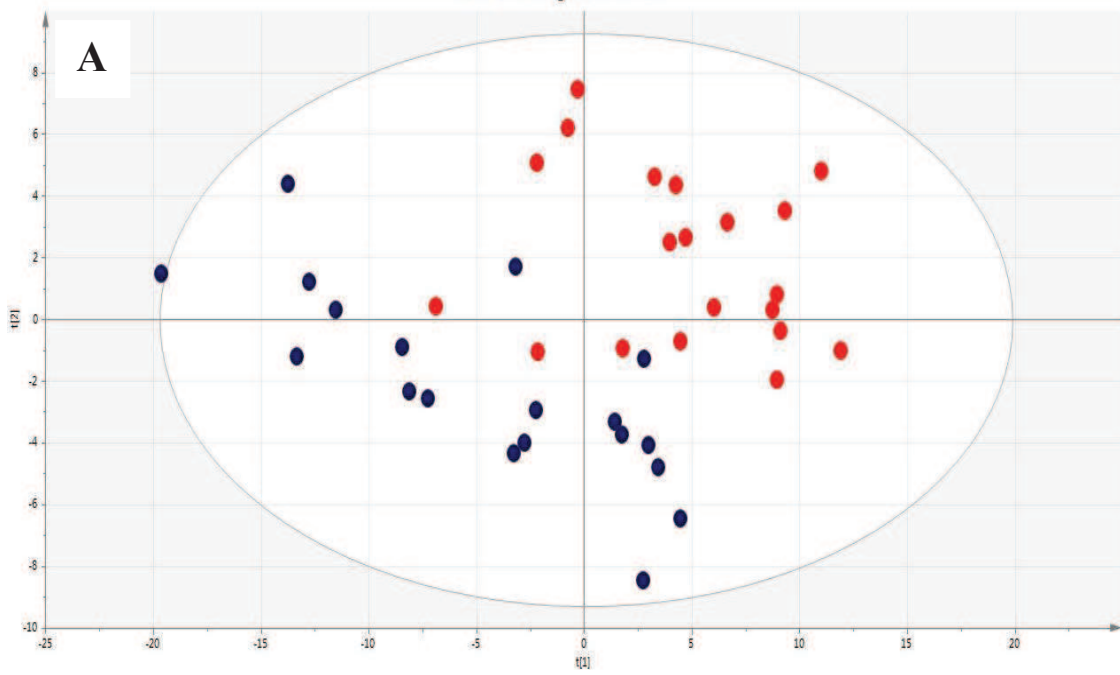
Figure 23. Checking the quality of analysis in all plasma metabolic fingerprinting experiments.

(A) Scores plot for a PCA model built with the data set obtained in HPLC-ESI(+)-QTOF-MS. Quality parameters for the model: explained variance $R^2 = 0.471$, predicted variance $Q^2 = 0.225$. (B) Scores plot for a PCA model built with the data set obtained in HPLC-ESI(-)-QTOF-MS. $R^2 = 0.455$, $Q^2 = 0.139$. (C) Scores plot for a PCA model built with the data set obtained in GC-Q-MS. $R^2 = 0.567$, $Q^2 = 0.193$. (D) The Hotelling's T2 range for GC-Q-MS

data set. QC samples, control and PAH group have been marked as black, blue and red spots, respectively.

7.1 Univariate and multivariate statistical analysis

After data reprocessing and multialignment the obtained datasets consisted of 27362 and 11498 features for HPLC-ESI(+)-QTOF-MS and HPLC-ESI(-)-QTOF-MS, respectively. In the case of GC-Q-MS based plasma metabolic fingerprinting, 114 compounds were aligned in all human plasma samples. Then, to clean up the obtained data sets from random signals the filtration step was performed. For both HPLC-ESI(+)-QTOF-MS and HPLC-ESI(-)-QTOF-MS data sets, the 90% filtration limit was used what meant that only features presented in 90% of all samples in at least one of the groups (i.e., in all control samples or all PAH samples) were considered in univariate statistical analysis. In the case of GC-Q-MS data matrix, the 75% frequency criterion was applied due to the complexity of derivatization process which can produce few various derivatives of the same compound. After filtration step the datasets were reduced to 838 and 637 features for HPLC-ESI(+)-QTOF-MS and HPLC-ESI(-)-QTOF-MS, respectively as well as 68 compounds for GC-Q-MS. Subsequently, the univariate statistical analysis employed both paired *t* tests and paired U Mann-Whitney test. 149 and 63 variables as well as 11 compounds, in the case of HPLC-ESI(+)-QTOF-MS, HPLC-ESI(-)-QTOF-MS and GC-Q-MS data, respectively, were selected as statistically significantly changed between compared groups. Then, only those significant variables were used to build multivariate supervised PLS-DA models for HPLC-QTOF-MS data from both polarity modes. Subsequently, the JK confidence interval criteria were applied as a multivariate statistical test to select variables which mainly contributed in samples discrimination. Therefore, only variables that passed through both univariate and multivariate statistical criteria were included in the metabolite identification. In the case of GC-Q-MS, all variables after data filtration step were used to build the PLS-DA model and then the metabolites that were statistically significant according to univariate tests or JK criteria were considered in biochemical interpretation. The PLS-DA models for three separate datasets were built with SIMCA P+ 13.03 software and were presented in Figure 24.



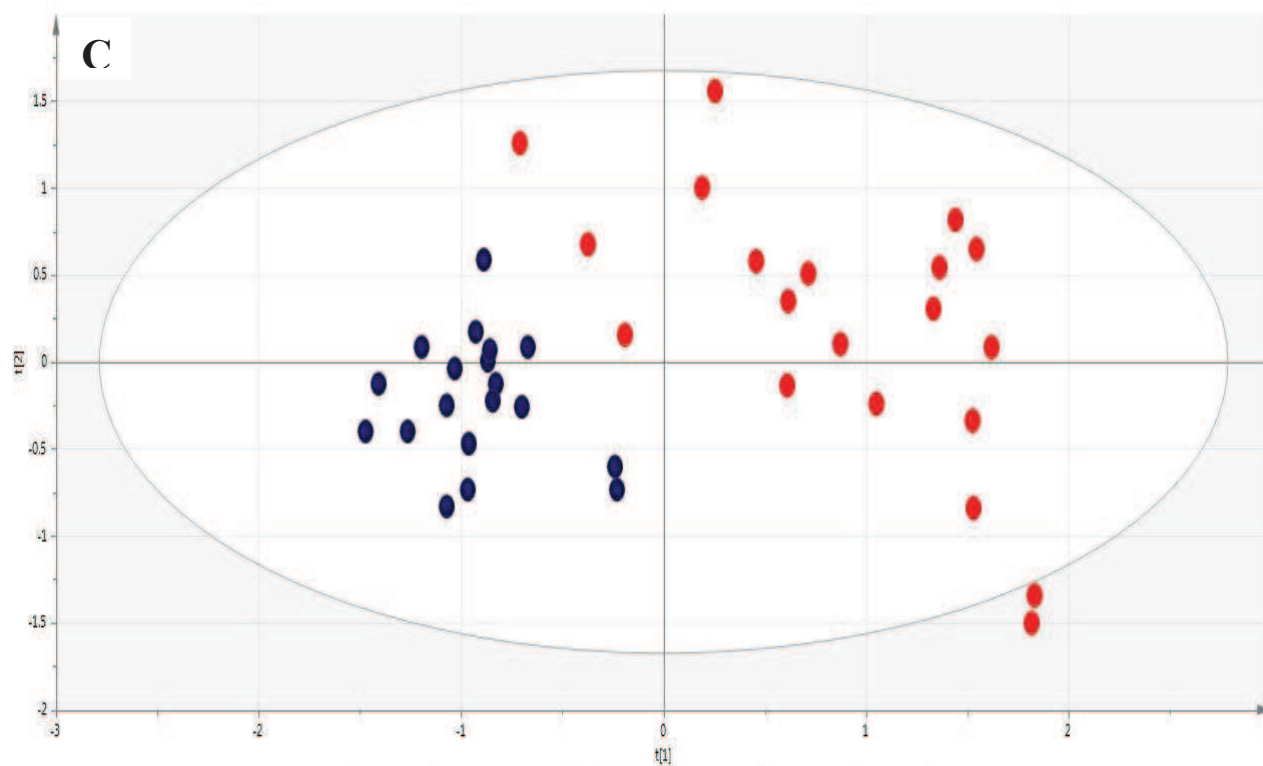


Figure 24. PLS-DA plots for human plasma metabolic fingerprints obtained for control and PAH groups.

(A) PLS-DA model ($R^2 = 0.845$, $Q^2 = 0.671$) for significantly changed variables detected in human plasma with HPLC-ESI(+)-QTOF-MS

(B) PLS-DA model ($R^2 = 0.896$, $Q^2 = 0.614$) for significantly changed variables detected in human plasma with HPLC-ESI(-)-QTOF-MS

(C) PLS-DA model ($R^2 = 0.825$, $Q^2 = 0.554$) for compounds detected in human plasma with GC-Q-MS, after data filtration.

The control and PAH plasma samples have been marked as blue or red spots, respectively.

7.2 Discriminant models validation

To avoid overfitting and check the predictive value of the obtained PLS-DA models, the leave-one-out cross-validation (LOOCV) method was applied with the use of Matlab 2007b software. The procedure of LOOCV approach was described in section 5.7. The correct classification rate (CCR) for training and test sets was calculated for each PLS-DA model. The sensitivity and specificity of particular independent discriminant model were also calculated based on confusion matrices. The predictive value (Q) of each PLS-DA model was assessed based on test sets prediction by the model built on training sets. The results of prediction and LOOCV procedure for three separate PLS-DA models were presented in Table 20.

Table. 20. The results of prediction and LOOCV procedure for separate discriminant models obtained for data from human plasma metabolic fingerprinting experiments.

PLS-DA models	LV	CCR_training set	CCR_test set	Q
HPLC-ESI(+)-QTOF-MS data	3	61%	75%	83%
HPLC-ESI(-)-QTOF-MS data	3	64%	83%	83%
GC-Q-MS data	3	81%	67%	75%

LV=latent variables used in PLS-DA construction

Based on LOOCV results the confusion matrix for each PLS-DA model was built. Then, the sensitivity and specificity were calculated with the use of the same formulas as was described in section 6.2. The confusion matrices, sensitivities and specificities of each discriminant model were presented in Tables 21 - 23.

Table 21. The confusion matrix, sensitivity and specificity of PLS-DA model based on HPLC-ESI(+)-QTOF-MS data set.

		Predicted		Sensitivity	Specificity	PPV	NPV
		C	PAH				
Actual	C	12	8	0.8	0.6	0.67	0.75
	PAH	4	16				

Table 22. The confusion matrix, sensitivity and specificity of PLS-DA model based on HPLC-ESI(-)-QTOF-MS data set.

		Predicted		Sensitivity	Specificity	PPV	NPV
		C	PAH				
Actual	C	14	6	0.75	0.7	0.71	0.74
	PAH	5	15				

Table 23. The confusion matrix, sensitivity and specificity of PLS-DA model based on GC- Q-MS data set.

		Predicted		Sensitivity	Specificity	PPV	NPV
		C	PAH				
Actual	C	15	5	0.7	0.75	0.74	0.71
	PAH	6	14				

7.3. Metabolite identification

The information about metabolites, significantly changed in human plasma during PAH in comparison to control group, which were identified both in HPLC-(ESI+)-QTOF-MS and HPLC-(ESI-)-QTOF-MS were collected in Table 24. For each particular metabolite, the RT, the measured monoisotopic mass, ionization mode, formula, p-value, percentage of change in PAH group, coefficient of variation (CV) for QC samples and identification based on fragments' analysis, were included. The percentage of change in PAH group comparing to control group were calculated with the same formulas described in section 6.3. In the case of metabolites identified in GC-Q-MS and significantly changed in human plasma of PAH group, the information concerning RT, RI, target ion, qualifier ions, p-value, percentage of change in PAH group and CV for QC samples were presented in Table 25.

Table 24. Metabolites significantly changed in human plasma during acute phase of PH, identified during HPLC-QTOF-MS metabolic fingerprinting experiment.

Name	Formula	RT	Ionization mode	Monoisotopic mass	p-value	% change	CV QCs	Identification
glutamine	C5H10N2O3	1.1	negative	146.0693	0.0143	59	6	145.0615, 127.0500, 109.0396, 58.0316, 41.9997
nonanoic acid	C9H18O2	12.7	positive	158.1304	0.0072	28	9	159.1375, 141.9564, 124.9622, 97.9679, 89.0596, 43.0545
uric acid	C5H4N4O3	0.7	negative	168.0262	0.0491	20	3	167.0195, 124.0147, 96.0198, 69.0089, 41.9990
hydroxybenzenesulfonic acid	C6H6O4S	1.2	negative	173.9984	0.0066	291	7	172.9901, 93.0343, 79.9569
tryptophan	C11H12N2O2	1.1	positive	204.0897	0.0376	-14	8	205.0984, 188.0706, 146.0599, 118.0651
palmitamide	C16H33NO	26.5	positive	255.2579	0.0257	-18	7	256.2644, 102.0911, 116.1065, 88.0756, 57.0701
oleamide	C18H35NO	27.3	positive	281.2741	0.0215	-14	7	281.2735, 265.2529, 247.2420, 135.1166, 97.1010, 83.0856, 69.0701, 57.0702
stearamide	C18H37NO	31.1	positive	283.2889	0.0266	-21	12	284.2962, 116.1072, 102.0911, 88.0756, 57.0699
ketosphingosine	C18H35NO2	20.3	positive	297.2664	0.0009	-34	17	298.2733, 281.2488, 95.0847, 81.0699, 67.0549, 57.0708
dimethylnonanoyl carnitine	C18H35NO4	8.7	positive	329.2564	0.0423	-21	10	329.2568, 271.1880, 85.0284, 60.0796
MG(16:0)	C19H38O4	27.8	positive	330.2777	0.0312	36	10	331.2850, 313.2728, 95.0852, 71.0856, 57.0700
hydroxy-oxo-cholanoic acid	C24H38O4	34.1	positive	390.2779	0.0274	40	27	391.2852, 167.0361, 149.0225, 71.0851, 57.0703
palmitoylcarnitine	C23H45NO4	18.1	positive	399.3347	0.0066	31	5	400.3418, 341.2682, 85.0285, 60.0809
vaccenyl carnitine	C25H47NO4	18.7	positive	425.3506	0.0168	36	4	426.3581, 309.2773, 85.0284, 60.0808
stearoylcarnitine	C25H49NO4	21.2	positive	427.3653	0.0016	31	4	428.3725, 311.2927, 85.0281, 60.0799
LPE(18:0)	C23H48NO7P	22.5	positive	481.318	0.0397	21	7	481.3179, 341.3044
LPC	C24H50NO8P	9.6	positive	511.3277	0.0008	70	29	512.3277, 184.0726, 104.1070, 86.0963
glycochenodeoxycholate sulfate	C26H43NO8S	8.5	negative	529.2697	0.0329	84	9	528.2620, 448.3069, 74.0236
LPC (22:6)	C30H50NO7P	17.8	positive	567.3331	0.0123	-20	12	568.3380, 184.0725, 104.1069, 86.0966
deoxycholic acid-3 glucuronide	C30H48O10	8.1	negative	568.3228	0.0124	63	9	567.3152, 505.3094, 391.2780, 113.0218, 85.0277, 75.0089, 44.9971
PC(26:1)	C34H66NO8P	24.1	positive	647.4436	0.0299	-29	26	648.4489, 184.0727, 104.1054, 86.0951

Table 25. Metabolites significantly changing in human plasma of PAH group, identified in GC-Q-MS metabolic fingerprinting experiment.

Name	T (target ion)	Q (qualifier ion)	RT (min)	RI	p- value	change PAH vs C [%]	CV for QCs [%]
pyruvic acid	174	89, 73, 59	6.584	721	0.025	71	19
lactic acid	117	191, 147, 73	6.749	733	0.042	123	10
glycerol	205	147, 117, 73	9.857	945	0.006	175	14
aminomalonic acid	218	73,147,320	12.5	889	0.037	84	28
cholesterol	129	329,73,368	27.6	2826	0.032	-9	27
creatinine	115	73,100,329	13.5	1232	0.004	77	29
threitol	73	147,217,103	12.9	1176	0.0005	115	24
isoleucine/norleucine	86	75,69, 188	8.4	853	0.001	-21	24
gluconic acid lactone	73	217,147,103	16.8	1560	0.023	54	25
glycolic acid	147	73,66, 205	6.9	748	0.031	18	28
urea	147	189, 73,66	9.4	923	0.038	39	17
citric acid	273	347, 147, 73	16.519	1494	JK	123	27
alanine	248	248,147,73	12.1	1107	JK	63	23
pyroglutamic acid	156	230,147,73	13.1	1196	JK	35	17
tetratriacontane	57	71,85, 99	29.3	3075	JK	-37	29
2-amino-1-phenylethanol	174	73, 147,86	15.3	1406	JK	66	12
ketobutyric acid	188	188,89, 59	6.9	773	JK	-40	29

7.4 External validation of potential markers of pulmonary hypertension

The external validation of potential markers (see Table 24 and 25) of PH condition was performed in independent test group, consisting of 20 PH patients and 12 healthy controls. The test groups were also matched according to age, sex and BMI. Plasma metabolic fingerprinting experiment was performed using the same analytical instruments and methods as described in sections 5.4. and 5.5. The further workflow regarding, data extraction, data treatment and statistical analysis were conducted in the same way, previously. The results of univariate statistical analysis in the test group were listed in Table 26. Additionally, the LOOCV approach was performed in Matlab 2013b and the test group was predicted by the PLS-DA models built based on data obtained in the first experiment. The predictive values were 63% and 82% for LC-MS and GC-MS datasets, respectively.

Table 26. The results of univariate statistical analysis in external test group in the study of human PH.

Metabolite	<i>p</i>-value in test group
glutamine	0.039
nonanoic acid	0.998
uric acid	0.626
hydroxybenzenesulfonic acid	0.045
tryptophan	0.024
palmitamide	0.047
oleamide	0.042
stearamide	0.021
ketosphingosine	0.024
MG(16:0)	0.743
hydroxy-oxo-cholanoic acid	0.309
palmitoylcarnitine	0.023
vaccenyl carnitine	0.179
stearoylcarnitine	0.027
LPE(18:0)	0.044
LPC	0.283
glycochenodeoxycholate sulfate	0.029
LPC (22:6)	0.041
deoxycholic acid-3 glucuronide	0.034
PC(26:1)	0.179
cholesterol	0.0039
creatinine	0.016
threitol	0.0017
gluconic acid lactone	0.565
glycerol	0.014
glycolic acid	0.075
lactic acid	0.0011
pyruvic acid	0.062
urea	0.0069
aminomalonic acid	0.012
isoleucine/norleucine	0.931

7.5 Biochemical interpretation and discussion

The identified metabolites representing significant differences in plasma of PAH patients in comparison to control group are associated with various metabolic pathways, including glycolysis, TCA cycle, pentose phosphate pathway, amino acid metabolism, purine metabolism and fatty acid metabolism. The global network of metabolite changes detected in human plasma in PAH development has been graphically presented in Figure 25.

In the context of central carbon metabolism (CCM), which centers on glycolysis and TCA cycle and deliver molecules to be catabolised in order to produce energy or for the biosynthesis of other compounds, few metabolites were significantly increased in PAH group. The elevated level of pyruvate and lactate has been observed in this study what can indicate the shift in energy production towards glycolysis. The similar metabolite changes underlining the energy imbalance (Warburg effect) was characteristic for hypoxic and an acute phase of PH in the animal model investigated in this thesis. However, recent report [135] suggested the reduced glycolysis in human PAH lung tissue compared to normal one. The explanation of these contrary results can be associated with the different PAH stage. In our study the patients with developing PAH were included while in the study based on lung tissue the severe and an advanced state of PAH was considered [135]. Interestingly, it is worth to note that metabolites derived from glycolysis could be involved in PAH progression and deliver new prognostic markers of the disease however further investigations based on larger population with different PAH stages are required to confirm the reliability of proposed metabolic markers. Other metabolites related to carbohydrate metabolism including threitol and gluconic acid lactone were observed to be increased in plasma of PAH group. Threitol is an end product of xylose metabolism whereas gluconic acid lactone derives from glucose oxidation and participates in pentose phosphate pathway which is a process involved in glucose turnover.

In the view of CCM, TCA cycle is employed in oxidation of carbohydrates, lipids and selected amino acids and its metabolic intermediates are continuously transported to the cytoplasm to increase energy production and fatty acids synthesis. In the present human based study of PAH, the significantly increased level of citric acid was observed in plasma of PAH group what can be a result of increased activity of citrate synthase. The same tendency was

reported in human lung tissue what can suggest an up-regulation of TCA cycle during the PAH development [135].

The disrupted energy production observed in this human based PAH model is also connected to alterations of fatty acid metabolism. The primary fatty acids amides (PFAMs) including palmitamide, stearamide and oleamide were found significantly decreased in plasma of PAH group. The PFAMs can be produced by two proposed routes involving ammonolysis of fatty acyl-CoA thioesters or the oxidative cleavage of *N*-fatty acylglycines [136]. The intensive studies on PFAMs revealed that they are important signaling molecules which control numerous of biological processes such as sleep, locomotion, angiogenesis, release of Ca^{2+} , blood vessels relaxation. Oleamide, as the best-studied of the PFAMs, has been recently reported to enhance the vasorelaxant effects in hypertension [137]. In addition, palmitamide, stearamide and oleamide were secreted by human atherothrombotic aneurysms [138] what suggests the potential role of PFAMs in pathogenesis of vascular diseases. In case of PAH, they can indicate the promising direction of further investigations.

The other group of metabolites representing the significant difference between PAH and control groups were long-chain acylcarnitines, which are the substrates for PFAMs synthesis. Carnitine and its derivatives are employed in the transport of activated long-chain fatty acids from cytoplasm into mitochondrial compartment where the enzymes involved in β -oxidation are located. The scheme of β -oxidation and connections with other metabolic pathways were presented in Figure 26. Carnitines play crucial role in maintenance of normal mitochondrial function and it is well known that alterations in carnitine metabolism result in mitochondrial dysfunction at the cellular level. In the present study, the significant decrease in palmitoylcarnitine, vaccenylcarnitine (or oleoylcarnitine) and steaorylcarnitine in plasma of PAH patients in comparison to the control group, was observed. The peroxisome proliferator-activated receptors (PPARs) are major regulators of energy balance and control the expression of genes involved in β -oxidation process [139]. The PPARs have been reported to be involved in various pathological processes as diabetes, cancer, inflammation or atherosclerosis [140]. Recently, the decreased level of palmitoylcarnitine, vaccenylcarnitine (or oleoylcarnitine) and steaorylcarnitine in plasma of aneurysm patients has been observed indicating the altered fatty

acid β -oxidation or deficiency of carnitine [141]. In addition, the experimental models also suggest that loss of PPARs signaling may result in the progression of pulmonary hypertension [142]. However, contrariwise to our results, the increase in palmitoylcarnitine, vaccenylcarnitine (or oleoylcarnitine) and steaorylcarnitine in human PAH lung tissue was reported [135]. Similarly to glycolysis derived metabolites, the alterations of carnitine metabolism may be specific for pathological stage of PAH and may be different in an acute or severe phase what indicate its potential role in the disease progression. Ketosphingosine, as a sphingolipid involved in sphingosine metabolism, was significantly decreased in plasma of PAH patients in comparison to healthy participants. Sphingolipids have been previously reported to be agonists of PPAR receptors which are, as described above, involved in fatty acids β -oxidation process [143]. Sphingolipids have also been suggested to play crucial role in cell proliferation, apoptosis and cell signaling what makes them important bioactive compounds [121]. In addition, the significant changes in few lysophospholipids as products of phospholipids metabolism were observed in plasma of PAH group what can indicate the PLA2 regulation. In the group of metabolites involved in lipid metabolism, glycerol and nonanoic acid were significantly increased in plasma of PAH patients when compared to controls what indicates the intensified rate of lipolysis which delivers new sources for energy production.

The statistically significant changes in cholesterol metabolism were also observed between compared groups in the present study. The decrease in cholesterol and increase in hydroxy-oxo-cholanoic acid, a bile acid product of cholesterol metabolism, were detected in plasma of PAH patients compared to controls. The similar tendency of change in the case of hydroxy-oxo-cholanoic acid was previously suggested to be secreted by abluminal part of human atherothrombotic aneurysms [138].

The other metabolite representing the significant change between PAH and control group, was uric acid. The increased level of this metabolite was observed in plasma of PAH patients. Uric acid is a heterocyclic final oxidation product of purine metabolism and it is a result of xanthine oxidase activity, which oxidizes oxypurines, for instance, xanthine into uric acid. The contributory role of uric acid in systemic hypertension has been previously reported [144]. Uric acid, although is known as an antioxidant in the extracellular part, induces oxidative stress within cells and leads to the renin-angiotensin system (RAS) activation. In

addition, uric acid inhibits an endothelial nitric oxide (NO) generation. These effects lead to systemic and renal vasoconstriction and hypertension development. Our results underline the potential role of uric acid in pathological processes involved in PAH development.

The next group of metabolites, with significant changes in plasma of compared groups, were amino acids. Among them, the elevated level of pyroglutamic acid (5-oxo-proline) was observed in plasma of PAH group. Pyroglutamic acid is employed in glutathione (GSH) turnover. The GSH is the best known cellular antioxidant so that alterations of GSH homeostasis observed in present study could be related to oxidative stress during PAH condition. In addition, GSH plays an crucial role in numerous cellular processes such as cell differentiation, proliferation or apoptosis, therefore disruptions in GSH turnover are likely to be involved in the pathogenesis or progression of cardiovascular and inflammatory diseases [145]. In addition, regarding amino acid metabolism, tryptophan and isoleucine (or norleucine) were decreased whereas glutamine, glycolic acid, alanine and creatinine were augmented in plasma of PAH patients in comparison to the control group. Especially, the changes in tryptophan level can be important in the case of PAH pathogenesis. Tryptophan is an essential amino acid in the human diet. In addition, it is transformed to serotonin by tryptophan hydrolase. Serotonin has been suggested to enhance pulmonary arterial smooth muscle cell proliferation, vasoconstriction and local microthrombosis [146]. In addition, it has been previously reported that expression of the gene regulating isoform 1 of tryptophan hydrolase was increased in lungs and pulmonary endothelial cells in an idiopathic PAH [147]. The other investigation aimed to study the genetic deletion of tryptophan hydroxylase 1 on hypoxia-induced pulmonary arterial hypertension in mice and confirmed its crucial role in disease development [148]. In our study, the decrease in tryptophan can be related to its metabolic conversion into serotonin which can be employed in cell proliferation and vascular remodeling in PAH.

Interestingly, as a result of present study, the significantly increased level of aminomalonic acid was observed in plasma of PAH group. The possible sources of the presence of aminomalonic acid include errors in protein synthesis or oxidative damage to amino acid residues in proteins [149]. However, the biochemical role of this metabolite is still

a question for further research, it is employed in the pyruvate conversion into alanine. Recently, increased plasma level of aminomalonic acid was observed in patients with aneurysm [150], however it was reduced in plasma of patients with acute coronary syndrome [151]. These reports together with our results may indicate the crucial role of aminomalonic acid in cardiovascular diseases.

To sum up, results presented in the thesis, confirmed that plasma metabolic fingerprinting may be powerful tool for understanding and explanation of pathological process involved in PAH progression. Although, it should be underlined that selected potential metabolic markers of PAH pathomechanism should be validated in larger human population to confirm their reliability and diagnostic or prognostic power. However, it also should be noted that PAH is relatively rare disorder so that the sample availability is limited. On the other hand, the frequency of PAH occurrence in human population can be underestimated due to the lack of characteristic clinical symptoms as consequently specific diagnostic biomarker. Therefore, metabolomics approach can provide new holistic insight into pathological processes involved in PAH development and thereby improve diagnosis, prognosis and treatment of the disease.

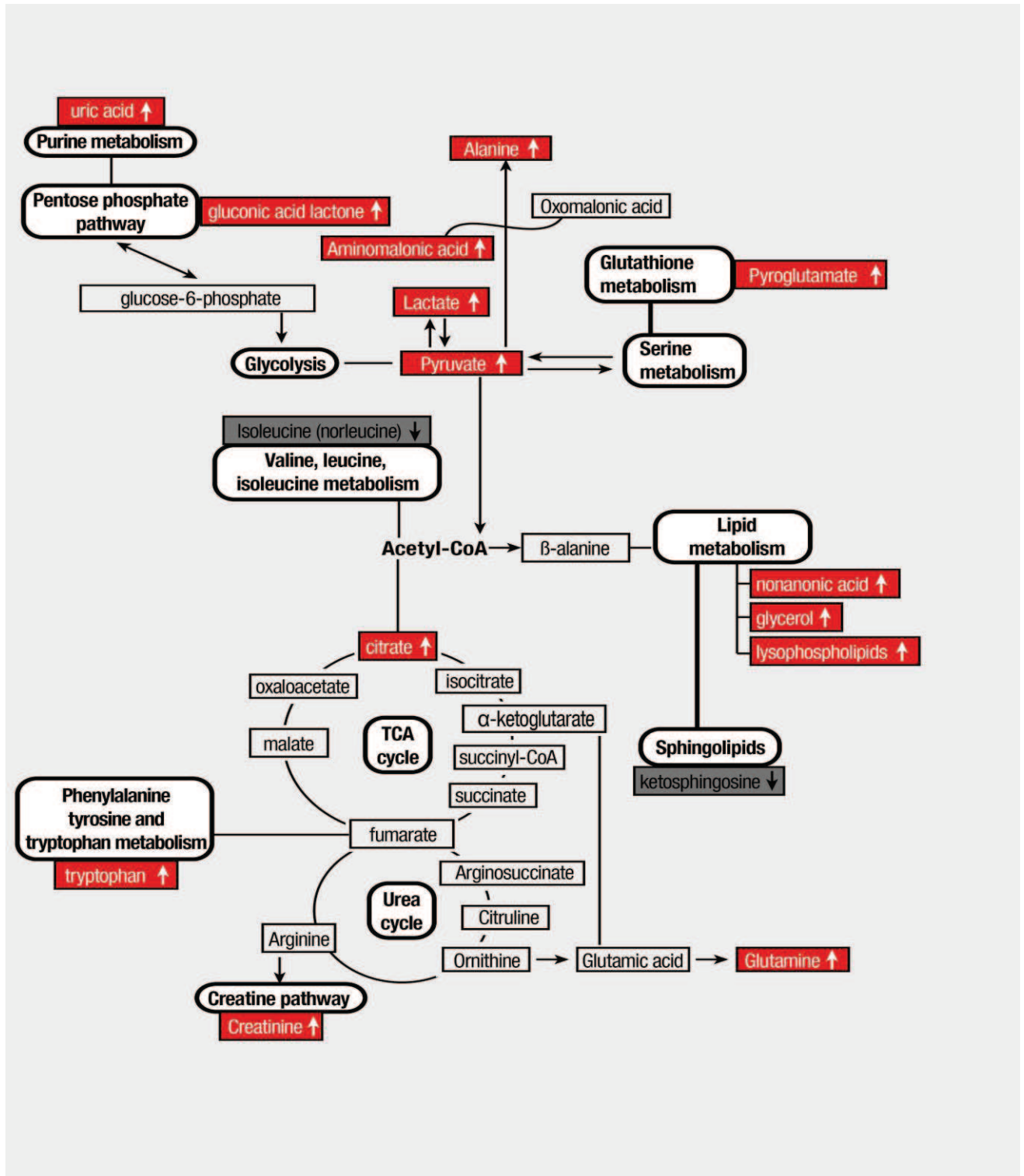


Figure 25. The global network of metabolite changes detected in human plasma in pulmonary arterial hypertension detected by HPLC-ESI-QTOF-MS or GC-Q-MS techniques. Those metabolites whose levels were increased in plasma of PAH patients are highlighted in red and those that decreased in grey boxes.

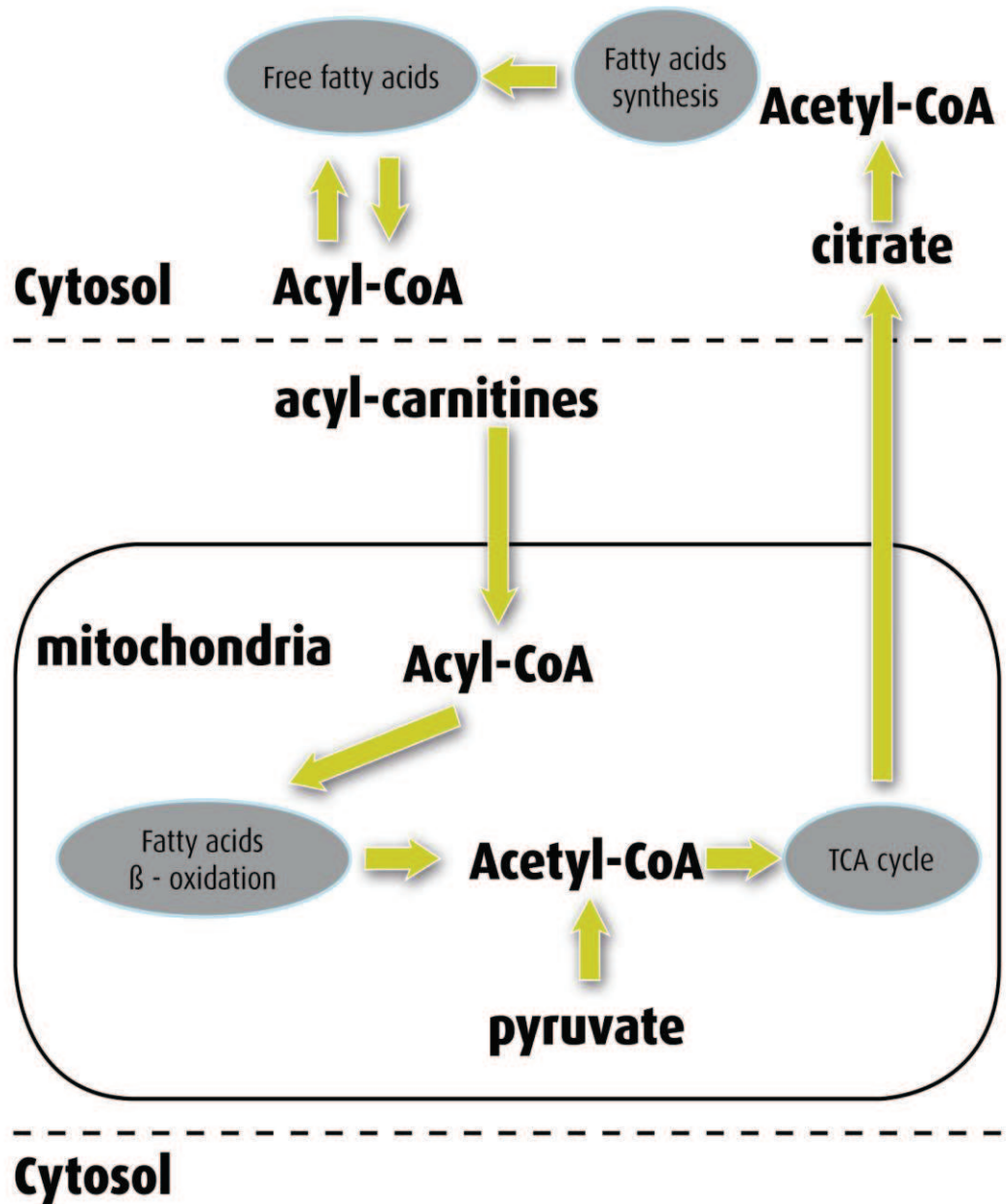


Figure 26. The role of carnitines in fatty acids β -oxidation and connections with other biochemical pathways.

V. CONCLUSIONS

- The presented doctoral thesis has proved that plasma metabolic fingerprinting with the use of modern and complementary platforms (LC-ESI-QTOF and GC-Q-MS) followed by multivariate data analysis is helpful to improve diagnosis and to study the global metabolic response to pathological processes involved in both acute and chronic stages of PH.
- The experiment based on the animal model of PH has revealed metabolite changes, which could be characteristic of an acute stage of PH. The increased plasma levels of lactate, pyruvate, pyroglutamate, α -hydroxybutyrate, acetoacetate, β -hydroxybutyrate, sphingosine, glycerol, citrate, malate, fumarate, tryptophan, phenylalanine, palmitic and oleic acid, as well as the decreased plasma levels of arginine, creatine, sphingomyelin, ceramide-1-phosphate, phospholipids and lysophospholipids, were observed as significantly changed between the compared groups.
- Those changes were associated with hypoxia, lipid-related energy imbalance, and cell signaling. Therefore, abnormal cellular metabolism such as glycolytic shift or alterations in mitochondrial function and signal transduction pathways, observed in the study, could be crucial pathological hallmarks of acute PE resulting in PH development.
- The study of PAH in human population has indicated metabolite alterations related to glycolysis, TCA cycle, pentose phosphate pathway, as well as amino acid, purine and fatty acid metabolic pathways, which could be specific for chronic phase of PAH progression. The increased plasma levels of uric acid, lactate, pyruvate, aminomalonic acid, glycerol, creatinine, palmitoylcarnitine, stearyl carnitine and glutamine, as well as decreased plasma levels of ketosphingosine, cholesterol, oleamide, palmitamide, stearamide, were found to represent statistically significant differences between PAH patients and healthy controls.

- Those changes indicated, that abnormal regulation of various metabolic pathways, as glycolytic shift, alternations of long chain carnitines and fatty acid metabolism, as well as signal transduction, revealed in the study, could be specific features of chronic stage of PAH.
- Metabolomics can turn out as a helpful tool in expanding current knowledge about pathogenesis of PH, what may consequently lead to discovery of new and more specific, diagnostic or prognostic markers of the disease.
- Potential metabolic markers, which were proposed in the presented doctoral thesis, should be validated on larger human populations, using the targeted and quantitative metabolomics approach, to confirm their probable diagnostic and prognostic power, which is obligatory in the studies focused on biomarkers discovery.

VI. SUMMARY

In the present doctoral thesis the untargeted plasma metabolic fingerprinting was used to study global metabolite alterations in pulmonary hypertension. To achieve this goal, the animal model was carefully designed and the human group was selected. Pigs were selected as an experimental animal model to provide the similarity to human, concerning the cardiovascular physiology, size, anatomy and blood perfusion distributions. Pulmonary hypertension in pigs was generated with the polydextrane microspheres injection. The animal model was designed in order to study an acute stage and therefore plasma metabolic fingerprinting was performed in two compared animal groups: before and 1 h after the initiation of the pulmonary embolism procedure resulting in pulmonary hypertension development. The human model of pulmonary hypertension was studied based on plasma metabolic fingerprints characteristic for the chronic pathological processes involved in the disease progression. During human model design, two groups were included and composed of PAH patients as well as healthy controls. The age, gender, BMI and associated diseases occurrence were considered to minimize the biological variation which is not related to the study aim but can affect the metabolomics results. Due to the complexity and chemical diversity of the metabolome, in order to detect as many as possible metabolites, two

complementary analytical platforms such as LC-ESI-QTOF-MS in both ionization modes (ESI+ and ESI-) and GC-Q-MS were applied to provide metabolites coverage in plasma metabolic fingerprints characterizing both an acute and a chronic stage of PAH.

First, the plasma sample pretreatment was performed to remove protein molecules and extract low-molecular-weight metabolites from complex biological matrices. In the case of metabolic fingerprinting with GC-Q-MS platform, an additional derivatization step was employed to increase volatility of compounds present in plasma samples. Then plasma extracts were fingerprinted with the use of optimized analytical methods with both LC-ESI-QTOF-MS and GC-Q-MS techniques. To control system stability and method reproducibility, QC samples were prepared as a pool of all plasma samples used in particular experiment. Subsequently, regular analysis of QC samples was conducted during the sequence run. Then, the acquired raw data obtained in LC-ESI-QTOF-MS and GC-Q-MS platforms, were reprocessed to extract compounds detected in all peaks of plasma metabolic fingerprints. Further data treatment was performed before statistical analysis. The alignment step was aimed to minimize the analytical variation concerning the retention time and mass shift occurring across analysis of all samples during the sequence runs. The sample multialignment step provided that each component of metabolic fingerprint was pointed as the same metabolite across all samples. Then, the filtration step, based on the frequency of particular metabolite in all samples analyzed, was conducted to remove random signals and remain only those with biological meaning.

Subsequently, the univariate statistical analysis was performed to selected metabolites representing significant difference between compared group. The *t* test or *U* Mann-Whitney test depending on the data distribution were applied to this purpose. Afterwards, the bioinformatic data analysis was required to study the relationships between multivariate plasma metabolic fingerprints and pathological stages of pulmonary arterial hypertension. As a first exploratory chemometric tool, principal component analysis was applied to reveal general trends in the obtained data, potential outliers and check quality of the analysis. Principal component analysis, as an unsupervised multivariate method, classifies samples based on their similarity included in data matrix without knowledge about class membership. In the present thesis, principal component analysis was mainly used to check systems performance and an

analytical method stability what was provided by QC samples grouping in the obtained score plots. The tightly clustering of QC samples ensured that biological variation between compared groups was real and not random or resulting from analytical variability. Subsequently, the partial least squares- discriminant analysis was applied to select metabolites contributed the most in group classification. As a supervised multivariate method, the partial least squares- discriminant analysis, apart from information included in data matrix utilizes the discrete data about samples membership, to find metabolites involved in group discrimination resulting from different biological state. The obtained multivariate discriminant models were validated with the use of leave-one-out cross-validation approach, to avoid the overfitting phenomenon and check the predictive value. The sensitivity and specificity of each independent discriminant models were assessed. All multivariate model were characterized by good sensitivity (at least 70%), specificity (at least 60%) and predictive value (at least 75%).

The identity of metabolites detected with LC-ESI-QTOF-MS platform and subsequently selected in either an univariate or a multivariate statistical analysis detected with LC-ESI-QTOF-MS platform was firstly confirmed by searching in publicly available databases such as METLIN, KEGG, LIPIDMAPS, HMDB and all simultaneously accessed by recently developed search engine, CEU MassMediator. The metabolites, found in databases mentioned above, were also confirmed by LC-MS/MS analysis. The metabolites detected with GC-Q-MS platform and representing the significant differences between compared groups were identified based on retention index, retention time and mass spectrum available in the NIST, Fiehn RTL and plasma in-house developed libraries. In the case of an animal model of pulmonary hypertension studied in the present thesis, 27 metabolites in LC-ESI-QTOF-MS and 19 in GC-Q-MS platforms were identified. In the human model of pulmonary hypertension, 21 metabolites in LC-ESI-QTOF-MS and 17 in GC-Q-MS were identified.

Finally, the analysis of biochemical pathways, in which the identified metabolites are involved, and connections between these routes were assessed to understand the global metabolic response to pathological processes associated with different phases of pulmonary hypertension. In the animal model, the metabolites found differentially distributed among compared groups were mainly involved in an energy imbalance such as glycolysis-derived metabolites, ketone bodies or TCA cycle intermediates, as well as lipid mediators which could

be employed in the signal transduction among cells such as sphingolipids and lysophospholipids. These metabolite changes confirmed the presence of the hypoxia-state in an acute phase of pulmonary hypertension. The obtained results revealed the important role of metabolic alterations in pathological processes involved in acute pulmonary hypertension. In the human model of the disease, the disruptions in glycolysis, TCA cycle, amino acids metabolism and mainly in fatty acids metabolism including β -oxidation or fatty acid amides synthesis have emerged among other biochemical pathways. These results suggested the potential role of glucose and lipids metabolic pathways in the molecular pathomechanisms associated with the progression of pulmonary hypertension. In addition, some new potential markers of the disease, such as oleamide, stearamide, palmitamide or aminomalonic acid have been revealed in the present study, however they have previously been reported to be related to various cardiovascular diseases but not to pulmonary hypertension.

To sum up, in the present doctoral thesis the plasma metabolic fingerprinting with the use of modern and complementary LC-ESI-QTOF and GC-Q-MS platforms followed by multivariate data analysis, was used to study global metabolic response to pathological processes involved in an acute and chronic stages of pulmonary hypertension. Since, the pathomechanisms of pulmonary hypertension are not completely understood yet, there is still a lack of specific biomarkers, which provide the effective diagnosis and prognosis of the disease. Therefore, the application of the metabolomics approach to study pathological processes at molecular level of both acute and chronic pulmonary hypertension was undertaken in the present doctoral thesis. The obtained results, have revealed that selected metabolites have a potency to be candidates for explanation the cellular mechanisms involved in disease pathogenesis. Metabolomics, among other *-omic* branches of systems biology approach, is closely related to molecular phenotype characteristic for particular biological state and therefore can provide the new insight into pathomechanisms involved in an acute and chronic stage of pulmonary hypertension. The results obtained in the present thesis open a new discipline for further research in order to improve current diagnosis, prognosis and therapeutic treatment of pulmonary hypertension. Metabolomics can turn out the helpful tool in expanding current knowledge about pathogenesis either of an acute or a chronic phase of pulmonary hypertension what can consequently lead to discovery and development of new diagnostic or prognostic biomarkers and more effective target therapies.

Table content

Table 1. The main advantages and drawbacks of MS and NMR application in metabolomics studies [25].

Table 2. The summary of advantages and limitations of the most commonly used analytical platforms in untargeted metabolomics [35].

Table 3. The comparison of various scaling techniques [44].

Table 4. Haemodynamic definition of PH [57].

Table 5. Updated risk factors for PAH development [66].

Table 6. The drugs and agents used in the currently licensed therapies [100].

Table 7. Hemodynamic parameters of animals at baseline state.

Table 8. Hemodynamic parameters of animals at acute pulmonary hypertension (PH) state.

Table 9. Statistical analysis of age and BMI difference in the studied groups.

Table 10. Clinical characteristics of individual participant included into the metabolomics study.

Table 11. The parameters of optimized method for UHPLC-ESI-QTOF-MS based plasma metabolic fingerprinting.

Table 12. The parameters of optimized method for HPLC-ESI-QTOF-MS based plasma metabolic fingerprinting.

Table 13. The characteristics of compounds included in the RI calibration file used for GC-Q-MS data processing.

Table 14. The results of prediction and LOOCV procedure for independent discriminant models obtained for data from pig plasma metabolic fingerprinting experiments.

Table 15. The confusion matrix, sensitivity and specificity of PLS-DA model based on UHPLC-ESI(+)-QTOF-MS data set.

Table 16. The confusion matrix, sensitivity and specificity of PLS-DA model based on UHPLC-ESI(-)-QTOF-MS data set.

Table 17. The confusion matrix, sensitivity and specificity of PLS-DA model based on GC-Q-MS data set.

Table 18. Metabolites significantly changed in pig plasma during acute phase of PH, identified during UHPLC-QTOF-MS metabolic fingerprinting experiment.

Table 19. Metabolites significantly changed in pig plasma during acute phase of PH, identified during GC-Q-MS metabolic fingerprinting experiment.

Table 20. The results of prediction and LOOCV procedure for separate discriminant models obtained for data from human plasma metabolic fingerprinting experiments.

Table 21. The confusion matrix, sensitivity and specificity of PLS-DA model based on HPLC-ESI(+)-QTOF-MS data set.

Table 22. The confusion matrix, sensitivity and specificity of PLS-DA model based on HPLC-ESI(-)-QTOF-MS data set.

Table 23. The confusion matrix, sensitivity and specificity of PLS-DA model based on GC-Q-MS data set.

Table 24. Metabolites significantly changed in pig plasma during acute phase of PH, identified during HPLC-QTOF-MS metabolic fingerprinting experiment.

Table 25. Metabolites significantly changing in human plasma of PAH group, identified in GC-Q-MS metabolic fingerprinting experiment.

Table 26. The results of univariate statistical analysis in external test group in the study of human PH.

Figure content

Figure 1. The general flow of biological information in the network –omic cascade.

Figure 2. Common research strategies in metabolomics [12].

Figure 3. Scheme of the typical workflow in untargeted metabolic fingerprinting approach.

Figure 4. Typical mass spectrometer construction.

Figure 5. The electrospray ionization mechanism [53].

Figure 6. The schematic construction of QqQ mass analyzer [56].

Figure 7. Clinical classification of pulmonary hypertension [66].

Figure 8. The major mechanisms in PAH pathogenesis [82].

Figure 9. The metabolic pathways in mitochondrion involved in energy production [82].

Figure 10. Current and emerging therapies and their targets in PAH treatment [100].

Figure 11. The histopathological changes in lung parenchyma of pig that underwent euthanasia 3 h after of acute PH induction by PE procedure. (A) Vessel obstruction by several microspheres marked as asterisk. (B) Macrophages infiltration around the microsphere obstructing the vessel marked as asterisk. (C) The hemorrhage pointed with arrowheads. (D) The hemorrhage marked as arrowhead and intraalveolar edema pointed with arrows. (E) The example of intraalveolar edema marked as arrow. (F) The severe perivascular and peribronchial inflammatory infiltration [102].

Figure 12. The simplified workflow of plasma sample pretreatment before LC-QTOF-MS metabolic fingerprinting.

Figure 13. The simplified scheme of plasma sample pretreatment prior to GC-Q-MS metabolic fingerprinting.

Figure 14. Representative UHPLC-ESI(+)-QTOF-MS chromatogram of pig plasma metabolic fingerprint form one pig plasma extract. A: Total Ion Chromatogram (TIC); B: overlay of all the individual features obtained after Molecular Feature Extraction (MFE) represented as extracted compound chromatogram (ECC) [102].

Figure 15. Representative UHPLC-ESI(-)-QTOF-MS chromatogram of pig plasma metabolic fingerprint form one pig plasma extract. A: Total Ion Chromatogram (TIC); B: overlay of all the individual features obtained after Molecular Feature Extraction (MFE) represented as extracted compound chromatogram (ECC) [102].

Figure 16. Representative GC-Q-MS Total Ion Chromatogram (TIC) of pig plasma metabolic fingerprint from one pig plasma extract [102].

Figure 17. Principal Component Analysis to verify quality of chromatographic analysis in all plasma metabolic fingerprinting experiments. (A) Scores plot for a PCA model built with the data set obtained in UHPLC-ESI(+)-QTOF-MS. Quality parameters for the model: explained variance $R^2 = 0.569$, predicted variance $Q^2 = 0.451$. (B) Scores plot for a PCA model built with the data set obtained in UHPLC-ESI(-)-QTOF-MS. $R^2 = 0.556$, $Q^2 = 0.308$. (C) Scores plot for a PCA model built with the data set obtained in GC-Q-MS. $R^2 = 0.649$, $Q^2 = 0.368$. QC samples have been marked as black spots. Animal groups before and after acute PE induction have been marked as blue spots or red spots, respectively.

Figure 18. PLS-DA plots for plasma metabolic fingerprints obtained before and after acute PE induction. (A) PLS-DA model ($R^2 = 0.959$, $Q^2 = 0.713$) for significantly changed variables detected in pig plasma with UHPLC-ESI(+)-QTOF-MS. (B) PLS-DA model ($R^2 = 0.999$, $Q^2 = 0.984$) for significantly changed variables detected in pig plasma with UHPLC-ESI(-)-QTOF-MS. (C) PLS-DA model ($R^2 = 0.924$, $Q^2 = 0.402$) for compounds detected in pig plasma with GC-Q-MS, after data filtration. The animal groups before and after acute PE have been marked as blue or red spots, respectively.

Figure 19. Metabolic changes in pig plasma during acute PH. Colored metabolites were detected using a GC-Q-MS or UHPLC-QTOF-MS platform. Those metabolites whose levels were increased in acute PH are highlighted in green and those that decreased in yellow boxes [102].

Figure 20. Representative HPLC-ESI(+)-QTOF-MS chromatogram of plasma metabolic fingerprint from exemplary human plasma extract. A: Total Ion Chromatogram (TIC), B: overlay of all the individual features obtained after Molecular Feature Extraction (MFE) represented as extracted compound chromatogram (ECC).

Figure 21. Representative HPLC-ESI(-)-QTOF-MS chromatogram of plasma metabolic fingerprint from exemplary human plasma extract. A: Total Ion Chromatogram (TIC), B: overlay of all the individual features obtained after Molecular Feature Extraction (MFE) represented as extracted compound chromatogram (ECC).

Figure 22. Representative GC-Q-MS Total Ion Chromatogram (TIC) of plasma metabolic fingerprint from exemplary human plasma extract.

Figure 23. Checking the quality of analysis in all plasma metabolic fingerprinting experiments. (A) Scores plot for a PCA model built with the data set obtained in HPLC-ESI(+)-QTOF-MS. Quality parameters for the model: explained variance $R^2 = 0.471$, predicted variance $Q^2 = 0.225$. (B) Scores plot for a PCA model built with the data set obtained in HPLC-ESI(-)-QTOF-MS. $R^2 = 0.455$, $Q^2 = 0.139$. (C) Scores plot for a PCA model built with the data set obtained in GC-Q-MS. $R^2 = 0.567$, $Q^2 = 0.193$. (D) The Hotelling's T² range for GC-Q-MS data set. QC samples, control and PAH group have been marked as black, blue and red spots, respectively.

Figure 24. PLS-DA plots for human plasma metabolic fingerprints obtained for control and PAH groups. (A) PLS-DA model ($R^2 = 0.845$, $Q^2 = 0.671$) for significantly changed variables detected in human plasma with HPLC-ESI(+)-QTOF-MS, (B) PLS-DA model ($R^2 = 0.896$, $Q^2 = 0.614$) for significantly changed variables detected in human plasma with HPLC-ESI(-)-QTOF-MS, (C) PLS-DA model ($R^2 = 0.825$, $Q^2 = 0.554$) for compounds detected in human plasma with GC-Q-MS, after data filtration. The control and PAH have been marked as blue or red spots, respectively.

Figure 25. The global network of metabolite changes detected in human plasma in pulmonary arterial hypertension detected by HPLC-ESI-QTOF-MS or GC-Q-MS techniques. Those metabolites whose levels were increased in plasma of PAH patients are highlighted in red and those that decreased in grey boxes.

Figure 26. The role of carnitines in fatty acids β -oxidation and connections with other biochemical pathways.

VII. REFERENCES

- [1] Snyder M., Li X.: Metabolomics as a robust tool in systems biology and personalized medicine: an open letter to the metabolomics community. *Metabolomics*, 2013, 9, 532–534.
- [2] Kitano H.: Systems biology: A brief overview, *Science*, 2002, 295, 1662-1664.
- [3] Peng L.: Tandem mass spectrometry: a new platform for fluxomics. *J Proteomics Bioinform*, 2012, 5 doi:10.4172/jpb.10000e14.
- [4] Nicholson J.K., Lindon J.C: Metabonomics, *Nature*, 2008, 455, 1054-1056.
- [5] Horning E.C., Horning M.G.: Metabolic profiles: gas-phase methods for analysis of metabolites, *Clin Chem*, 1971, 17, 802-809.
- [6] Horning E.C., Horning M.G.: Human metabolic profiles obtained by GC and GC/MS, *J Chromatogr Sci*, 1971, 9, 129-140.
- [7] Pauling L., Robinson A.B., Teranishi R., Cary P.: Quantitative analysis of urine vapor and breath by gas-liquid partition chromatography, *Proc Natl Acad Sci USA*, 1971, 68, 2374-2376.
- [8] Nicholson J.K, Lindon J.C, Holmes E.: “Metabonomics”: understanding the metabolic responses of living systems to pathophysiological stimuli via multivariate statistical analysis of biological NMR spectroscopic data, *Xenobiotica*, 1999, 29, 1181-1189.
- [9] Fiehn O.: Combining genomics, metabolome analysis, and biochemical modeling to understand metabolic networks, *Comp Funct Genom*, 2001, 2, 155-168.
- [10] Nobeli I., Ponsting H., Krissinel E.B., Thornton J.M.: A structure-based anatomy of the *E. coli* metabolome, *J Mol Biol*, 2003, 334, 697-719.
- [11] Wikoff W.R, Anfora A.T., Liu j., Schultz P.G., Lesley S.A., Peters E.C, Siuzdak G.: Metabolomics analysis reveals large effects of gut microflora on mammalian blood metabolites, *PNAS*, 2009,10, 3698-3703.[12] Barderas M.G, Laborde C.M, Posada M., de la Cuesta F., Zubiri I., Vivanco F., Alvarez-Llamas G. Metabolomic profiling for identification

of novel potential biomarkers in cardiovascular diseases, *J Biomed Biotechnol.* 2011, 790132. doi: 10.1155/2011/790132.

[13] Patti J.G., Yanes O., Siuzdak G.: Metabolomics: the apogee of the omic trilogy. *Nat Rev Mol Cell Biol*, 2013, 13, 263–269.

[14] Holmes E., Loo R.L., Stamler J., Bictash M., Yap I.K., Chan Q., Ebbels T., de Iorio M., Brown I.J., Veselkov K.A., Davignus M.L., Kesteloot H., Ueshima H., Zhao L., Nicholson J.K., Elliott P.: Human metabolic phenotype diversity and its association with diet and blood pressure, *Nature*, 2008, 453, 396-400.

[15] Lindon J.C., Nicholson J.K., Holmes E., Keun H.C., Craig A., Pearce J.T., Bruce S.J., Hardy N., Sansone S.A., Antti H.: Summary recommendations for standardization and reporting of metabolic analyses. *Nat Biotechnol*, 2005, 23, 833-838.

[16] Teahan O., Gamble S., Holmes E.: Impact of analytical bias in metabonomic studies of human blood serum and plasma. *Anal Chem*, 2006, 78, 4307–4318.

[17] Lenz E.M., Bright J., Wilson I.D., Morgan S.R., Nash A.F.A.: ¹H NMR-based metabonomic study of urine and plasma samples obtained from healthy human subjects, *J Pharm Biomed Anal*, 2003, 33, 1103-1115.

[18] Want E.J., Wilson I.D., Gika H., Theodoridis G., Plumb R.S., Shockcor J., Holmes E., Nicholson J.K.: Global metabolic profiling procedures for urine using UPLC-MS, *Nat Protoc*, 2010, 5, 1005-1018.

[19] Gangl E.T., Annan M.M., Spooner N., Vouros, P.: Reduction of signal suppression effects in ESI-MS using a nanosplitting device. *Anal Chem*, 2001, 73, 5635–5644.

[20] Godzien J., Ciborowski M., Whiley L., Legido-Quigley C., Ruperez F.J., Barbas C.: In-vial dual extraction liquid chromatography coupled to mass spectrometry applied to streptozotocin-treated diabetic rats. Tips and pitfalls of the method. *J Chromatogr A*, 2013, 1304, 52-60.

[21] Lenz E.M., Wilson I.D.: Analytical Strategies in Metabonomics, *J Proteome Res*, 2007, 6, 443-458.

- [22] Fiehn O., Kopka J., Trethewey R.N., Willmitzer L.: Identification of uncommon plant metabolites based on calculation of elemental compositions using gas chromatography and quadrupole mass spectrometry, *Anal Chem*, 2000, 75, 3573-3580.
- [23] Chan E.C., Pasikanti K.K., Nicholson J.K.: Global urinary metabolic profiling procedures using gas chromatography–mass spectrometry, *Nat Protoc*, 2011, 6, 1483–1499.
- [24] Lindon J.C., Nicholson, J.K.: Analytical technologies for metabonomics and metabolomics, and multi-omic information recovery. *Trac-Trend Anal Chem*, 2008, 27, 194-204.
- [25] Lindon J.C., Nicholson J.K.: Spectroscopic and statistical techniques for information recovery in metabonomics and metabolomics, *Annu Rev Anal Chem*, 2008, 1, 45-49.
- [26] Lindon J.C., Nicholson J.K., Holmes E., Antti H., Bollard M.E., Keun H., Beckonert O., Ebbels T.M., Reily M.D., Robertson D., Stevens G.J., Luke P., Breau A.P., Cantor G.H., Bible R.H., Niederhauser U., Senn H., Schlotterbeck G., Sidemann U.G., Laursen S.M., Tymiak A., Car B.D., Lehman-McKeeman L., Colet J.M., Loukaci A., Thomas C.: Contemporary issues in toxicology. The role of metabonomics in toxicology and its evaluation by the COMET project, *Toxicol App Pharmacol*, 2003, 187, 137-146.
- [27] Coen M., Ruepp S.U., Lindon J.C., Nicholson J.K., Pognan F., Lenz E.M., Wilson I.D. Integrated application of transcriptomics and metabonomics yields new insight into the toxicity due to paracetamol in the mouse. *J Pharm Biomed Anal*, 2004, 1;35(1):93-105.
- [28] Chauton M.S., Størseth T.R., Johnsen G.: High-resolution magic angle spinning 1 H NMR analysis of whole cells of *Thalassiosira pseudonana* (Bacillariophyceae): Broad range analysis of metabolic composition and nutritional value. *J App Phycol*, 2003, 15, 533-542.
- [29] Tolstikov V.V., Fiehn O.: Analysis of highly polar compounds of plant origin: combination of hydrophilic interaction chromatography and electrospray ion trap mass spectrometry, *Anal Biochem*, 2002, 301, 298-307.
- [30] Wilson I.D., Nicholson J.K., Castro-Perez J., Granger J.H., Johnson K.A., Smith B.W., Plumb R.S.: High resolution "ultra performance" liquid chromatography coupled to oa-TOF

mass spectrometry as a tool for differential metabolic pathway profiling in functional genomic studies, *J Proteome Res*, 2005, 4, 591-598.

[31] Corcoran O., Spraul M.: LC-NMR-MS in drug discovery. *Drug Discov Today*, 2003, 8, 624–631.

[32] Shellie R.A., Welthagen W., Zrostlikova J., Spranger J., Ristow M., Fiehn O., Zimmermann R.: Statistical methods for comparing comprehensive two-dimensional gas chromatography-time-of-flight mass spectrometry results: metabolomic analysis of mouse tissue extracts, *J Chromatogr A*, 2005, 1086, 83-90.

[33] Naz S., Garcia A., Rusak M., Barbas C.: Method development and validation for rat serum fingerprinting with CE-MS: application to ventilator-induced-lung-injury study. *Anal Bioanal Chem*, 2013, 405, 4849-4858.

[34] Moraes E.P., Rupérez F.J., Plaza M., Herrero M., Barbas C.: Metabolomic assessment with CE-MS of the nutraceutical effect of *Cystoseira* spp extracts in an animal model, *Electrophoresis*, 2011, 32, 2055-2062.[35] Dunn W.B., Bailey N.J., Johnson H.E.: Measuring the metabolome: current analytical technologies. *Analyst*, 2005, 130, 606-625.

[36] Dunn W.B., Ellis D.I.: Metabolomics: current analytical platforms and methodologies, *Trac-Trend Anal Chem*, 2005, 24, 285-294.

[37] Godzień J., Ciborowski M., Angulo S., Barbas C.: From numbers to a biological sense: How the strategy chosen for metabolomics data treatment may affect final results. A practical example based on urine fingerprints obtained by LC-MS, *Electrophoresis*, 2013, 34, 2812–2826.[38] Eliasson M., Rännar S., Madsen R., Donten M.A., Marsden-Edwards E., Moritz T., Shockcor J.P., Johansson E., Trygg J.: Strategy for optimizing LC-MS data processing in metabolomics: a design of experiments approach. *Anal Chem*, 2012, 84, 6869-6876.

[39] Behrends V., Tredwell G.D., Bundy J.G.: A software complement to AMDIS for processing GC-MS metabolomic data, *Anal Biochem*, 2011, 206–208.

[40] van Nederkassel A.M., Daszykowski M., Eilers P.H., Vander Heyden Y.: A comparison of three algorithms for chromatograms alignment. *J Chromatogr A*, 2006, 1118, 199-210.

- [41] Szymanska E., Markuszewski M.J., Capron X., van Nederkassel A.M., Heyden Y.V., Markuszewski M., Krajka K., Kaliszan R.: Increasing conclusiveness of metabonomic studies by chemoinformatic preprocessing of capillary electrophoresis data on urinary nucleoside profiles, *J Pharm Biomed Anal*, 2007, 43, 413-420.
- [42] Broil R., Smilde A.K.: Centring and scaling in component analysis, *J Chemometrics*, 2003, 17, 16-33.
- [43] Warrack B.M., Hnatyshyn S., Ott K.-H., Reily M.D., Sanders M., Zhang H., Drexler D.M.: Normalization strategies for metabonomic analysis of urine samples, *J Chromatogr B Analyt Technol Biomed Life Sci*, 2009, 877, 547-552.
- [44] van den Berg R.A., Hoefsloot H.C.J., Westerhuis J.A., Smilde A.K., van der Werf M.J.: Centering, scaling, and transformations: improving the biological information content of metabolomics data, *BMC Genomics*, 2006, 7, doi: 10.1186/1471-2164-7-142.
- [45] Lindon J.C., Holmes E., Nicholson J.K.: Metabonomics techniques and applications to pharmaceutical research and development, *Pharm Res*, 2006, 23, 1075-1088.
- [46] Fonville J.M., Richards S.E., Barton R.H., Boulange C.L., Ebbels T.M.D., Nicholson J.K., Holmes E., Dumas M.E.: The evolution of partial least squares models and related chemometric approaches in metabonomics and metabolic phenotyping, *J Chemometr*, 2010, 24, 636-649.
- [47] Bylesjö M., Rantalainen M., Cloarec O., Nicholson J.K., Holmes E., Trygg J.: OPLS discriminant analysis: combining the strengths of PLS-DA and SIMCA classification, *J Chemometr*, 2006, 20, 341-351.
- [48] Broadhurst D.I., Kell D.B.: Statistical strategies for avoiding false discoveries in metabolomics and related experiments, *Metabolomics*, 2006, 2, 171-196.
- [49] Westerhuis J.A., Hoefsloot H.C.J., Smit S., Vis D.J., Smilde A.K., van Velzen E.J.J., van Duijnhoven J.P.M., van Dorsten F.A.: Assessment of PLS-DA cross validation, *Metabolomics*, 2008, 4, 81-89.

- [50] Wehrens R., Putter H., Buydens L.M.C.: The bootstrap: a tutorial. *Chemometrics and Intelligent Laboratory Systems*, 2000, 54, 35–52.
- [51] Quintás G., Portillo N., García-Cañaveras J.C., Castell J.V., Ferrer A., Lahoz A.: Chemometric approaches to improve PLS-DA model outcome for predicting human non-alcoholic fatty liver disease using UPLC-MS as a metabolic profiling tool, *Metabolomics*, 2012, 8, 86-98.
- [52] Lee D.Y., Bowen B.P., Northen T.R.: Mass spectrometry-based metabolomics, analysis of metabolite-protein interactions, and imaging, *Biotechniques*, 2010, 49, 557–565.
- [53] www.chm.bris.ac.uk/ms/theory/esi-ionisation.html
- [54] Karas M., Bahr U., Dülcks T.: Nano-electrospray ionization mass spectrometry: addressing analytical problems beyond routine, *Fresenius J Anal Chem*, 2000, 366, 669-676.
- [55] Ciborowski M., Lipska A., Godzien J., Ferrarini A., Korsak J., Radziwon P., Tomasiak M., Barbas C.: Combination of LC-MS- and GC-MS-based Metabolomics to Study the Effect of Ozonated Autohemotherapy on Human Blood, *J Proteome Res*, 2012, 11, 6231–6241.
- [56] <http://departments.agri.huji.ac.il/zabam/triplequad.html>.
- [57] Galie N., Torbicki A., Barst R., Darteville P., Haworth S., Higenbottam T., Olschewski H., Peacock A., Pietra G., Rubin L.J., Simonneau G.: Guidelines for the diagnosis and treatment of pulmonary hypertension, *Eur Heart J*, 2009, 30, 2493–2537.
- [58] Humbert M.: The burden of pulmonary hypertension, *Eur Respir J*, 2007, 30, 1–2.
- [59] Hyduk A., Croft J.B., Ayala C., Zheng K., Zheng Z.J., Mensah G.: Pulmonary hypertension surveillance-United States, 1980–2002, *MMWR*, 2005, 54, 1–28.
- [60] Peacock A.J., Murphy N.F., McMurray J.J.V., Caballero L., Stewart S.: An epidemiological study of pulmonary arterial hypertension, *Eur Respir J*, 2007, 30, 104–109.
- [61] Humbert M., Sitbon O., Chaouat A.: Pulmonary arterial hypertension in France: results from a National Registry, *Am J Respir Crit Care Med*, 2006, 173, 1023–1030.

- [62] Lapa M., Dias B., Jardim C., Fernandes C.J., Dourado P.M., Figueiredo M., Farias A., Tsutsui J., Terra-Filho M., Humbert M., Souza R.: Cardio-pulmonary manifestations of hepatosplenic schistosomiasis, *Circulation*, 2009, 119, 1518–1523.
- [63] Penaloza D., Arias-Stella J.: The heart and pulmonary circulation at high altitudes: healthy highlanders and chronic mountain sickness, *Circulation*, 2007, 115, 1132–1146.
- [64] Simonneau G., Robbins I.M., Beghetti M., Channick R.N., Delcroix M., Denton C.P., Elliott C.G., Gaine S.P., Gladwin M.T., Jing Z.C., Krowka M.J., Langleben D., Nakanishi N., Souza R.: Updated clinical classification of pulmonary hypertension, *J Am Coll Cardiol*, 2009, 54, 43–54.
- [65] Hatano S., Strasser T.: Primary pulmonary hypertension. Report on a WHO Meeting. Geneva: World Health Organization, 1975.
- [66] Simonneau G., Robbins I.M., Beghetti M., Channick R.N., Delcroix M., Denton C.P., Elliott C.G., Gaine S.P., Gladwin M.T., Jing Z.C., Krowka M.J., Langleben D., Nakanishi N., Souza R.: Updated clinical classification of pulmonary hypertension, *J Am Coll Cardiol*, 2009, 54, 43–54.
- [67] Mukerjee D., St George D., Coleiro B., Knight C., Denton C., Davar J., Black C. J.: Prevalence and outcome in systemic sclerosis associated pulmonary arterial hypertension: application of a registry approach, *Ann Rheum Dis*, 2003, 62, 1088–1093.
- [68] Hervé P., Lebrec D., Brenot F., Simonneau G., Humbert M., Sitbon O., Duroux P.: Pulmonary vascular disorders in portal hypertension, *Eur Respir J*, 1998, 11, 1153–66.
- [69] Krowka M.J., Swanson K.L., Frantz R.P., McGoan M.D., Wiesner R.H.: Portopulmonary hypertension: results from a 10-year screening algorithm, *Hepatology*, 2006, 44, 1502–1510.
- [70] Lapa M., Dias B., Jardim C., Fernandes C.J., Dourado P.M., Figueiredo M., Farias A., Tsutsui J., Terra-Filho M., Humbert M., Souza R.: Cardio-pulmonary manifestations of hepatosplenic schistosomiasis, *Circulation*, 2009, 119, 1518 –1523.

- [71] Reiter C.D., Wang X., Tanus-Santos J.E., Hogg N., Cannon R.O., Schechter A.N., Gladwin M.T.: Cell-free hemoglobin limits nitric oxide bioavailability in sickle-cell disease, *Nat Med*, 2002, 8, 1383–1389.
- [72] Robin H. Steinhorn, M.D.: Neonatal pulmonary hypertension, *Pediatr Crit Care Med*, 2010, 11, 79–84.
- [73] Rabinovitch M.: Pathobiology of pulmonary hypertension, *Ann Rev Pathol*, 2007, 2, 369–399.
- [74] Kreymborg K., Uchida S., Gellert P., Schneider A., Boettger T., Voswinckel R., Wietelmann A., Szibor M., Weissmann N., Ghofrani A.H., Schermuly R., Schranz D., Seeger W., Braun T.: Identification of right heart-enriched genes in a murine model of chronic outflow tract obstruction, *J Mol Cell Cardiol*, 2010, 49, 598–605.
- [75] Wharton J., Strange J.W., Møller G.M., Growcott E.J., Ren X., Franklyn A.P., Phillips S.C., Wilkins M.R.: Antiproliferative effects of phosphodiesterase type 5 inhibition in human pulmonary artery cells. *Am J Respir Crit Care Med*, 172, 2005, 105–113.
- [76] Leiper, J., Nandi M., Torondel B., Murray-Rust J., Malaki M., O'Hara B., Rossiter S., Anthony S., Madhani M., Selwood D., Smith C., Wojciak-Stothard B., Rudiger A., Stidwill R., McDonald N.Q., Vallance P.: Disruption of methylarginine metabolism impairs vascular homeostasis, *Nat Med.*, 2007, 13, 198–203.
- [77] Christman B.W., McPherson C.D., Newman J.H., King G.A., Bernard G.R., Groves B.M., Loyd J.E.: An imbalance between the excretion of thromboxane and prostacyclin metabolites in pulmonary hypertension, *N Engl J Med*, 1992, 327, 70–75.
- [78] Eddahibi S., Guignabert C., Barlier-Mur A.M., Dewachter L., Fadel E., Dartevielle P., Humbert M., Simonneau G., Hanoun N., Saurini F., Hamon M., Adnot S.: Cross talk between endothelial and smooth muscle cells in pulmonary hypertension: critical role for serotonin-induced smooth muscle hyperplasia. *Circulation*, 2006, 113, 1857–1864.

- [79] Davie N., Haleen S.J., Upton P.D., Polak J.M., Yacoub M.H., Morrell N.W., Wharton J.: ETA and ETB receptors modulate the proliferation of human pulmonary artery smooth muscle cells, *Am J Respir Crit Care Med*, 165, 2002, 398–405.
- [80] Launay J.M., Hervé P., Peoc'h K., Tournois C., Callebert J., Nebigil C.G., Etienne N., Drouet L., Humbert M., Simonneau G., Maroteaux L.: Function of the serotonin 5-hydroxytryptamine 2B receptor in pulmonary hypertension, *Nat Med*, 2002, 8, 1129–1135.
- [81] Ooi C.Y., Wang Z., Tabima D.M., Eickhoff J.C., Chesler N.C.: The role of collagen in extralobar pulmonary artery stiffening in response to hypoxia-induced pulmonary hypertension, *Am J Physiol Heart Circ Physiol*, 2010, 299, 1823–1831.
- [82] Schermuly R.T., Ghofrani H.A., Wilkins M.R., Grimminger F.: Mechanisms of disease: pulmonary arterial hypertension, *Nat Rev Cardiol*, 2011, 8, 443–455.
- [83] Lepetit H., Eddahibi S., Fadel E., Frisdal E., Munaut C., Noel A., Humbert M., Adnot S., D'Ortho M.P., Lafuma C.: Smooth muscle cell matrix metalloproteinases in idiopathic pulmonary arterial hypertension, *Eur Respir J*, 2005, 25, 834–842.
- [84] Rudarakanchana N., Flanagan J.A., Chen H., Upton P.D., Machado R., Patel D., Trembath R.C., Morrell N.W.: Functional analysis of bone morphogenetic protein type II receptor mutations underlying primary pulmonary hypertension, *Hum Mol Genet*, 2002, 11, 1517–1525.
- [85] Yang X., Long L., Southwood M., Rudarakanchana N., Upton P.D., Jeffery T.K., Atkinson C., Chen H., Trembath R.C., Morrell N.W.: Dysfunctional Smad signaling contributes to abnormal smooth muscle cell proliferation in familial pulmonary arterial hypertension, *Circ Res*, 2005, 96, 1053–1063.
- [86] Li X., Zhang X., Leathers R., Makino A., Huang C., Parsa P., Macias J., Yuan J.X., Jamieson S.W., Thistlethwaite P.A.: Notch3 signaling promotes the development of pulmonary arterial hypertension, *Nat Med*, 15, 2009, 1289–1297.
- [87] Duan S.Z., Usher M.G., Mortensen R.M.: Peroxisome proliferator-activated receptor-gamma-mediated effects in the vasculature, *Circ Res*, 2008, 102, 283–294.

- [88] Jiang C., Ting A.T., Seed B.: PPAR-gamma agonists inhibit production of monocyte inflammatory cytokines, *Nature*, 1998, 391, 82–86.
- [89] Khakoo A.Y., Finkel T.: Endothelial progenitor cells, *Annu Rev Med*, 2005, 56, 79–101.
- [90] Tuder R.M., Groves B., Badesch D.B., Voelkel N.F.: Exuberant endothelial cell growth and elements of inflammation are present in plexiform lesions of pulmonary hypertension, *Am J Pathol*, 1994, 144, 275–285.
- [91] Toshner M., Voswinckel R., Southwood M., Al-Lamki R., Howard L.S., Marchesan D., Yang J., Suntharalingam J., Soon E., Exley A., Stewart S., Hecker M., Zhu Z., Gehling U., Seeger W., Pepke-Zaba J., Morrell N.W.: Evidence of dysfunction of endothelial progenitors in pulmonary arterial hypertension, *Am J Respir Crit Care Med*, 2009, 180, 780–787.
- [92] Tuder R.M., Groves B., Badesch D.B., Voelkel N.F.: Exuberant endothelial cell growth and elements of inflammation are present in plexiform lesions of pulmonary hypertension, *Am J Pathol*, 1994, 144, 275–285.
- [93] Itoh T., Nagaya N., Ishibashi-Ueda H., Kyotani S., Oya H., Sakamaki F., Kimura H., Nakanishi N.: Increased plasma monocyte chemoattractant protein-1 level in idiopathic pulmonary arterial hypertension, *Respirology*, 2006, 11, 158–163.
- [94] Dorfmueller P., Chemokine RANTES in severe pulmonary arterial hypertension, *Am J Respir Crit Care Med*, 2002, 165, 534–539.
- [95] Sanchez O., Marcos E., Perros F., Fadel E., Tu L., Humbert M., Dartevielle P., Simonneau G., Adnot S., Eddahibi S.: Role of endothelium-derived CC chemokine ligand 2 in idiopathic pulmonary arterial hypertension, *Am J Respir Crit Care Med*, 2007, 176, 1041–1047.
- [96] Tournier A., Wahl D., Chaouat A., Max J.P., Regnault V., Lecompte T., Chabot F.: Calibrated automated thrombography demonstrates hypercoagulability in patients with idiopathic pulmonary arterial hypertension, *Thromb Res*, 2010, 126, 418–422.
- [97] Cottrill K.A., Chan S.Y.: Metabolic dysfunction in pulmonary hypertension: the expanding relevance of the Warburg effect, *Eur J Clin Invest*, 2013, 43, 855–865.

- [98] Warburg O.: On the origin of cancer cells, *Science*, 1956, 123, 309–314.
- [99] Reinartz P., Wildberger J.E., Schaefer W., Nowak B., Mahnken A.H., Buell U.: Tomographic imaging in the diagnosis of pulmonary embolism: a comparison between V/Q lung scintigraphy in SPECT technique and multislice spiral CT, *J Nucl Med*, 2004, 45, 1501-1508.
- [100] O'Callaghan D.S., Savale L., Montani D., Jaïs X., Sitbon O., Simonneau G., Humbert M.: Treatment of pulmonary arterial hypertension with targeted therapies, *Nat Rev Cardiol*, 2011, 8, 526–538.
- [101] O'Callaghan D.S., Gaine S.P.: Combination therapy and new types of agents for pulmonary arterial hypertension, *Clin Chest Med*, 2007, 28, 169–185.
- [102] Bujak R., García-Álvarez A., Rupérez F.J., Nuño-Ayala M., García A., Ruiz-Cabello J., Fuster V., Ibáñez B., Barbas C.: Metabolomics reveals metabolite changes in acute pulmonary embolism, *J Proteome Res*, 2014, 13, 805–816.
- [103] Dun W.B., Broadhurst D., Begley P., Zelena E., Francis-McIntyre S., Anderson N., Brown M., Knowles J.D., Halsall A., Haselden J.N., Nicholls A.W., Wilson I.D., Kell D.B., Goodacre R.: Procedures for large-scale metabolic profiling of serum and plasma using gas chromatography and liquid chromatography coupled to mass spectrometry, *Nat Protoc*, 2011, 6, 1060-1083.
- [104] Huisman M.V., Klok F.A.: Diagnostic management of clinically suspected acute pulmonary embolism, *J Thromb Haemostasis*, 2009, 7, 312-317.
- [105] Solaini G., Baracca A., Lenaz G., Sgarbi G.: Hypoxia and mitochondrial oxidative metabolism, *Biochim Biophys Acta*, 2010, 1797, 1171–1177.
- [106] Archer S.L., Fang Y.-H., Ryan J.J., Piao L.: Metabolism and bioenergetics in the right ventricle and pulmonary vasculature in pulmonary hypertension, *Pulm Circ*, 2013, 3, 144–52.
- [107] LaManna J.C., Salem N., Puchowicz M., Erokwu B., Koppaka S., Flask C., Lee Z.: Ketones suppress brain glucose consumption, *Adv Exp Med Biol*, 2009, 645, 301–306.

- [108] Sylvester J.T., Shimoda L.A., Aaronson P.I., Ward J.P.T.: Hypoxic pulmonary vasoconstriction, *Physiol Rev*, 2012, 92, 367–520.
- [109] Leach R.M., Hill H.M., Snetkov V.A., Robertson T.P., Ward J.P.: Divergent roles of glycolysis and the mitochondrial electron transport chain in hypoxic pulmonary vasoconstriction of the rat: identity of the hypoxic sensor, *J Physiol*, 2011, 536, 211–224.
- [110] Rubin M., Tuder L., Davis A., Graham B.B.: Targeting energetic metabolism. A new frontier in the pathogenesis and treatment of pulmonary hypertension, *Am J Respir Crit Care Med*, 2012, 185, 260–266.
- [111] Piao L., Fang Y.-H., Cadete V.J.J., Wietholt C., Urboniene D., Toth P.T., Marsboom G., Zhang H.J., Haber I., Rehman J., Lopaschuk, G.D., Archer S.L.: The inhibition of pyruvate dehydrogenase kinase improves impaired cardiac function and electrical remodeling in two models of right ventricular hypertrophy: resuscitating the hibernating right ventricle, *J Mol Med*, 2010, 88, 47–60.
- [112] Rehman J., Archer S.L.A.: Proposed mitochondrial-metabolic mechanism for initiation and maintenance of pulmonary arterial hypertension in fawn-hooded rats: The Warburg model of pulmonary arterial hypertension. In: Membrane Receptors, Channels and Transporters in Pulmonary Circulation, Advances in Experimental Medicine and Biology, Yuan J. X.-J., Ward J. P.T., Eds.; Springer: New York, 2010, 661, 171–185.
- [113] Lord R.S., Bralley J.A.: Clinical applications of urinary organic acids. Part I: Detoxification markers, *Altern Med Rev*, 2008, 13, 205–215.
- [114] Frezza C., Zheng L., Tennant D.A., Papovsky D.B., Hedley B.A., Kalna G., Watson D.G., Gottlieb E.: Metabolic profiling of hypoxic cells revealed a catabolic signature required for cell survival, *PLoS One*, 2011, 6, doi: 10.1371/journal.pone.0024411.
- [115] Yin J., Gao Z., He Q., Ye J.: Role of hypoxia in obesity-induced disorders of glucose and lipid metabolism in adipose tissue, *Am J Physiol Endocrinol Metab*, 2009, 296, 333–342.
- [116] Lambert I. H., Pedersen S. F., Poulsen K.A.: Activation of PLA2 isoforms by cell swelling and ischaemia/hypoxia, *Acta Physiol (Oxford)*, 2006, 187, 75–85.

- [117] Funk C.D.: Prostaglandins and leukotrienes: advances in eicosanoid biology, *Science*, 2001, 294, 1871-75.
- [118] Raj J.U., Chen P.: Role of eicosanoids in hypoxic vasoconstriction in isolated lamb lungs, *Am J Physiol Heart Circ Physiol*, 1987, 253, 626-633.
- [119] Jones J.E., Walker J.L., Song Y., Weiss N., Cardoso W.V., Tuder R.M., Loscalzo J., Zhang Y.Y.: Effect of 5-lipoxygenase on the development of pulmonary hypertension in rats, *Am J Physiol Heart Circ Physiol*, 2004, 286, 1775-1784.
- [120] Weissmann N., Sommer N., Schermuly R.T., Ghofrani H.A., Seeger W., Grimminger F.: Oxygen sensors in hypoxic pulmonary vasoconstriction, *Cardiovasc Res*, 2006, 71, 620-629.
- [121] Bartke N., Hannun Y.A.: Bioactive sphingolipids: metabolism and function, *J Lipid Res*, 2009, 50, 91-96.
- [122] Cogolludo A., Moreno L., Frazziano G., Moral-Sanz J., Menendez C., Castañeda J., González C., Villamor E., Perez-Vizcaino F.: Activation of neutral sphingomyelinase is involved in acute hypoxic pulmonary vasoconstriction, *Cardiovasc Res*, 2009, 82, 296–302.
- [123] Geoffroy K., Wiernsperger N., Lagarde M., El Bawab S.: Bimodal effect of advanced glycation end products on mesangial cell proliferation is mediated by neutral ceramidase regulation and endogenous sphingolipids, *J Biol Chem*, 2004, 279, 34343–34352.
- [124] Ma S., Turino G.M., Lin Y.Y.: Quantitation of desmosine and isodesmosine in urine, plasma, and sputum by LC-MS/MS as biomarkers for elastin degradation *J Chromatogr B Anal Technol Biomed Life Sci*, 2011, 879, 1893-1898.
- [125] Huang J.T.H., Chaudhuri R., Albarbarawi O., Barton A., Grierson C., Rauchhaus P., Weir C.J., Messow M., Stevens N., McSharry C., Feuerstein G., Mukhopadhyay S., Brady J., Palmer C.N.A., Miller D., Thomson N.C.: Clinical validity of plasma and urinary desmosine as biomarkers for chronic obstructive pulmonary disease, *Thorax*, 2012, 67, 502-508.
- [126] Cottrill K.A., Chan S.Y.: Metabolic dysfunction in pulmonary hypertension: the expanding relevance of the Warburg effect, *Eur J Clin Invest*, 2013, doi: 10.1111/eci.12104.

- [127] Agrawal A., Guttapalli A., Narayan S., Albert T.J., Shapiro I.M., Risbud M.V.: Normoxic stabilization of HIF-1 drives glycolytic metabolism and regulates aggrecan gene expression in nucleus pulposus cells of the rat intervertebral disk, *Am J Physiol Cell Physiol*, 2007, 293, 621-631.
- [128] Marsboom G., Wietholt C., Haney C.R., Toth P.T., Ryan, J. J., MorrowE., ThenappanT., Bache-Wiig P., Piao L., Paul J., Chen C-T., Archer S.L.: Lung 18F-Fluorodeoxyglucose positron emission tomography for diagnosis and monitoring of pulmonary arterial hypertension, *Am J Respir Crit Care Med*, 2012, 185, 670-679.
- [129] Lopez-Barneo J., Pardal R., Ortega-Sáenz P.: Cellular mechanism of oxygen sensing. *Annu Rev Physiol*, 2001, 63, 259–287.
- [130] Land S.C., Tee A.R.: Hypoxia-inducible factor 1alpha is regulated by the mammalian target of rapamycin (mTOR) via an mTOR signaling motif, *J Biol Chem*, 2007, 282, 20534-20543.
- [131] Laplante M., Sabatini D.M.: An emerging role of mTOR in lipid biosynthesis, *Curr Biol*, 2009, 19, 1046-1052.
- [132] Wymann M.P., Schneider R.: Lipid signalling in disease, *Nat Rev Mol Cell Biol*, 2008, 9, 162-176.
- [133] Gurbanov E., Shiliang X.: The key role of apoptosis in the pathogenesis and treatment of pulmonary hypertension, *Eur J Cardiothorac Surg*, 2006, 30, 499-507.
- [134] Goncharova E.A.: mTOR and vascular remodeling in lung diseases: current challenges and therapeutic prospects, *FASEB J*, 2013, 27, 1796–1807.
- [135] Zhao Y., Peng J., Lu C., Hsin M., Mura M., Wu L., Chu L., Zamel R., Machuca T., Waddell T., Liu M., Keshavjee S., Granton J., de Perrot M. Metabolomic heterogeneity of pulmonary arterial hypertension, *PLoS ONE*, 2014, 9, doi:10.1371/journal.pone.0088727.
- [136] Farrell E.K., Chen Y., Barazanji M., Jeffries K.A., Cameroamortegui F., Merkler DJ.: Primary fatty acid amide metabolism: conversion of fatty acids and an ethanolamine in N 18 TG 2 and SCP cells 1, *J Lipid Res*, 2012, 53, 247-256.

- [137] Jamie J. Hopps, William R. Dunn, Michael D. Randall. Enhanced vasorelaxant effects of the endocannabinoid-like mediator, oleamide, in hypertension, *Eur J Pharmacol*, 2012, 684, 102-107.
- [138] Ciborowski M., Martin-Ventura J.L., Meilhac O., Michel J.B., Ruperez F.J., Tunon J., Egido J., Barbas C.: Metabolites secreted by human atherothrombotic aneurysms revealed through a metabolomic approach, *J Proteome Res*, 2011, 10, 1374-1382.
- [139] van Raalte D.H., Li M., Pritchard P.H., Wasan K.M.: Peroxisome proliferator-activated receptor (PPAR)-alpha: a pharmacological target with a promising future, *Pharm Res*, 2004, 21, 1531-1538.
- [140] Kersten S., Desvergne B., Wahli W.: Roles of PPARs in health and disease. *Nature*, 2000, 405, 421-424.
- [141] Ciborowski M., Teul J., Martin-Ventura J.L., Egido J., Barbas C.: Metabolomics with LC-QTOF-MS permits the prediction of disease stage in aortic abdominal aneurysm based on plasma metabolic fingerprint, *PLoS ONE*, 2012, 7, doi:10.1371/journal.pone.0031982.
- [142] Sutliff R.L., Kang B.Y., Hart C.M.: PPARgamma as a potential therapeutic target in pulmonary hypertension, *Ther Adv Respir Dis*, 2010, 4, 143-160.
- [143] Tsuji K., Satoh S., Mitsutake S., Murakami I., Park J.J., Li Q., Chang Y.T., Chung S.K., Igarashi Y.: Evaluation of synthetic sphingolipid analogs as ligands for peroxisome proliferator-activated receptors. *Bioorg Med Chem Lett*, 2009, 19, 1643-1646.
- [144] Mazzali M., Kanbay M., Segal M.S., Shafiu M., Jalal D., Feig D.I., Johnson R.J.: Uric acid and hypertension: cause or effect? *Curr Rheumatol Rep*, 2010, 12, 108-117.
- [145] Ballatori N., Krance S., Notenboom S., Shi S., Tieu K., Hammond C.: Glutathione dysregulation and the etiology and progression of human diseases, *Biol Chem*, 2009, 390, 191-214.
- [146] MacLean M.R., Herve P., Eddahibi S., Adnot S.: 5-hydroxytryptamine and the pulmonary circulation: receptors, transporters and relevance to pulmonary arterial hypertension, *Br J Pharmacol*, 2000, 131, 161-168.

- [147] Eddahibi S., Guignabert C., Barlier-Mur A.M., Dewachter L., Fadel E., Dartevielle P., Humbert M., Simonneau G., Hanoun N., Saurini F., Hamon M., Adnot S.: Cross talk between endothelial and smooth muscle cells in pulmonary hypertension - critical role for serotonin-induced smooth muscle hyperplasia, *Circulation*, 2006, 113, 1857–1864.
- [148] Morecroft I., Dempsie Y., Bader M., Walther D.J., Kotnik K., Loughlin L., Nilsen M., MacLean M.R.: Effect of tryptophan hydroxylase 1 deficiency on the development of hypoxia-induced pulmonary hypertension, *Hypertension*, 2007, 49, 232-236.
- [149] Copley S.D., Frank E., Kirsch W.M., Koch T.H.: Detection and possible origins of aminomalonic acid in protein hydrolysates, *Anal Biochem*, 1992, 201, 152-157.
- [150] Rupérez F.J., Ramos-Mozo P., Teul J., Martinez-Pinna R., Garcia A., Malet-Martino M., Camafeita E., Lopez J.A., Pastor-Vargas C., Egado J., Balayssac S., Gilard V., Barbas C., Martin-Ventura J.L.: Metabolomic study of plasma of patients with abdominal aortic aneurysm, *Anal Bioanal Chem*, 2012, 403, 1651–1660.
- [151] Teul J., Garcia A., Tuñón J., Martin-Ventura J.L., Tarín N., Bescós L.L., Egado J., Barbas C., Rupérez F.J.: Targeted and non-targeted metabolic time trajectory in plasma of patients after acute coronary syndrome, *J Pharm Biomed Anal*, 2011, 56, 343-351.

VIII. ABSTRACT

Pulmonary hypertension is a complex disorder, characterized by a multifactorial pathophysiology. The common hallmark of the pulmonary hypertension is its severity and progressiveness. When it is misdiagnosed, may lead to right ventricle failure and premature death. Pathogenesis of the pulmonary hypertension is still not fully explained and understood yet, and derived mainly from experimental animal models.

The objective of the presented doctoral thesis was untargeted metabolomic analysis of plasma samples in pulmonary hypertension. Both animal (*Sus scrofa*) and human models were considered to study metabolic changes occurring in this disorder. In the doctoral thesis, the comparative analysis of control and pulmonary hypertensive groups was performed.

In the presented doctoral thesis, untargeted metabolic fingerprinting approach with the use of complementary analytical techniques, such as: liquid chromatography coupled with quadrupole and time of flight mass spectrometry (LC-QTOF-MS) and gas chromatography coupled with quadrupole mass spectrometry (GC-Q-MS), was applied. The obtained raw datasets were pretreated (deconvolution, alignment, filtration, normalization) and subjected to univariate statistical analysis with the use of both *t*-test and *U* Mann-Whitney test. The multivariate techniques, such as: principal component analysis (PCA) and partial least squares-discriminant analysis (PLS-DA), were used in order to select metabolites, which contributed to groups' classification and discrimination. The selected, statistically significant metabolites, were identified based on searching through publicly available databases (METLIN, HMDB, KEGG, LIPIDMAPS, CEU Mass Mediator, NIST), as well as fragmentation pattern analyses.

Metabolites, which represented statistically significant differences between compared groups, were related to various biochemical pathways, mainly glycolysis, tricarboxylic acid cycle as well as fatty acid, lipid and amino acid metabolism.

IX. STRESZCZENIE

Nadciśnienie płucne jest hemodynamicznym schorzeniem patofizjologicznym o bardzo złożonej etiopatogenezie. Nieprawidłowo zdiagnozowane lub nierozpoznane nadciśnienie płucne może prowadzić do dysfunkcji prawej komory serca, a w konsekwencji do przedwczesnej śmierci. Procesy patofizjologiczne leżące u podstaw tej jednostki chorobowej nie są do końca wyjaśnione, a wiedza na temat potencjalnych patomechanizmów nadciśnienia płucnego opiera się głównie na eksperymentalnych modelach zwierzęcych. Do tej pory nie zostały zaproponowane specyficzne markery diagnostyczne nadciśnienia płucnego.

Celem głównym niniejszej pracy doktorskiej była niecelowana analiza metabolomiczna próbek osocza w nadciśnieniu płucnym. Badania zostały przeprowadzone w oparciu o model zwierzęcy oraz na wybranej grupie z populacji ludzkiej. Cel główny pracy doktorskiej został osiągnięty poprzez realizację poszczególnych celów cząstkowych, obejmujących następujące etapy:

- Niecelowaną analizę metabolomiczną (metaboliczny „odcisk palca”) próbek osocza z zastosowaniem zaawansowanych i komplementarnych technik analitycznych, takich jak HPLC-ESI-QTOF-MS, GC-EI-Q-MS, co umożliwiło oznaczenie szerokiego spektrum metabolitów o zróżnicowanych właściwościach fizykochemicznych;
- Przygotowanie otrzymanych danych metabolomicznych o złożonej strukturze wielowymiarowej do analizy statystycznej, obejmujące wyrównanie pików (ang. peak alignment), filtrację oraz normalizację;
- Jednowymiarową oraz wielowymiarową bioinformatyczną analizę danych w celu wyselekcjonowania związków o potencjalnym znaczeniu klasyfikacyjnym oraz dyskryminacyjnym;
- Identyfikację istotnych statystycznie różnic w poziomach metabolitów;
- Analizę szlaków biochemicznych, w których biorą udział metabolity o potencjalnym znaczeniu klasyfikacyjnym;
- Kompleksową interpretację biochemiczną uzyskanych wyników przeprowadzonych badań.

W modelu zwierzęcym nadciśnienia płucnego, jako organizm modelowy została wybrana świnia domowa (*Sus scrofa*), ze względu na podobieństwo anatomiczne, fizjologiczne oraz genetyczne do populacji ludzkiej. U zwierząt ostre nadciśnienie płucne zostało wywołane przez iniekcję do żyły udowej mikrosfer polidekstranowych. Próbki osocza zostały pobrane przed zainicjowaniem nadciśnienia płucnego oraz godzinę po stwierdzeniu ciężkiego ($> 40\text{mmHg}$) nadciśnienia płucnego. Przygotowanie próbek osocza obejmowało etapy odbiałczania, odwirowania oraz filtracji supernatantu w przypadku techniki LC-MS, a w przypadku techniki GC-MS dodatkowo przeprowadzono dwustopniowy proces upochodniania. Analiza metabolicznych „odcisków palca” została przeprowadzona za pomocą dwóch komplementarnych technik analitycznych: UHPLC-ESI-QTOF-MS (w dwóch trybach polaryzacji: dodatniej oraz ujemnej) oraz GC-Q-MS. Po wstępnym przygotowaniu danych analitycznych (wyrównanie pików, filtracja, normalizacja), została przeprowadzona jedno- oraz wielowymiarowa analiza statystyczna. W analizie jednowymiarowej zastosowano test t-Studenta oraz U Manna-Whitneya. Natomiast w wielowymiarowej analizie chemometrycznej wykorzystano analizę składowych głównych (PCA) oraz analizę dyskryminacyjną częściowych najmniejszych kwadratów (PLS-DA). Kolejnym etapem przeprowadzonego badania była identyfikacja istotnych statystycznie metabolitów na podstawie dostępnych baz danych (METLIN, KEGG, HMDB, LIPIDMAPS, CEU Mass Mediator, NIST) oraz analizy fragmentacyjnej, zapewniającej wiarygodne potwierdzenie tożsamości chemicznej wyselekcjonowanych metabolitów. W grupie zwierząt z ostrym nadciśnieniem tętniczym zaobserwowano istotnie podwyższony poziom kwasu mlekowego, pirogronianu, kwasu piroglutaminowego, kwasu α -hydroksymasłowego, acetoctanu, kwasu β -hydroksymasłowego, sfingozyny, glicerolu, kwasu cytrynowego, kwasu jabłkowego, kwasu fumarowego, tryptofanu, fenyloalaniny, kwasu palmitynowego oraz oleinowego, jak również istotnie obniżony poziom argininy, kreatyny, sfingomieliny, fosforanu-1-ceramidu, fosfolipidów oraz lizofosfolipidów, w porównaniu z grupą zwierząt przed inicjacją nadciśnienia płucnego. Interpretacja szlaków biochemicznych, w których obserwowane są zidentyfikowane metabolity, pozwoliła na kompleksową interpretację biologiczną uzyskanych wyników. Potencjalne znaczenie w patogenezie ostrego nadciśnienia płucnego mogą mieć metabolity pochodzące ze szlaków glikolizy, cyklu Krebsa, metabolizmu kwasów

tłuszczowych oraz lipidów, których zmieniony poziom może prowadzić do hipoksji, zaburzeń równowagi energetycznej na poziomie komórkowym oraz dysfunkcji mitochondriów.

W modelu nadciśnienia płucnego opartym na populacji ludzkiej, przeprowadzono analizę porównawczą dwóch grup badanych: grupy kontrolnej oraz grupy ze zdiagnozowanym nadciśnieniem płucnym. Porównywane grupy obejmowały 20 pacjentów ze zdiagnozowanym nadciśnieniem płucnym oraz 20 osób zdrowych. Grupy badane zostały dobrane pod względem wieku (50.3 ± 14.8 w grupie kontrolnej, 50.7 ± 15.2 w grupie z nadciśnieniem płucnym), BMI (25.1 ± 3.6 w grupie kontrolnej, 25.3 ± 3.7 w grupie z nadciśnieniem płucnym), jak i rozkładu płci (15 kobiet i 5 mężczyzn w każdej z porównywanych grup). Materiałem biologicznym do oznaczeń metabolomicznych było osocze krwi żyłnej. Przygotowanie próbek biologicznych obejmowało etapy: odbiałczania, odwirowania oraz filtracji supernatantu w przypadku techniki LC-MS, a w przypadku techniki GC-MS, dodatkowo przeprowadzono dwustopniowy etap upochadniania. Metaboliczne „odciski palca” przygotowanych próbek osocza zostały oznaczone za pomocą komplementarnych technik analitycznych HPLC-ESI-QTOF-MS (w trybie polaryzacji dodatniej i ujemnej) oraz GC-EI-Q-MS. Przygotowanie uzyskanych danych analitycznych obejmowało ich dekonwolucję, wyrównanie pików, filtrację oraz normalizację. Następnie została przeprowadzona jednowymiarowa analiza statystyczna z wykorzystaniem testu t-Studenta lub testu U Manna-Whitneya, w zależności od rozkładu danych. W wielowymiarowej analizie chemometrycznej zastosowano analizę składowych głównych (PCA) oraz analizę dyskryminacyjną częściowych najmniejszych kwadratów (PLS-DA), wyselekcjonować te metabolity, które wykazują największą korelację ze stanem patofizjologicznym, jakim jest nadciśnienie płucne. Kolejnym etapem badań przeprowadzonych w niniejszej pracy doktorskiej była identyfikacja istotnych statystycznie metabolitów na podstawie dostępnych baz danych (METLIN, HMDB, KEGG, LIPIDMAPS, CEU Mass Mediator, NIST) oraz analizy fragmentacyjnej. W grupie pacjentów z nadciśnieniem płucnym zaobserwowano podwyższony poziom kwasu moczowego, kwasu mlekowego, pirogronianiu, kreatyniny, glicerolu, glutaminy, palmitoilokarnityny, stearoilokarnityny oraz kwasu aminomalonowego, jak również obniżony poziom cholesterolu, ketosfingozyny oraz amidów kwasu palmitynowego, oleinowego oraz stearynowego, w porównaniu z grupą osób zdrowych. Przeprowadzona analiza szlaków biochemicznych

wykazała, że zaburzenia w procesie glikolizy, metabolizmie kwasów tłuszczowych oraz lipidów mogą mieć potencjalnie znaczenie w patogenezie przewlekłego nadciśnienia płucnego.

Wyniki badań przeprowadzonych w niniejszej pracy doktorskiej potwierdzają potencjalną rolę niecelowanej analizy metabolomicznej, wykorzystującej komplementarne techniki analityczne (LC-QTOF-MS i GC-Q-MS) oraz zaawansowane bioinformatyczne metody analizy danych, w poszukiwaniu nowych, czułych i specyficznych markerów nadciśnienia płucnego. Planowane jest w ramach dalszej pracy przeprowadzenie walidacji na większej populacji z wykorzystaniem celowanej oraz ilościowej analizy metabolomicznej, aby potwierdzić wartość diagnostyczną oraz prognostyczną, wyselekcjonowanych w niniejszej pracy doktorskiej, potencjalnych markerów nadciśnienia płucnego.